

Charles University

Faculty of Science

Study programme: Biology

Branch of study: Cell and Developmental Biology

Specialization: Cell Physiology



Jarmila Havelková

## The source of endogenous DNA damage in neurodegenerative disease

Původ endogenního poškození DNA u neurodegenerativních onemocnění

DIPLOMA THESIS

Supervisor: Mgr. Hana Hanzlíková, Ph.D.

Advisor: Prof Keith Caldecott, Ph.D.

Prague, 2020

**Prohlášení:**

Prohlašuji, že jsem závěrečnou práci zpracovala samostatně a že jsem uvedla všechny použité informační zdroje a literaturu. Tato práce, ani její podstatná část, nebyla předložena k získání jiného nebo stejného akademického titulu.

V Praze 8. 8. 2020

Podpis:

### **Acknowledgements:**

At this point, I would like to thank my supervisor Hana Hanzlíková for her professional guidance and helpfulness in consulting the results. I thank Keith Caldecott for his expert advice, support, and resources for this work. I also thank to Mark Adamowicz for preparing stable gene-edited cell lines. I would like to thank my colleagues, namely Zuzana Cihlářová, Kateřina Krejčíková, Ilona Kalasová and Margarita Sobol, for their willingness and valuable advices for the experimental part of my work. My thanks belongs to the Institute of Molecular Genetics of the ASCR for providing space and equipment for the elaboration of this work. From the service workplaces, I would like to thank Ivan Novotný for his patience and help in the field of fluorescence microscopy.

Last but not least, a big thank you goes to my family, partner, classmates and friends, who were a constant support and motivation during my studies.

## Abstract

DNA single-strand breaks (SSBs) are amongst the most frequent DNA lesions arising in cells and can threaten genetic integrity and cell survival, as indicated by the elevated genetic deletion, embryonic lethality and neurological disease observed when single-strand break repair (SSBR) is attenuated.

One of the proteins important for rapid repair of SSBs is XRCC1, which is a molecular scaffold protein that interacts with multiple DNA repair enzymes (e.g. PARP1, PNKP, POL $\beta$ , APTX, LIG3) and thus, promotes their stability and/or function. Defects in SSBR have been associated with hereditary neurodegeneration in humans, cerebellar ataxias and seizures. Here, I focus on genetic disease *spinocerebellar ataxia autosomal recessive-26 (SCAR26)*, which has been shown to be linked to mutations in *XRCC1*.

I investigate the amount of XRCC1 protein in *XRCC1*-defective cells and reveal that cells from patients with mutations in *XRCC1* exhibit greatly reduced XRCC1 levels. I show that reduced levels of XRCC1 protein in cells correlate with the increasing number of endogenous SSBs, measured by quantification of ADP-ribose in the chromatin.

In addition, I confirm that the most endogenous SSBs arise in S phase of the cells cycle during replication. Moreover, I prove that the main sources of the endogenous SSBs in *XRCC1*-defective cells are not an aberrant Topoisomerase I activity-induced lesions, neither lesions, whose repair require the PNKP activity. Ultimately, I propose a hypothesis that unrepaired oxidative lesions are those, which might trigger the neurodegenerative disease associated with *XRCC1* mutation.

**Key words:** XRCC1, SSB, SSBR, DNA damage, DNA damage repair pathway, neurodegeneration, ataxia

## Abstrakt

Jednovláknové zlomy DNA (single-strand breaks, SSBs) patří mezi nejčastější DNA poškození vznikající v buňkách a mohou ohrozit genetickou integritu a přežití buněk, jak ukazuje zvýšená genetická delece, embryonální letalita a neurologické onemocnění vzniklé z důvodu narušení opravné dráhy těchto jednovláknových zlomů (single-strand break repair, SSBR).

Jedním z proteinů důležitých pro rychlou opravu jednovláknových zlomů v DNA je XRCC1, molekulární scaffold protein, který v rámci oprav poškozené DNA interaguje s několika enzymy (např. PARP1, PNKP, POL $\beta$ , APTX, LIG3), a tak podporuje jejich stabilitu a/nebo funkci. Narušení opravných drah jednovláknových zlomů DNA bylo již v minulosti spojeno s dědičnou neurodegenerací u lidí, cerebelárními ataxiemi a záchvaty.

V této práci se zaměřuji na geneticky podmíněné onemocnění autozomálně recesivní spinocerebelární ataxii (*spinocerebellar ataxia autosomal recessive-26; SCAR26*), u níž bylo prokázáno, že je spojena s mutacemi v *XRCC1* genu

Zkoumám množství proteinu XRCC1 v *XRCC1*-defektivních buňkách, což odhaluje, že buňky pacientů s mutacemi v *XRCC1* vykazují velmi nízké hladiny XRCC1 proteinu. Popisují také, že snížené hladiny proteinu XRCC1 v buňkách korelují s rostoucím počtem endogenních jednovláknových zlomů DNA, měřitelným pomocí kvantifikace ADP-ribózy v chromatinu.

Dále potvrzují, že nejvíce endogenních jednovláknových zlomů DNA vzniká v S fázi buněčného cyklu, během replikace. Dokazují zde, že hlavním zdrojem endogenních DNA SSBs v *XRCC1*-defektivních buňkách není ani aberantní aktivita enzymu topoisomerasa I, ani jednovláknové zlomy v DNA, jejichž oprava vyžaduje účast enzymu PNKP.

Nakonec navrhuji hypotézu, že primárním zdrojem jednovláknových zlomů v DNA, jež mohou představovat jednu z molekulárních příčin dědičného neurodegenerativního onemocnění spojeného s mutací *XRCC1*, jsou neopravené oxidativní léze v DNA.

**Klíčová slova:** XRCC1, SSB, SSBR, DNA poškození, opravné dráhy DNA poškození, neurodegenerace, ataxie

## List of abbreviations

3'-PG	3'-phosphoglycolate
5'AMP	5'-adenylate terminus
Ab	antibody
AD	Alzheimer's disease
ADPr	ADP-ribose
ALS	amyotrophic lateral sclerosis
AOA1	ataxia oculomotor apraxia 1
AOA2	ataxia oculomotor apraxia 2
AOA4	ataxia oculomotor apraxia 4
AOA4/MSZ	ataxia oculomotor apraxia 4/microcephaly with seizures
AOA-XRCC1	ataxia oculomotor apraxia-XRCC1
AP site	apurinic/aprimidinic site
APE1	AP endonuclease 1
APEH	acylpeptide hydrolase
APLF	aprataxin- and PNKP-like factor
APTX	aprataxin
ARH1	ADP-ribosylhydrolase 1
ARH3	ADP-ribosylhydrolase 3
ART	ADP-ribosyl transferase
ARTDs	ADP-ribosyl transferases
ATB	antibiotic
ATLD	ataxia-telangiectasia-like disorder
ATM	ataxia telangiectasia mutated kinase and ATR
ATR	ataxia telangiectasia and Rad3 related inase
BCA	bicinchoninic acid assay
BER	base excision repair
BRCA1	breast cancer type 1 susceptibility protein
BRCA2	breast cancer type 2 susceptibility protein
BRCT1	BRCA1 C-terminal domain 1
BRCT2	BRCA1 C-terminal domain 2
CK2	cysteine-kinase 2

CMT2B2	Charcot-Marie-Tooth disease
CPT	camptothecin
CRISPR/Cas9	clustered regularly interspaced short palindromic repeats/Caspase 9
DAPI	4',6-diamidino-2-phenylindole
DDR	DNA damage response/repair
DGs	DNA glycosylases
DMEM	Dulbecco's modified Eagle's medium
DMSO	dimethyl sulfoxide
DNA	deoxyribonucleic acid
dNTP	deoxyribonucleoside triphosphate
DSB	double-strand break
DSBR	double-strand break repair
EdU	5-Ethynyl-2'-deoxyuridine
EV	empty vector
FA	formaldehyde
FBS	fetal bovine serum
FEN1	flap endonuclease 1
FHA	forkhead-associated domain
FTD	frontotemporal dementia
G	guanine
8-oxoG	8-oxoguanine
H <sub>2</sub> O <sub>2</sub>	hydrogen peroxide
HD	helical domain
HD	Huntington's disease
HR	homologous recombination
I	inosine
IMG	Institute of Molecular Biology AV CS
KD	knock-down
KO	knock-out
LIG1	DNA ligase 1
LIG3 $\alpha$	human DNA ligase III alfa
MAR	mono ADP-ribose

MEM	Minimum Essential Eagle's medium
MG132	proteasome inhibitor
MGMT	O <sup>6</sup> -methylguanine-DNA methyltransferase
MMR	mismatch repair
MMS	methyl methanesulfonate
mRNA	messenger RNA
MSCZ	microcephaly with seizures
MUTYH	human mutY DNA glycosylase
<i>Mutyh</i>	MutY homolog in mice coding adenine DNA glycosylase
NAD <sup>+</sup>	nicotinamide adenine dinucleotide
NEIL1	endonuclease VIII-like 1
NEIL2	endonuclease VIII-like 2
NEIL3	endonuclease VIII-like 3
NEILs	endonuclease VIII-like enzymes
NER	nucleotide excision repair
NHEJ	non-homologous end-joining
NLS	nuclear localization sequence
NT	N-terminal domain
NTH1	endonuclease III-like protein 1
O <sup>6</sup> -meG	O <sup>6</sup> -methylguanine
OGG1	human oxoguanine glycolase 1
Ogg1	mouse oxoguanine glycolase 1
P/S	penicillin/streptomycin
PAGE	polyacrylamide gel electrophoresis
PAM	polyacrylamide
PAR	poly ADP-ribose
PARG	poly ADP-ribose glycohydrolase
PARGi	poly ADP-ribose glycohydrolase inhibitor
PARP	poly ADP-ribose polymerase
PARP1	poly ADP-ribose polymerase 1
PARP2	poly ADP-ribose polymerase 2
PARP3	poly ADP-ribose polymerase 3
PARPi	poly ADP-ribose polymerase inhibitor



PARylation	poly ADP-ribosylation
PBS	phosphate-buffered saline
PCNA	proliferating cell nuclear antigen
PD	Parkinson's disease
PNKP	polynukleotide kinase 3'-phosphatase
POL $\beta$	DNA polymerase beta
RER	ribonucleotide excision repair
RIR	Rev1 interacting region
RNA	ribonucleic acid
rNT	ribonucleotide
rNTP	ribonucleoside triphosphate
ROS	reactive oxygen species
RPKM	reads per kilobase milion
SB	sample buffer
SCAN1	spinocerebellar ataxia with axonal neuropathy 1
SD	standard deviation
SDS-PAGE	sodium dodecyl sulfate-polyacrylamide gel electrophoresis
SEM	standard error of the mean
siNT	small non-target RNA
siRNA	small interfering RNA
siXRCC1	small XRCC1interfering RNA
SMUG1	single-strand selective monofunctional uracil DNA glycosylase
SSB	single-strand break
SSBR	single-strand break repair
ssDNA	single-stranded DNA
T	thymine
TARG	terminal ADP-ribose protein hydrolase 1
TDG	thymine DNA glycosylase
TDP1	tyrosil-DNA phosphodiesterase 1
TOP1	DNA topoisomerase I
TOP1-cc	TOP1-cleavege complex
U	uracil

UNG	uracil DNA glycosylase
WB	western blotting/blot
WGR	Trp-Gly-Arg DNA binding domain
WT	wild type
XRCC1	X-ray cross-complementing protein 1
<i>XRCC1</i>	gene coding X-ray cross-complementing protein protein 1
ZN-F	Zinc fingers (Zn1, Zn2, Zn3) domain

# Contents

1	Introduction .....	1
1.1	DNA damage and repair .....	3
1.2	DNA single strand breaks and repair .....	4
1.2.1	Sources and consequences of SSB lesions in the DNA .....	4
1.2.2	Recognition of SSB and ADP-ribosylation .....	8
1.2.3	Regulation of poly-ADP-ribosylation .....	9
1.2.4	X-ray repair cross-complementing protein (XRCC1) .....	11
1.2.5	End-processing, gap-filling and ligation of SSBs .....	13
1.3	DNA damage and neurodegeneration .....	17
1.3.1	XRCC1, XRCC1-interacting partners and neuropathologies .....	18
2	Aims of the thesis .....	22
3	Materials and methods .....	23
3.1	Chemicals, antibodies, inhibitors and solutions .....	23
3.2	Commercial molecular biology assay kits .....	27
3.3	Cell lines, vectors and siRNA .....	27
3.4	Cell culture, cryopreservation and storage .....	28
3.5	RNA interference .....	29
3.6	Preparation of cell lysates, protein concentration quantification .....	30
3.7	SDS-PAGE, Western blotting, immunostaining and protein detection .....	30
3.8	Cell pre-extraction and fixation .....	31
3.9	Immunofluorescence .....	31
3.10	Click-iT EdU Proliferation Assay .....	32
3.11	Microscopy and Scan-R cell analysis system .....	32
3.12	Data analysis and statistics .....	34
3.13	Graphic .....	35
4	Results .....	36

4.1	Reduced XRCC1 protein levels in <i>XRCC1</i> -mutated patient fibroblasts.....	36
4.2	ADP-ribosylation in <i>XRCC1</i> -mutated patient fibroblasts is detected primarily during S phase.....	37
4.2.1	The level of ADP-ribosylation in G1/G2 cells correlates with the amount of the remaining XRCC1 protein.....	41
4.3	Abortive human DNA topoisomerase I activity is not responsible for elevated endogenous ADP-ribosylation in <i>XRCC1</i> -deleted cells.....	46
4.4	XRCC1 interaction with PNKP is not essential for SSBR of endogenous BER-induced lesions in <i>XRCC1</i> -mutated U2OS cells.....	50
5	Discussion .....	57
6	Conclusions .....	68
7	References .....	69

# 1 Introduction

Among the crucial cellular processes, which allow the cell to be living and functional, is maintaining the genome integrity. Genetic information must resist several types of damage, which may arise from various sources. Fortunately for all eukaryotic organisms, our cells have many strategies how to achieve a successful repairment of both exogenous and endogenous DNA damage.

When DNA damage is too severe for cell's future functioning, the purpose of DNA damage response (DDR) signalling is to guide the cell towards apoptosis. In other cases, DDR activates requisite signalling pathways and provides an important information about the severity of genome-threatening DNA damage. Based on the output, the cell can decide whether stalling of the cell cycle or senescence should follow.

During last decades, naturally occurring DNA damage became a favourite subject in many research areas, such as cancer, aging, neurodevelopment and neurodegeneration. Further research revealed that hydrolysis of DNA sugar backbone, DNA damage caused by either alkylating agents or damaging compounds from metabolism (e.g. oxygen metabolism, lipid peroxidation and some other processes) is frequently occurring on daily basis to a large extent.

Nowadays, there is no doubt that among these types of damage, arising spontaneously throughout a day, single-strand breaks are the most abundant with number of events estimated to more than 10 000 per cell per day (Ciccia & Elledge, 2010).

As there are many types of damage, there are also several repair pathways, which can be cursorily divided into single- and double-strand break repair (SSBR, DSBR, respectively). Single-strand breaks (SSBs) are the most common DNA lesions and SSBR might include base excision repair (BER) pathways and nucleotide excision repair (NER) pathway, ribonucleotide excision repair pathway (RER), mismatch repair (MMR) and other. The specific DNA repair strategy is determined by the type of the lesion. Since SSBs arise on daily basis in every DNA containing cell, these mechanisms for maintaining the genome integrity are available in all eukaryotic cells independently on cell cycle phase. The ratio of individual pathways utilized in the cells although may differ in a tissue-, organelle- and environment-specific manner.

The other impending cell catastrophes represented by double-strand breaks (DSBs) in the DNA can be averted via homologous recombination (HR) and non-homologous end-joining (NHEJ) repair pathway (Lieber, 2010).

In actively replicating cells, both DSBR pathways mentioned above are available. Contrary, in non-dividing cells (therefore, non-replicating), the option to repair these breaks via HR is lacking. NHEJ pathway (although repairing DSBs, just as like it happens during HR in replicating cells) is always available and quite fast, but also more error-prone than HR, as was shown in yeasts by Emerson et al., 2018.

There is a plethora of non-replicating cell types. Some can stay in reversible nonproliferating state called G0 phase of the cell cycle (G0=description of a cell arrested in G1, therefore, not exiting the G1 cell cycle phase). These cells are referred to as quiescent cells and can re-entry the replicative cycle in response to external or internal stimuli (e.g. tissue stem cells and glial cells). After that, HR, again, becomes an option as a DNA repair strategy. Mentioned quiescent state although, is not reversible in senescent and in terminally differentiated cells (although this allegation is still questionable (Sharma et al., 2017)), which lose their ability to divide completely (e.g. post-mitotic neurons, keratinocytes and other) or almost completely (e.g. cardiomyocytes).

In neurons, the lost DNA damage repair options together with some non-replicative state requirements and cell metabolism bring an extra genome-threatening stress to the cell. With such a burden, even slight disruption of DNA repair processes in neurons can result in an impaired neurological functioning. Taking into account the accumulation of mutations (Verheijen et al., 2018) and the fact that each unrepaired SBB might eventually lead to generation of double-strand break, lacking HR might be seen as disadvantageous for these cells. In neurodegeneration context, this might be true particularly throughout aging (Jeppesen, Bohr, & Stevnsner, 2011; Moreira et al., 2001; Coppede & Migliore, 2010; Lodato et al., 2018).

Moreover, insufficient repair of either single- or double-strand breaks in DNA has been connected to several neurodegenerative diseases including Alzheimer's disease (AD), Parkinson's disease (PD), Huntington's disease (HD), amyotrophic lateral sclerosis (ALS), frontotemporal dementia (FTD) and last, but not least, several spinocerebellar ataxias.

Interestingly, ataxias seem to have impaired repair of single-strand breaks in common, the source of which remains unclear. Unravelling the origin of DNA lesions, which underpin

disease pathology, may help us to understand the very basis of genome instability and neurodegeneration in DDR-deficient neuronal dysfunctions.

## 1.1 DNA damage and repair

Life of the cell is possible thanks to the genome integrity, which is protected by a systematic recognition and repair of DNA damage by a fine network of many DNA repair pathways (Fig. 1).

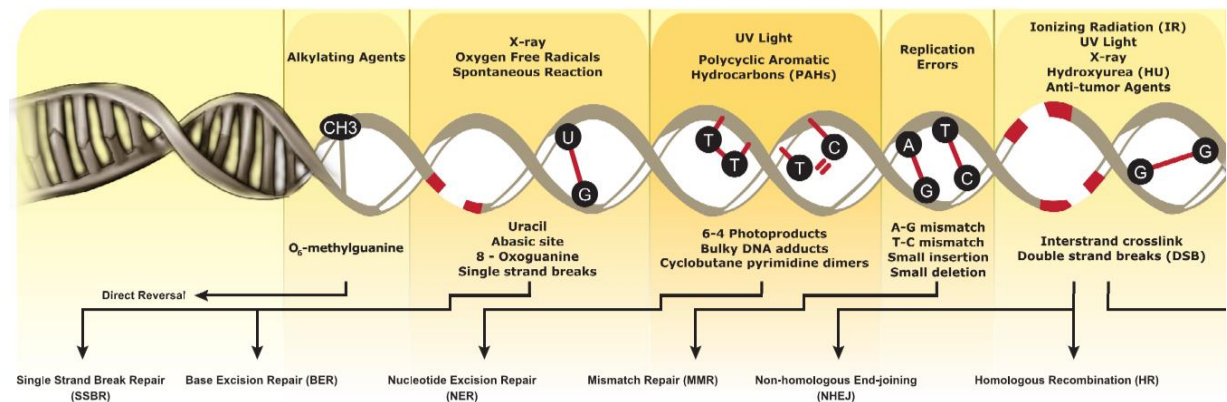


Figure 1: DNA damage and relevant repair pathways. Adapted from Genetex ([URL1](#)).

Some direct repair of DNA damage caused by alkylating agents is possible via single enzymes (Belanich et al., 1996), however, common attribute of most of these repair pathways is signalling via detectors/sensors, transducers, mediators and effectors.

Every cell must cope with both endogenous and exogenous DNA damage. This involves DNA alterations and DNA lesions. Depending on the DNA damaging agent, we observe either single- (single-strand break, SSB) or double-stranded (double-strand break, DSB) breaks of DNA double-helix. These lesions are not necessarily produced directly, but they can also be generated as intermediates during the repair of DNA itself (Abbotts & Madhusudan, 2010).

Among directly produced lesions in replicating cells, the most common are replication machinery-caused DSBs and mismatched bases. In actively replicating cells, when DSB occur, it can be repaired by suitable DSB repair pathway (either homologous recombination or NHEJ). The DSBs in DNA may arise, apart from the replication-connected processes, in response to exposure to ionizing radiation or genotoxic agents. Endogenous sources of DSBs are cellular metabolism (generation of DNA-damaging ROS, which might subsequently result in DSB), and

also normal programmed process of genomic recombination (either in purpose to provide the gametic variety during meiosis or a class switch to ensure the antibody diversity) (Yoon & Caldecott, 2018).

Anyway, in both replicating and non-replicating cells, the most abundant endogenous DNA lesions are single-strand breaks. Sources causing DNA alterations which are later on capable of SSB-induction are transcriptional stress, spontaneous deamination (causing apurinic or apyrimidinic sites (AP sites)), hydrolysis of bases, modification of bases, inter- and intra-strand cross-links, bulky adducts and free radicals (reactive oxygen species, ROS) doing (Iyama & Wilson, 2013).

## 1.2 DNA single strand breaks and repair

So far, we have briefly discussed double-strand breaks and some other replication-induced genome integrity challenging events. Aside these lesions, there are other which deserve our attention - SSBs.

Coming from various sources, SSBs may get involved various DNA repair pathways, which are tightly connected (discussed in greater detail below). The central mechanism of the recognition and subsequent processing of SSBs is poly(ADP-ribose) labelling of the damaged site, scaffold assembly, processing of DNA damaged, DNA synthesis filling the gap in the damaged strand and ligation (Figure 2).

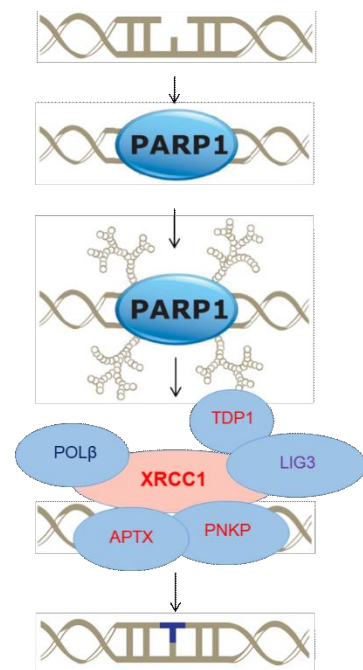


Figure 2: Simplified steps of SSB recognition and subsequent repair by SSBR enzymes.

### 1.2.1 Sources and consequences of SSB lesions in the DNA

As double-stranded breaks in DNA might arise from exposure to ionizing radiation or genotoxic agents, as well as from normal cellular processes, the origin of SSBs also vary. In general, these include mainly direct disintegration of oxidized DNA sugar backbone, abortive activity of topoisomerase I, cell metabolism (respiration and lipid peroxidation) and some



internal steps of DNA repair pathways (e.g. BER and RER). The most common lesions which pose a threat in the form of subsequent SSB formation are summarized in Figure 3.

Among other events indirectly generating SSBs, but significantly threatening the DNA are unique DNA-damaging structures formed. At many sites in the eukaryotic genome, including the transcribed regions, if the nascent RNA transcript hybridizes with complementary DNA template, RNA-DNA hybrids arise. These hybrids, together with displaced ssDNA, are three-stranded structures called the R-loops and may serve as a transcription-stress effectors (Santos-Pereira & Aguilera, 2015).

As the transcription machinery (and in replicating cells, the replication machinery in addition) itself needs the DNA to be unwind, independently on the formation of RNA-DNA hybrids, there is a forward positive torsion stress generated by RNA polymerase. This torsional stress is than relieved by the DNA topoisomerase I (TOP1).

This ATP-independent enzyme possesses an endonuclease activity and covalently binds DNA. The enzyme catalysis transient single-strand break, which allows the mechanical unwinding of the DNA. Under normal conditions, such breakage is not recognized as a DNA damage, because DNA strand is re-ligated by the TOP1, and the enzyme is then liberated from the site without activating DDR pathway.

On the other hand, perturbation of the normal cellular TOP1 activity may lead to the accumulation of TOP1-cleavage complexes (TOP1-cc), and trapping those complexes on the DNA leads to the activation of DDR (Pommier et al., 2006).

The normal cellular processes which can become the source of genome-threatening DNA damage are DNA repair pathways called base excision repair (BER) and nucleotide excision pathway (NER). So called “helix-distorting” lesions (e.g. bulky adducts, inter- and intra-strand crosslinks) caused by either UV radiation or chemical substances are repaired by excision of multiple nucleotides (usually about 30 nucleotides) via NER specific enzymes (NER mechanisms reviewed in (Sugasawa, 2010)). On the other side, there are non-bulky lesions, which can be eliminated by BER, also requiring the initial enzymatic DNA cleavage.

The base excision pathway and the pathway for SSBs’ repair share some core proteins, but the pathway preventing the deleterious consequences of SSBs is often called single-strand break repair (SSBR) and seen as a separate genome-protective mechanism, rather, then sub-pathway of BER (discussed in detail in chapter 1.2.5 End-processing, gap-filling and ligation).

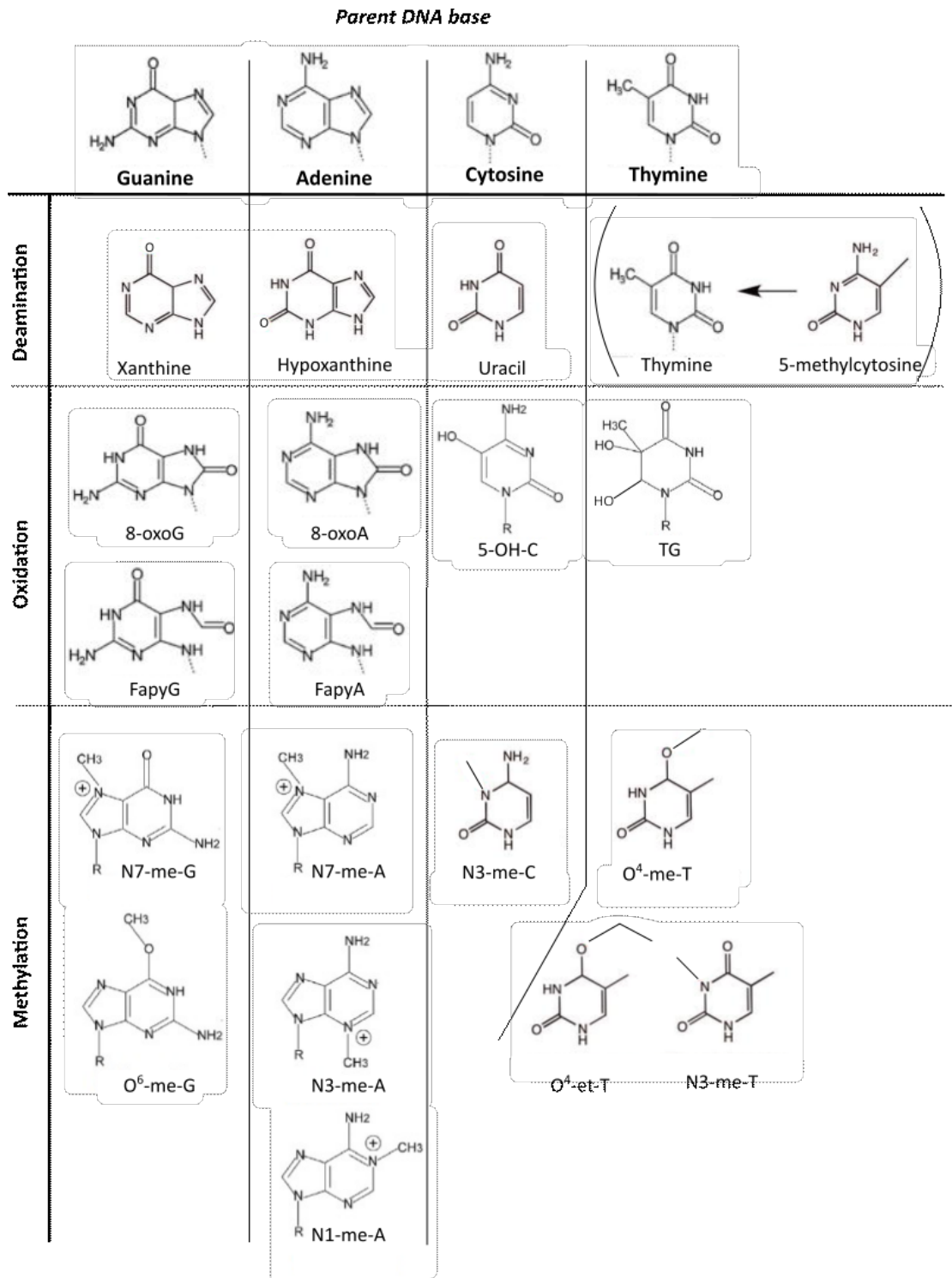


Figure 3: **Common non-bulky lesions.** Nucleotide derivatives listed by the parent base and separated into groups based on the type of modification.

BER serves as a key defensive mechanism against oxidative, alkylating and deamination (e.g. cytosine deamination) events in the cell coming from either normal cellular metabolism, spontaneous mutations or exogenous agents. These events result in a damaged DNA site, which does not necessarily distort the DNA, but leads to a formation of SSB, which can subsequently be turned into DSB (Yang et al., 2004). Non-bulky DNA lesions include apurinic/apyrimidinic sites (AP sites), nucleotide derivatives and deaminated bases (most of which are summarized in Fig. 3).

As was previously mentioned, BER is a pathway requiring DNA incision. Two main BER pathways were established. Short-patch BER pathway dealing with single damaged nucleotide and long-patch BER pathway, incising two or more nucleotides (Matsumoto et al., 1994; Fortini et al., 1998), a system requiring some replication-associated factors (Klungland & Lindahl, 1997). These two branches share four essential core enzymes (DNA glycosylase, AP endonuclease or AP DNA lyase, DNA polymerase and DNA ligase), although, in context of SSBR, the process of BER generally consists of 7 major steps summarized and compared to the 5 steps of SSBR pathway in Figure 4.

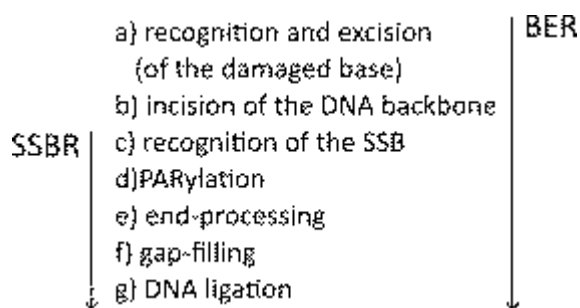


Figure 4: The inclusion of BER and SSBR general steps.

The long-patch BER branch is important mainly in S phase, because the recognition and subsequent repair of Okazaki fragment-caused SSBs is dependent on proliferating cell nuclear antigen (PCNA) (Kedar et al., 2002) and flap endonuclease 1 (FEN1) (Prasad et al., 2000; Klungland & Lindahl, 1997). In G1/G2 cell cycle phases, the short-patch branch of BER becomes the key DNA repair pathway, which is able to repair the most common endogenous lesions. As you can notice in the comparison of BER and SSBR (Fig. 3), BER is causing an additional DNA single-strand break, which is then recognized and resolved by SSBR proteins and enzymes.

### 1.2.2 Recognition of SSB and ADP-ribosylation

The additional SSBs arising from BER were connected to the first step of SSBR which involves DNA and protein modification (covalently attached ADP-ribose molecules) done by specialized sensory enzymes. So far, there is not enough scientific data, which would clarify the role of such modification in the NER-pathway (King et al., 2012).

The first step in SSBR is detection of such damage and activation of the pathway by signalling the threat to the cell. This ability belongs to some of the members of poly(ADP-ribose) polymerase (PARP) protein family (so far consisting of 17 enzymes).

These enzymes, known as ADP-ribosyl transferases (ARTDs), are capable of poly/mono(ADP-ribose) synthesis. Consuming the  $\text{NAD}^+$ , PARPs can modify proteins with single mono(ADP-ribose) molecules (MARylation)<sup>1</sup> or chains of poly(ADP-ribose) molecules (so called “PARylation” by PARP1, PARP2, and Tankyrases 5a and 5b), which then serve as a cellular signalisation (further referred to as “labelling”) (Vyas et al., 2014). Altering the biochemical properties of proteins and molecules (e.g. histones, DNA, RNA), this modification is utilized in crucial pathways: regulation transcription, apoptosis, cell division and DDR.

For the purpose of labelling the SSBs in the DNA, only a few PARPs can do so: PARP1, PARP2 and PARP3. This is thanks to their capacity to bind DNA. These three enzymes share a conserved DNA-binding domain WGR (Trp, Gly, Arg) (Fig. 5). PARP1 and PARP2 are capable of PARylation, whereas PARP3 (according to Grundy et al., 2016; Belousova et al., 2018) can synthesize and covalently link only single molecules of ADP-ribose. Although all three mentioned proteins share similar structure (including the catalytic domain), compared to PARP1 and PARP2, PARP3 lacks the N-terminal Zn-finger domains (Zn1, Zn2, Zn3) and BRCT domain (Fig. 5).

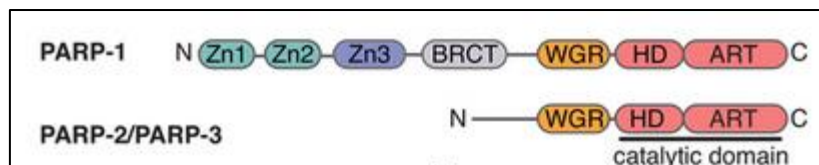


Figure 5: **Schematic structure of human PARP-1, PARP-2, and PARP-3 domain organization.** Zinc fingers: Zn1, Zn2, and Zn3; BRCT – BRCA C-terminus; WGR: Trp-Gly-Arg domain; HD –helical domain; ART – ADP-ribosyltransferase. Adapted from: Li, G. M. (2008). Mechanisms and functions of DNA mismatch repair. In *Cell Research* (Vol. 18, Issue 1, pp. 85–98).

<sup>1</sup> Capable of the mono(ADP-ribose) modification is the majority of the PARP protein family members.

Within the catalytic domain, PARPs have auto-modification moiety, which accepts auto-PARylation. When the conformation of the enzyme changes (by binding to ssDNA), dimerization occurs and the enzyme becomes fully active, generating ADP-ribose polymers (Pion et al., 2005).

The abundance of PARP1, PARP2 and PARP3 does not differ dramatically (according to data published in (GeneCards®: The Human Gene Database, 2020); [URL2](#), [URL3](#), [URL4](#)), but the main enzyme ensuring about 85 % of nuclear PARylation after induction of oxidative damage is PARP1 (Hanzlikova et al., 2017).

The reason for that is the presence of the Zn-finger domains, which provide strong DNA-binding (Fig. 6). Chains of (ADP-ribose) molecules are recognized by the X-ray cross complementing protein 1 (XRCC1). XRCC1 does not exhibit an enzymatic activity, instead, it serves as a scaffold protein and a linkage between PARylation and other DNA-repairing enzymes. Thus, it accelerates SSBR.

### 1.2.3 Regulation of poly-ADP-ribosylation

Even though PARylation might be very robust (as result of hyperactivation of PARPs by DNA damage (Hoch et al., 2017), it is a very transient process. Aside the auto-regulatory function and conformational changes (Langelier et al., 2018), the PARylation process itself is regulated by hydrolases, sometimes called erasers of PARylation (simplified schema of PAR chains' metabolism is illustrated in Fig. 7).

Poly(ADP-ribose) glycohydrolase (PARG) is a necessary enzyme and provides very adroit regulation of the length of PAR chains by cleavage of ribose-ribose bonds within the polymer, therefore, releasing free single ADP-ribose molecules (Slade et al., 2011).

Importantly, this enzyme is not able to cleave the very last ADP-ribose molecule attached to the protein. For this purpose, there are several mono(ADP-ribose) hydrolases, for example ADP-

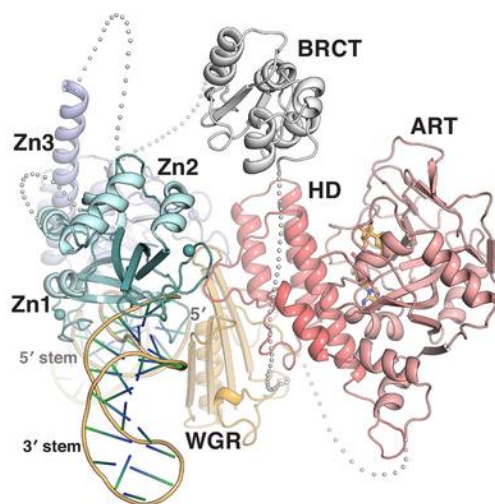


Figure 6: A composite model for full-length PARP-1 detecting a single-strand DNA break. Adapted from: Li, G. M. (2008). Mechanisms and functions of DNA mismatch repair. In *Cell Research* (Vol. 18, Issue 1, pp. 85–98).

ribosylhydrolase 1 (ARH1), ADP-ribosylhydrolase 3 (ARH3) and terminal ADP-ribose protein glycohydrolase 1 (TARG) with the ability to remove the terminal mono(ADP-ribose) molecule. These enzymes are not redundant, their function is limited by the amino acid, on which is the terminal ADPr bound (e.g. serine-ADPr is cleaved by ARH3 (Bonfiglio et al., 2017; Abplanalp et al., 2017) and ADPr attached to glutamate or aspartate residue are cleaved by TARG (Sharifi et al., 2013)).

PARPs are one the therapeutic targets in cancer research due to the exploration of PARP inhibition (PARP inhibitors, PARPi) synthetic lethality (Bryant et al., 2005; Dedes et al., 2011; Ali et al., 2018). Connection between the inhibition of PARPs' counterpart enzyme PARG and synthetic lethality in BRCA1/BRCA2 deficient cancers is not as clear as in the case of PARPi, but the use of PARG inhibitor (PARGi) is very helpful tool in SSB research.

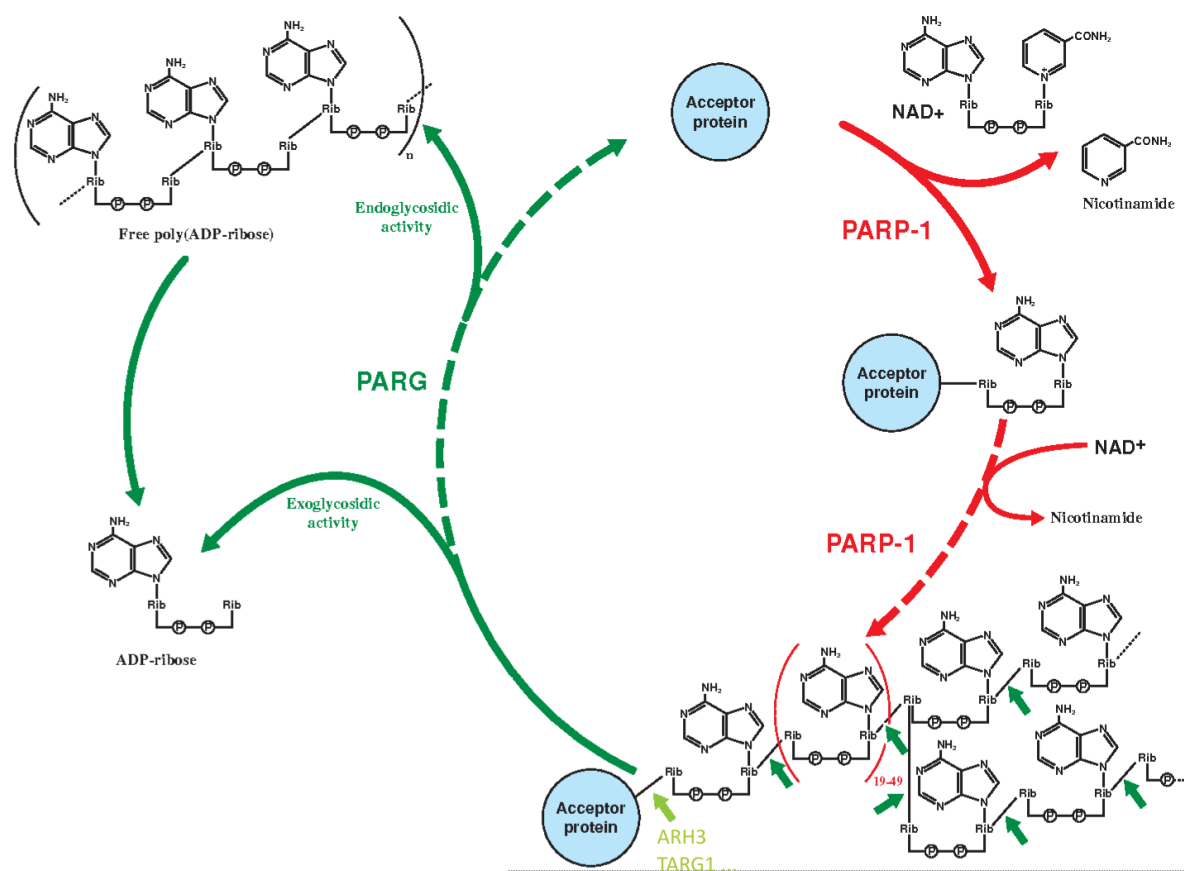


Figure 7: **Simplified schema of the ADP-ribose polymers.** Polymerization of ADP-ribose units by PARP1 (consuming  $\text{NAD}^+$ ) (red). Hydrolysis of ribose-ribose bonds by PARG is shown in dark green. Site of the terminal mono(ADPr) cleavage is indicated by light green arrow. Adapted from (Rouleau et al., 2004).

There are few methods for SSB visualization in cells, but currently the most efficient way to explore SSBs in the DNA seems to be PARG inhibition (for mechanistic description of the method see chapter 3.4.6 Immunofluorescence). It is very accurate, less time-consuming and cheap, compared to the other DNA-breaks detection methods (Luczak & Zhitkovich, 2018; Biernacka et al., 2018; Kordon et al., 2019).

#### 1.2.4 X-ray repair cross-complementing protein (XRCC1)

After PARylation, the key scaffold protein of SSBR, X-ray repair complementing protein 1 (XRCC1) mediates the assembly of SSBR machinery and accelerates the whole process of repairment.

Its mRNA abundance in tissues was described in Fagerberg's RNA-sequencing study (Fagerberg et al., 2014). The XRCC1 mRNA can be found in at least 27 different tissues, including placenta, thyroid, endometrium, testes and ovaries (mean RPKM ranging from  $10,3631 \pm 1,506$  to  $16,043 \pm 0,377$ , respectively;) and in brain, colon, duodenum, oesophagus, small intestine and stomach similarly (mean RPKM ranging from  $6,150 \pm 0,518$  to  $7,124 \pm 1,66$ , respectively; as analysed in "XRCC1 X-ray repair cross complementing 1", 2020; [URL5](#)). In case of the brain, XRCC1 mRNA is present in most human, pig and mouse brain regions, such as olfactory region, cerebellar cortex, basal ganglia, cerebellum and other according to two transcriptomics datasets (Yoon & Caldecott, 2018).

This protein is located on chromosome 19 (19q13.31), consists of 633 amino acids coded by 17 exons and has molecular weight 85 kDa. XRCC1 exists in form of a monomer, as well as a homodimer (Mani et al., 2004). This protein has a Rev1 interacting region (RIR) motif (interacting with PNKP with low affinity; (Breslin et al., 2017)), nuclear localization sequence (NLS) motif and several interacting domains. One of such interacting domains is N-terminal domain, which interacts with Pol $\beta$ , another domain is central BRCT1 (Breast cancer type 1 susceptibility protein C-terminus domain 1), interacting with DNA, ADP-ribosylated PARP1 and PARP2, and is also involved in homodimerization of XRCC1 (Lévy et al., 2006) (Fig. 8).

On the C-terminus there is BRCT2 domain (Breast cancer type 1 susceptibility protein C-terminal domain 2), interacting with human DNA ligase III (LIG3 $\alpha$ ). Two linker domains interact with PNKP. As was previously said, linker 1 provides low affinity binding site for

PNKP, but the linker has also a modification site present (important for the repair of G/T mismatches, for more detailed information see (Wiest & Tomkinson, 2019)).

In context of SSB, the linker 2 (between BRCT1 and BRCT2 domain) is essential due to three clusters of cysteine-kinase 2 (CK2)-phosphorylation sites (depicted as clustered black asterisks in Fig. 8). Phosphorylation of XRCC1 by the constitutively active protein kinase CK2 enables XRCC1 translocation to the nucleus (in response to oxidative DNA damage) and also provides successful binding with PNKP (high affinity XRCC1/PNKP interaction), APTX and APLF, as depicted in Fig. 8) (A. A. E. Ali et al., 2009; Rulten et al., 2008; Loizou et al., 2004; Clements et al., 2004).

The scaffold protein XRCC1 was shown to bind also some important DNA glycosylases (e.g. AP endonuclease 1 (APE1), oxoguanine glycosylase 1 (OGG1) and endonuclease VIII-like enzymes (NEILs); Fig. 8) with take part in SSB too.

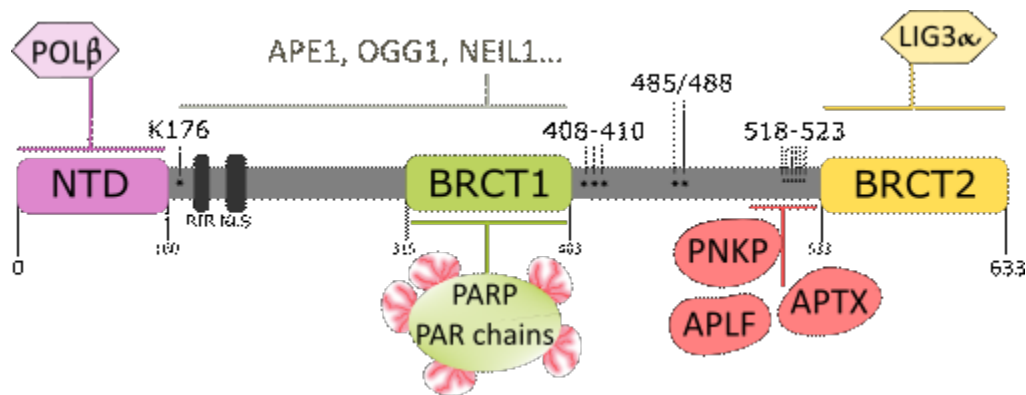


Figure 8: **XRCC1 protein structure and interactions.** Simplified XRCC1 protein structure with following domains depicted: N-terminal domain (purple), two linker domains (grey), BRCT domains (green and yellow). Relevant domain interacting partners depicted in an according lighter colour. Abbreviations: APE1 = AP endonuclease 1; APLF = aprataxin- and PNKP-like factor; APTX = aprataxin; BRCT1 = BRCA1 C-terminal domain 1; BRCT2 = BRCA1 C-terminal domain 2; LIG3α = human ligase III alfa; NEIL1 = endonuclease VIII-like 1; NLS = nuclear localization signal; NTD = N-terminal domain; OGG1 = oxoguanine glycolase 1; PAR = poly(ADP-ribose); PARP= poly(ADP-ribose) polymerase; PNKP = polynucleotide kinase phosphatase; POLβ = DNA polymerase beta; RIR = Rev1 interacting region; \* = modification site.



### 1.2.5 End-processing, gap-filling and ligation of SSBs

Following the track of SSB pathway, the next major step is called end-processing. After spontaneously arisen SSBs or exposure to SSB-causing agents, there are several combinations of damaged DNA ends left behind (summarized in Fig. 9). SSBR machinery restore the necessary conventional 3'-OH and 5'-P ends via several damaged end-specific enzymes (Repair enzymes in Fig. 9), which allows the repair machinery to proceed.

As you can see in Figure 9, there are several different ssDNA damaged ends, which might appear in the cell. The enzymes of SSBR pathway are able to eliminate such, based on the chemical properties. Among the events which leave a 3'-phosphate and 5'-hydroxyl termini are ionizing radiation, AP-lyase enzymatic cleavage or ROS attack ( $\cdot\text{OH}$ ). Resolving these unligable ends is the main task of DNA end-processing enzyme which possesses DNA 5'-kinase and 3'-phosphatase activity called polynucleotide kinase phosphatase (PNKP) (Fig. 9, left).

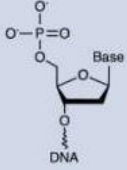
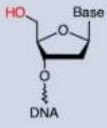
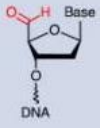
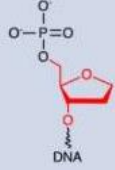
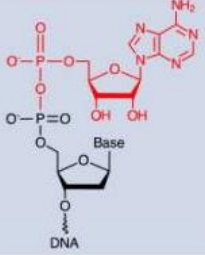
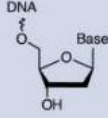
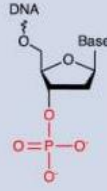


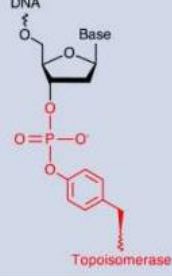
5' lesions	5'-hydroxyl	5'-aldehyde	5'-deoxyribose phosphate	5'-adenylate (AMP)
				
Repair enzyme:	PNKP	POL $\beta$ , FEN1	POL $\beta$	APTX, FEN1
3' lesions	3'-phosphate	3'-phosphoglycolate	3'-phospho- $\alpha,\beta$ -unsaturated aldehyde	3'-TOP1 adduct
				
Repair enzyme:	PNKP	APE1	APE1	TDP1

Figure 9: **Examples of damaged DNA termini at SSB.** Possible forms of 3' and 5' DNA ends and DNA repair enzymes involved in end-specific repair. Green: XRCC1-interacting partners, orange: XRCC1- and PARP1-interacting partners, blue: XRCC1- and PAR-interacting enzymes. PNKP: polynucleotide kinase 3'-phosphatase; POL $\beta$ : DNA polymerase  $\beta$ ; FEN1: flap endonuclease 1; APTX: aprataxin; APE1: apurinic/apyrimidinic endonuclease 1; TDP1: tyrosyl DNA phosphodiesterase 1.

Also, previously mentioned mechanism of torsional stress relieve via TOP1 brings the problem of unresolved TOP1-cleavage complex (TOP1-cc), indirectly causing persisting SSB, whose proper processing of TOP1-cc is dependent on the PNKP enzyme too. In normal cells, formation of TOP1-cleavage complex is a reversible process. Topoisomerase I is able to perform an incision of the DNA as well as its ligation afterwards. In the situation, when TOP1 enzyme is stalled at the site of the single-strand cleavage<sup>2</sup>, it forms a complex with ssDNA via tyrosyl phosphate bond. The stalled complex activates the ubiquitin-26S proteasome pathway, which leads to a partial degradation of TOP1. Tyrosyl phosphate link remains at the site and is subsequently cleaved by tyrosyl-DNA phosphodiesterase I (TDP1), leaving a 3'-phosphate moiety, which can be PARylated, recognized by XRCC1 and then processed by SSB pathway (Fig. 10).

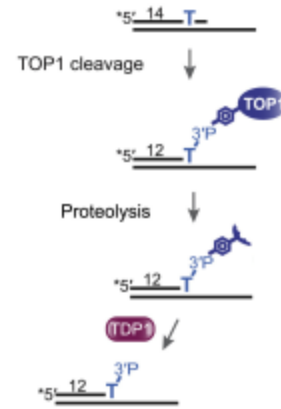


Figure 10: **Simplified steps of TOP1-cleavage complex dissolution by TDP1 enzyme.** Adapted from (Álvarez-Quilón et al., 2020).

TDP1 is recruited to the SSB by PARP1 and the PAR chains generated by the enzyme. TDP1 was also shown to co-localize with XRCC1, to bind LIG3 $\alpha$  (which might be in complex with XRCC1), and, also to promote XRCC1 recruitment (Plo et al., 2003; El-Khamisy, Hartsuiker, & Caldecott, 2007; El-Khamisy et al., 2005). Its function although is not perfect to the point of processing the damaged ends into the conventional form, which would directly facilitate subsequent gap-filling and ligation of the strand. After TDP1 cleaves TOP1 peptide (remaining at the SSB from previously partially degraded TOP1), there are damaged ends left. The ends are specific based on their origin and, in this case, the damaged ends must be processed by the PNKP enzyme (Álvarez-Quilón et al., 2020).

This PNKP enzyme can bind to DNA (Havali-Shahriari et al., 2017) and is one of the major XRCC1-interacting partners (Breslin et al., 2015; Breslin et al., 2017). Aside the mentioned low-affinity binding site upstream BRCT1 of XRCC1, which is phosphorylation independent, it has been shown that N-terminal FHA domain of the PNKP enzyme interacts with

<sup>2</sup> Stalling of TOP1 might be induced by topoisomerase I inhibitor camptothecin (CPT).

phosphorylated XRCC1 (A. A. E. Ali et al., 2009). It support the retention of these proteins, accelerating the SSBR in response to alkylating agents (Della-Maria et al., 2012), and also stimulates the PNKP activity (Loizou et al., 2004; Hanzlikova et al., 2017).

The FHA domain is crucial for the enzyme, because it does not only bind to a specific phosphorylated site on XRCC1 (A. A. E. Ali et al., 2009). Its folding creates secondary structure similarly to BRCT1 domain (“PAR-binding pocket”), which is responsible for early recruitment of the protein to the DNA damage sites (M. Li et al., 2013) , which were PARylated afore by the PARPs.

The CK2-phosphorylated motif of XRCC1 mediates the interaction with another end-processing enzymes aprataxin (APTX) and aprataxin- and PNKP-like factor (APLF), which both possess the amino-terminal FHA domain (Moreira et al., 2001; Iles, Rulten, El-Khamisy, & Caldecott, 2007). Aprataxin resolves 5'-adenylate (5'-AMP) terminus (Fig. 9; top right) arising from abortive ligation intermediates, and, same as with PNKP, interaction between XRCC1 and APTX promotes the recruitment of the protein to the SSBs in nucleus (Horton et al., 2018). APLF is also recruited to sites of DNA damage in PAR-dependent manner, but its specific function has not been fully described yet (Iles et al., 2007).

Apurinic or apyrimidinic lesions (AP sites, Figure 11), induced by ROS attack or resulting from DNA glycosylase-catalyzed reactions, and 3'-phosphoglycolate (3'-PG) are excised by the apurinic/apyrimidinic endonuclease 1 (APE1). APE1 possess 3'-phosphodiesterase and 3'-5' exonuclease activities. Working in close cooperation with DNA glycosylases, APE 1 can cleave the phosphodiester backbone at 5' of the AP site, leaving a 3'-OH terminus and 5'-dRP (Fig. 9) behind. This enzyme, although upstream of the SSB origin, was also reported to bind XRCC1 (Vidal et al., 2001a).

Nevertheless, taking into account the contradictory observations and conclusions (Vidal et al., 2001; Fan et al., 2004; Wong et al., 2005; Caldecott, 2019), this interaction seem to be indirect and the relevance of APE1/XRCC1 interaction remains blurry.

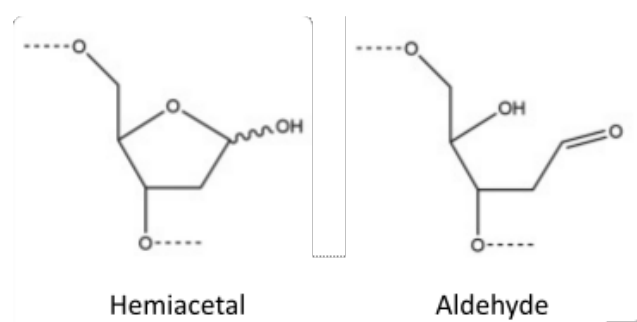


Figure 11: Baseless sugar moieties called AP sites.

Next step is gap-filling of the SSB-caused gap in the DNA performed by DNA polymerase  $\beta$  (POL $\beta$ ). This and following steps utilize the same set of proteins during BER and SSBR. POL $\beta$  cleaves the sugar backbone at 3' of the AP site and is able to fill the gap by synthesis of proper nucleotides (Prasad et al., 1998).

It also has the ability to bind XRCC1 NTD domain via palm-thumb domains in its active site (Marintchev et al., 2003; Gryk et al., 2002), whilst the thumb domain is important for XRCC1/POL $\beta$  affinity (Cuneo & London, 2010). Binding XRCC1, once again, promotes recruitment of POL $\beta$  to the site of DNA damage caused by low doses of irradiation and positively affects its stability (Hanssen-Bauer et al., 2011; Fang et al., 2019).

Alkylating agent- and oxidative agent-induced DNA damage repair studies (Wong & Wilson, 2005; Dianova et al., 2004, respectively) support the hypothesis that this interaction participate in BER efficiency coordination, therefore, also in SSBR pathway (Lan et al., 2004). This is consistent with the finding that POL $\beta$  is involved in long-patch BER pathway downstream of XRCC1 (Havali-Shahriari et al., 2017), where it interacts with another set of enzymes (including proliferating cell nuclear antigen (PCNA) (Kedar et al., 2002) and flap endonuclease 1 (FEN1) (Prasad et al., 2000; Klungland & Lindahl, 1997). POL $\beta$  in SSBR pathway might be partially dispensable in case of oxidative damage (Caldecott, 2019), but either way (alkylating or oxidative agents-caused DNA SSBs), POL $\beta$  is tightly connected with the final step of ligation, which completes the repair of SSB.

In case of long-patch DNA repair, DNA ligase 1 (LIG1) and its interaction with PCNA is needed (Levin et al., 2000), but the pathway which includes XRCC1 is the short-patch branch of SSBR (Mortusewicz et al., 2006a). Ligation of the latter is conducted by XRCC1-interacting enzyme DNA ligase III $\alpha$  (LIG3 $\alpha$ ), one of the two isoforms present in the nucleus. Only this isoform possesses C-terminal domain which promotes the enzyme's stability and, as it has been seen with other XRCC1-interacting partners, recruitment to the DNA damage site (Ljungquist et al., 1994; Caldecott et al., 1995; Mortusewicz et al., 2006) via binding to XRCC1 (Taylor et al., 1998). Noteworthy is the fact that most of the LIG3 $\alpha$  (about 80%) is in heterodimer with XRCC1, and that in XRCC1-deficient mammal cells, the cellular level of LIG3 $\alpha$  is greatly reduced (~5 fold) (Caldecott et al., 1995; Ljungquist et al., 1994). As can be concluded from

above information, the XRCC1 (with bound LIG3 $\alpha$ ) plays a role in recruitment of the ligase and presumably provides more efficient continuity of SSBR steps.

### 1.3 DNA damage and neurodegeneration

Although all living cells fight to maintain the genome integrity, neurons with their specific requirements for the functionality, indeed, are very specialized cells in the human body. Constantly occurring endogenous DNA damage-causing events threaten the neural genome integrity during neurodevelopment and mature neurons face even more threats. Many neurologic diseases are caused by perturbation of neurodevelopment, which projects to the adult life, often shortening the lifespan of an individual.

As proliferation drives the neurodevelopment, replication stress is a major cause of DNA damage during neurogenesis. Additionally (to DSBs arising from the replication machinery itself), one of the most frequent errors during DNA replication involve incorporation of ribonucleoside triphosphate (rNTP) instead of deoxyribonucleoside triphosphate (dNTP). Although, transcription-associated and oxidative stress-caused DNA damage take place in immature neural cells as well as in mature neurons,

As was previously said, many neurological problems originate from the proliferating cells during the development. In a mature brain, the situation is distinctly changed. Since the mature brain consists mostly of post-mitotic non-proliferating neurons, often with high transcriptional activity and high respiratory rate, genotoxic events are most likely to happen on a bigger scale. The increased respiration leads to a high ROS production, oxidization of bases and, possibly even to a breakage of phosphodiester backbone of DNA. It is not surprising that these extra threats require efficient DDR, and any perturbation might be potentially fatal.

In last decades, neurodegeneration was directly and indirectly linked to defectiveness in BER and SSBR, as well as DSBR, NER, MMR and mitochondrial dysfunction (Jeppesen et al., 2011). Aside the individual diseases and syndromes (summarized in Fig. 12), the DNA breaks seem to contribute to the process of aging (Jeppesen et al., 2011). It has been shown that DSBs may lead to disrupted neurodevelopment, however, the most frequent lesions in the non-dividing cells are SSBs. Therefore, it is possible that SSBs in SSBR-defective mature neurons pose a bigger threat to the genome than the highly toxic DSBs.

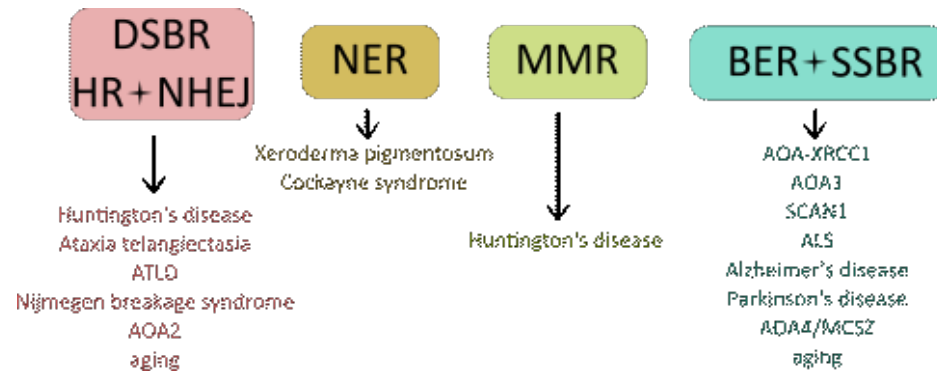


Figure 12: **Summary of DDR-defects and attributed diseases/syndromes.** ALS = amyotrophic lateral sclerosis, AOA1 = ataxia oculomotor apraxia 1, AOA2 = ataxia oculomotor apraxia 2, AOA4/MCSZ = ataxia oculomotor apraxia 4/microcephaly with seizures, AOA-XRCC1 = ataxia oculomotor apraxia-XRCC1, ATLD = ataxia-telangiectasia-like disorder, BER = base excision repair, DSBR = double-strand break repair, HR = homologous recombination, MMR = mismatch repair, NER = nucleotide excision repair, NHEJ = non-homologous end-joining, SCAN1 = spinocerebellar ataxia with axonal neuropathy, SSBR = single-strand break repair.

### 1.3.1 XRCC1, XRCC1-interacting partners and neuropathologies

Defective DNA repair pathways caused by altered *XRCC1* (or simply XRCC1 polymorphism) and/or by several other proteins, which somehow affect either XRCC1 itself or its interactions, were previously linked to cancer (e.g. cervical cancer, breast cancer, non-small cell lung cancer and others, respectively; acute myeloid leukemia (the established contribution of impaired DNA damage repair to cancer reviewed in Broustas & Lieberman, 2014)).

Moreover, mutations in several SSBR proteins affecting either directly their function or their interactions, were found to be connected to neurodegenerative diseases (e.g. hereditary ataxias (Yoon & Caldecott, 2018), amyotrophic lateral sclerosis, Alzheimer's disease, Parkinson's disease, Huntington's disease, reviewed in (Wang et al., 2018)).

The medical term ataxia represents loss of muscle control and movement coordination. Such condition affects daily life to a large extent. Patients diagnosed with ataxia may experience difficulties with speech, swallowing, walking, loss of balance; loss of hand, arm or leg muscle coordination and other. The symptoms might graduate and result in problematic fulfilling of daily tasks (such as putting clothes on, brushing teeth, hygiene, eating and communication). Such medical condition might eventually require wheelchair for patient's mobility and even fulltime assistance.

In general, the cause of developed ataxia vary (stroke, head trauma, infections, brain abnormalities, vitamin deficiencies, multiple sclerosis and other), but an important subgroup are hereditary ataxias. These are divided into autosomal dominant and autosomal recessive ataxias nevertheless, the main features are progressive cerebellar degeneration, peripheral neuropathy, oculomotor apraxia and gait and limb ataxia (for more detailed information see “Hereditary Ataxia Overview - GeneReviews® - NCBI Bookshelf,” accessible here [URL6](#)).

Recently, mutations in *XRCC1* gene, which contribute or directly cause neurodegeneration in humans, were described (Hoch et al., 2017; O’Connor et al., 2018) and are referred to as ataxia oculomotor apraxia XRCC1 (AOA-XRCC1; previously SCAN26 or AOA5).

*XRCC1* mutated on both alleles (heterozygous) was found in a 47-year-old- woman (for simplicity and consistency within this text, this proband is referred to as XD1 patient), who was initially, six years before the mutation was earmarked, examined and diagnosed with cerebellar atrophy, gait and limb ataxia, oculomotor apraxia and peripheral neuropathy. Among ataxic abnormalities, also dysmetria, dysdiadochokinesis, slow fast finger movements, dysarthria and affected proprioception were observed. Early development and cognitive functions were not affected, but at approximately 28 years, difficulties with balance and gait began. Then, around 39 year of age, speech difficulties appeared and later on, also swallowing became problematic.

Brain scan at the age of 40 revealed massive cerebellar atrophy, and by the age of 47, the atrophy progressed (cerebellar vermis and hemispheres affected) (Fig. 13). Her condition accelerated throughout these years into muscle cramps and severe pain, often falls, choking episodes and difficulties with daily tasks (such as eating, standing, putting clothes on, walking, personal hygiene).

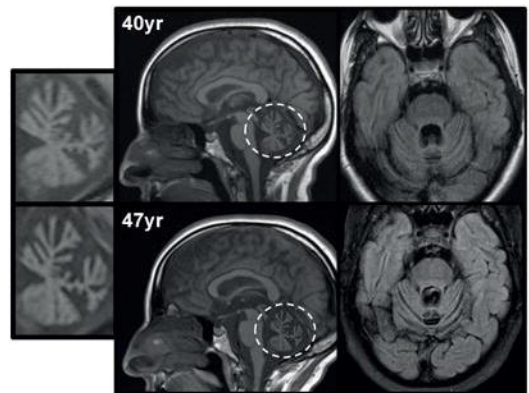


Figure 13: **MRI examination of XD1 patient brain at the age of 40 (top) and 47 (bottom).** Adapted from (Hoch et al., 2017).

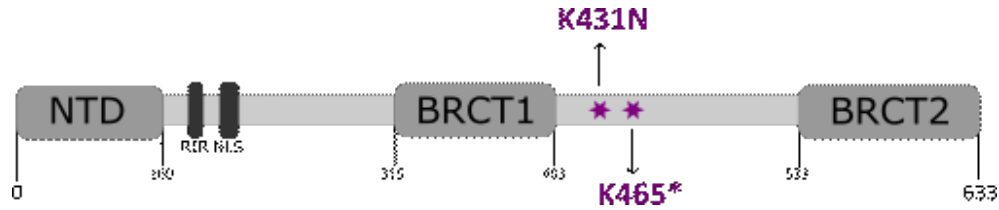


Figure 14: **AOA-XRCC1 patients' mutations in XRCC1.** Patient with biallelic heterozygous mutation (XD1) carry c. 1293G>C (p.K431N) and c. 1393C>T (p.Q465\*) mutations. Patient with biallelic homozygous mutation carry c. 293G>C (p.K431N) and c. 293G>C (p.K431N).

Genetic tests did not reveal any other neurologic disease-caused mutations (tested for spinocerebellar ataxias types 1, 2, 3, 6, 7, 8 and 17, Friedrich a., APTX, SETX and POLG1), only heterozygous mutations of *XRCC1* were identified (Fig. 14): c. 1293G>C (p.K431N) and c. 1393C>T (p.Q465\*). Mutation c. 1293G>C (p.K431N) is within a consensus donor splice site and results in aberrant splicing. Mutation c. 1393C>T (p.Q465\*) causes a premature stop codon. The resulting shortened mRNA is most likely degraded by nonsense mediated mRNA decay (Hoch et al., 2017).

Later, in 2018, O'Connor et al. broaden the AOA-XRCC1 phenotype of two new patients. These two unrelated men carry a biallelic homozygous mutation in *XRCC1* gene, which is identical with XD1 mutation c. 1293G>C (p.K431N). Unlike the previously described heterozygous AOA-XRCC1 patient, both homozygous patients come from consanguineous parents.

Patient 1 (referred to as #424) experienced ataxic gait and recurrent falls by the age of 3. During school years, he developed dysarthria, dysdiadochokinesis and experienced painful cramps. MRI at the age of 15 did not reveal any remarkable changes, but other nerve conduction studies showed sensorimotor neuropathy of axonal type. By the age of 22, the patient experienced recurrent falls, broad-based gait and lacked reflexes in lower limbs. Also, hypometria, nystagmus on lateral gaze and impaired proprioception was shown. The control MRI revealed cerebellar atrophy.

Patient 2 (hereinafter referred to as #428) experienced first signs of ataxic features as an infant. This worsened throughout his childhood and brought muscle cramps, lower limbs stiffness and dysarthria. He was diagnosed with myotonia congenita (myotonic disorder). By the age of 30, his gait was clearly ataxic and developed nystagmus on lateral gaze. Impairment



of lower limb sensation and lack of reflexes was observed. Electromyography revealed sensorimotor axonal neuropathy and MRI showed cerebellar atrophy.

In the first described patient (XD1), it was shown that carrying the heterozygous mutation in scaffold protein gene *XRCC1*, patient-derived fibroblast exposed to oxidative DNA damaging compound show reduced SSBR in response to oxidative stress, reduced *XRCC1* levels and its recruitment to the chromatin (which negatively alters the kinetics of SSBR). This was confirmed in *XRCC1*<sup>-/-</sup> RPE-1 cells, where the phenotype was even stronger.

Further experiments showed reduced levels of *XRCC1*-interacting partner *LIG3α* and the level of *XRCC1* in patient cells to be very low (~5 %). Additionally, conditional knock-out of *Xrcc1* in mice exhibited elevated ADP-ribose in the cerebellum, loss of cerebellar interneurons and ataxia (Hoch et al., 2017). The SSBR capacity, *XRCC1* levels and chromatin recruitment in the patients with homozygous mutation in *XRCC1* was not described yet.

It is not surprising that mutations in most of the SSBR enzymes interacting with the scaffold *XRCC1* protein (namely *PNKP*, *TDP1* and *APTX*) are also connected to neurodegeneration (Fig. 15). Mutations in the *PNKP* enzyme are connected to microcephaly and early onset seizures (MCSZ), Charcot-Marie-Tooth disease (CMT2B2) and, importantly, also to ataxia oculomotor apraxia 4 (AOA4) (Kalasova et al., 2019; Leal et al., 2018; Scholz et al., 2018, respectively). AOA4 share the main SSBR-defective phenotype features with *XRCC1*-mutated individuals, namely the progressive cerebellar atrophy (Fig. 16), gait ataxia, ocular motor apraxia and peripheral neuropathy.

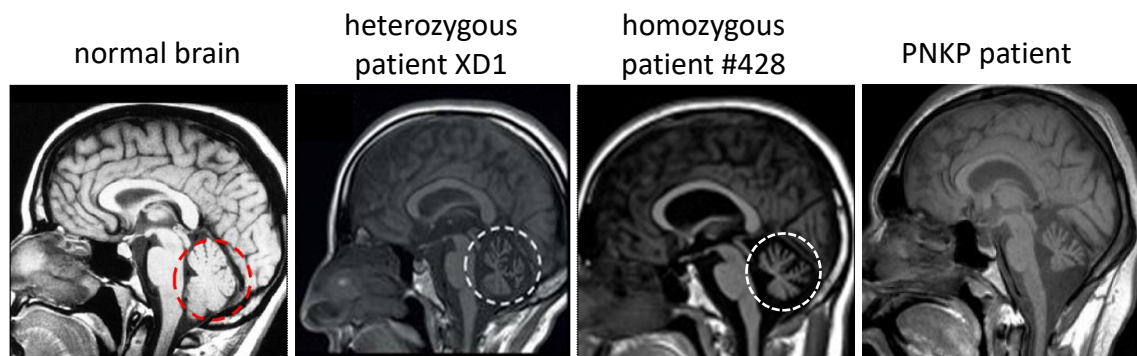


Figure 15: Comparison of brain scans showing cerebellar atrophy (white circles) in *XRCC1*-mutated patients and one *PNKP*-mutated patient. Brain scans of the two *XRCC1*-mutated patients and one *PNKP*-mutated patient in comparison to a healthy individual.

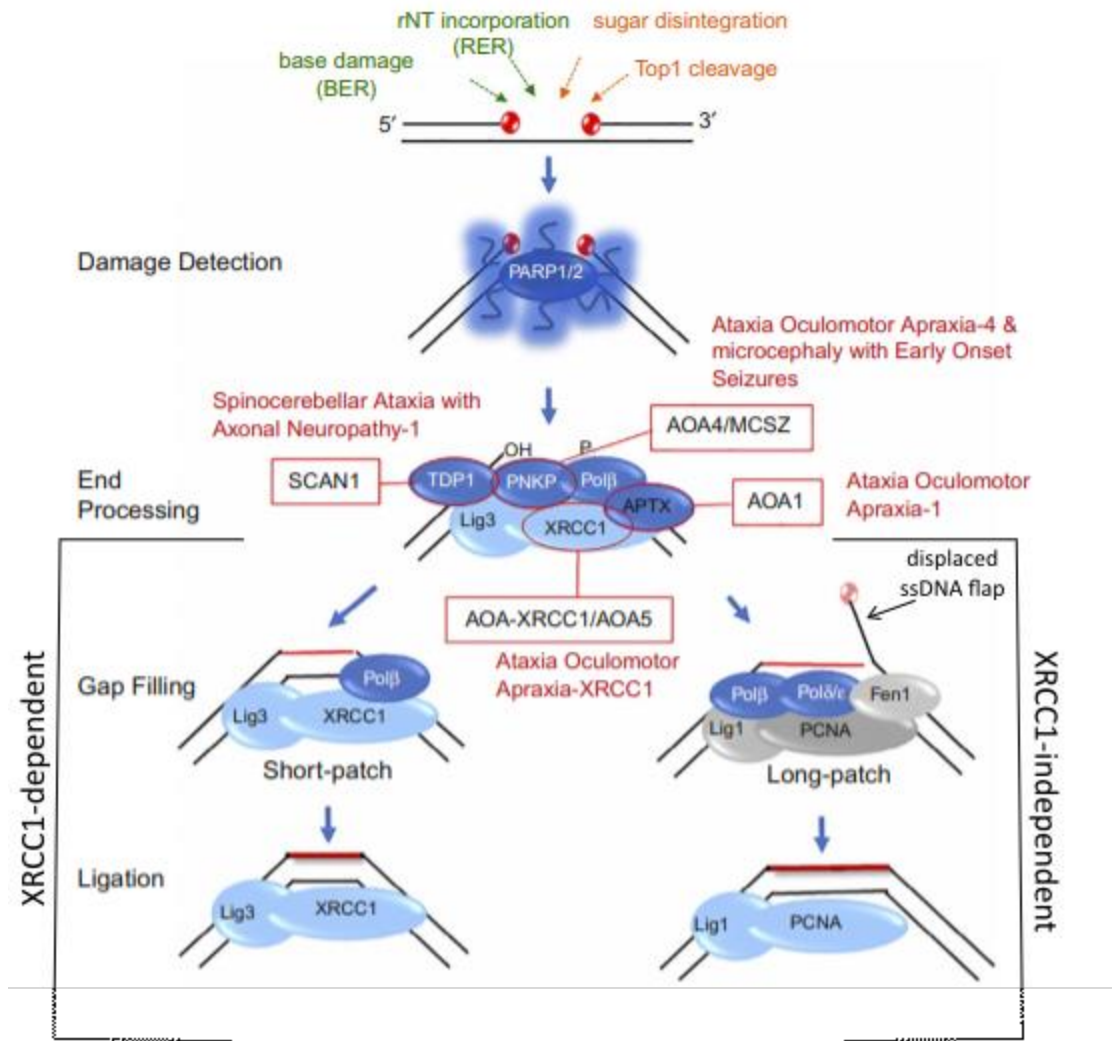


Figure 16: **Single-strand break repair (SSBR), XRCC1 and XRCC1-interacting partners in the context of neurological pathologies.** The sources of SSBs in the DNA followed by main SSBR steps. End-processing enzymes interact with scaffold protein XRCC1 and allow the pathway to proceed via short-patch branch, which is also a part of base excision repair pathway XRCC1 and its interacting proteins linked to neurodegeneration are highlighted in red-outlined ovals with corresponding disease (AOA-XRCC1, AOA1, AOA4, SCAN1) or syndrome (MCSZ) in red rectangles. Other depicted pathway (long-patch, also identical with long-patch BER steps) is XRCC1-independent and involves displacement of ssDNA, which then require enzymes such as PCNA, FEN1. The long-patch branch is utilized for example in RER pathway (Potenski & Klein, 2014). With permission adapted from (Yoon & Caldecott, 2018a).

Similar disease manifestations appear in individuals diagnosed with the hereditary disease ataxia oculomotor apraxia 1 (AOA1) caused by a complete deletion/mutation in the gene which codes aprataxin<sup>3</sup>, the end-processing enzyme which can resolve the 5'-AMP damaged end. Cells

<sup>3</sup>more than 20 different pathogenic mutations of the *APT*X gene were identified as the primary cause of the AOA1 (as stated in the (Yoon & Caldecott, 2018) review)

lacking *APTX* show impaired DDR in response to SSB-causing agents (Hirano et al., 2007; Crimella et al., 2011).

A mutation in *TDP1* was reported as the genetic cause of another hereditary ataxia, the spinocerebellar ataxia with axonal neuropathy 1 (SCAN1) (Takashima et al., 2002). In mice, the *TDP<sup>-/-</sup>* knock-out animals recapitulate SCAN1 clinical features, mainly the progressive cerebellar atrophy. In this study, the mice-derived *TDP<sup>-/-</sup>* neurons were shown to accumulate SSBs (Katyal et al., 2007) due to the impaired SSBR.

Here, I would like to present one more protein. Although it does not interact with XRCC1 protein, mutations in the gene coding RNA/DNA helicase senataxin (*SETX*) represent another genetic cause of hereditary ataxia (ataxia oculomotor apraxia 2, AOA2) (Nanetti et al., 2013). Senataxin helicase can resolve toxic R-loop structures (RNA/DNA hybrids) and its disrupted function can result in AOA2 and, also to another neurodegenerative disease called juvenile amyotrophic lateral sclerosis (ALS4). The AOA2 manifestation involves some of the clinical features as AOA1, mainly cerebellar atrophy and axonal neuropathy, but most of the patients do not show oculomotor apraxia (Nanetti et al., 2013). Additionally, this year (Richard et al., 2020), showed that senataxin is apparently a part of autophagy regulation. In context of the ALS and ataxia disease pathologies, this might be a new interesting direction of the neurodegeneration research.

## 2 Aims of the thesis

The primary aims of this thesis are as follows:

- To measure the amount of residual XRCC1 protein in XRCC1-mutated patient-derived fibroblasts.
- To investigate the level of endogenous ADP-ribose/the DNA single-strand breaks in *XRCC1*-defective cells during the cell cycle.
- To identify the source of the endogenous DNA single-strand breaks in *XRCC1*-defective cells.

### 3 Materials and methods

#### 3.1 Chemicals, antibodies, inhibitors and solutions

<b>Chemical</b>	<b>Abbreviation</b>	<b>Storage</b>	<b>Company [catalog number]</b>
acetone	ac	RT	Lach-ner, s.r.o. [20001-AT0-M10001]
ammonium persulfate	APS	4°C	Fisher Scientific, s.r.o. [A/P470/46]
$\beta$ -mercaptoethanol	-	RT	Sigma-Aldrich, s.r.o. [M3148-100ML]
bromophenol blue	-	RT	Sigma-Aldrich, s.r.o. [B0126]
butanol	but	RT [1:1 but:dH <sub>2</sub> O]	Lach-ner, s.r.o. [20010-CT0-M1000-1]
4',6-diamidino-2-phenylindole dihydrochloride	DAPI	-20°C	Fisher Scientific, s.r.o. [A202710100]
dimethylsulfoxide	DMSO	RT	Serva [20385.02]
distilled water	dH <sub>2</sub> O	RT	Provided by IMG
dithiothreitol	DTT	-20°C	Fisher Scientific, s.r.o. [B172/5]
5-Ethynyl-2'-deoxyuridine	EdU	4°C	Invitrogen [A10044; E10187; E10415]
Ethylenediaminetetraacetic acid	EDTA	RT	Sigma-Aldrich, s.r.o. [EDS-100G]; [E5134-1KG];
formaldehyde	FA	4°C	VWR [5167.1000]
glycerol	-	RT	Lach-ner, s.r.o. [40058-AT0-M1000-1]
glycine	-	RT	Fisher Scientific, s.r.o. [G/0800/600]
L-glutamine	Glut	- 20°C	Gibco [25030024]
Hydrochloric acid 37%	HCl	RT	VWR [20252.290]

4-(2-hydroxyethyl)-1-piperazineethanesulfonic acid	HEPES	4°C	Fisher Scientific, s.r.o. [BP310-500]
Lipofectamine RNAiMAX	RNAiMAX	4°C	Thermo Fisher Scientific [13778150]
methanol	met	RT	VWR [20847.318]
penicillin/streptomycin	P/S	-20°C	Gibco [15140122]
Polysorbate 20	Tween-20	RT	Sigma-Aldrich, s.r.o. [P1379]
Ponceau S	-	RT	Sigma-Aldrich, s.r.o. [141194]
Sodium dodecyl sulphate	SDS	RT	Sigma-Aldrich, s.r.o. [L3771]
Tetramethylethylenediamine	TEMED	4°C	Sigma-Aldrich, s.r.o. [T9281]
2-amino-2-(hydroxymethyl)propane-1,3-diol hydrochloride	Tris	RT, solutions of Tris max 2 weeks on RT/4°C	Fisher BioReagents [BP152-1]
RNase-free water	RNase-free dH <sub>2</sub> O	4°C	Dharmacon [B-003000-WB-100]
Vectashield antifading mounting medium	vectashield	4°C	Vector Laboratories [H-1000]
Triton X-100	Triton-X	RT	Sigma-Aldrich, s.r.o. [X100-1L]
trypsin	T/E (1:1 trypsin:EDTA)	-20°C	Sigma-Aldrich, s.r.o.

Primary antibody (animal)	Used abbreviation	Method	Company [catalog number]	Storage
Poly(ADP-ribose) polymerase 1 (mouse)	PARP1 ab	WB	Serotec [MCA1522G]	4°C
Poly(ADP-ribose) polymerase 1 (mouse)	PARP1 ab	IF	Santa Cruz [sc-8007]	4°C
X-ray repair cross complementing protein 1 (rabbit)	XRCC1 ab	IF	Novus Biologicals [NBP1-87154]	-20°C

X-ray repair cross complementing protein 1 (rabbit)	XRCC1 ab	WB	Millipore [ABC738]	-20°C
pan-ADP-ribose (mono + poly ADPR) (rabbit)	PAN ab	IF	Millipore [MABE1016]	
poly-ADP-ribose binding reagent (rabbit)	PAR ab	IF	Trevigen [4336-BPC-100]	
$\alpha$ -tubulin (mouse)	$\alpha$ -tubulin ab	WB	Santa Cruz [sc-23948]	4°C
<b>Secondary antibody</b>				
Alexa Fluor 488 (goat anti rabbit)	-	IF	Invitrogen [A11011]	-20°C
Alexa Fluor 568 (goat anti rabbit)	GAR 568	IF	Life Technologies [A11011]	4°C
Goat anti mouse IgG HRP	GAM	WB	BioRad [170-6516]	4°C
Goat anti rabbit IgG HRP	GAR	WB	BioRad [170-6516]	4°C
<b>Protein ladders</b>				
PageRuler™ Prestained Protein Ladder 10-180 kDa	marker	WB	Thermo Scientific [26616]	-20°C

<b>Inhibitor</b>	<b>Abbreviation</b>	<b>Storage</b>	<b>Company [cat. n.]</b>
Poly(ADP-ribose) glycohydrolase inhibitor	PARGi	Stock solution 10 mM in DMSO, -80°C	Sigma-Aldrich, s.r.o. [SML1781-25MG]
Proteasome inhibitor MG132	MG132	-20°C	Selleckhem [S2619]
Topoisomerase inhibitor camptothecin	CPT	-20°C	Sigma-Aldrich, s.r.o. [C9911]

<b>Solution</b>	<b>Compounds (company)</b>	<b>Abbreviation</b>	<b>Storage</b>
CSK lysis buffer	<ul style="list-style-type: none"> <li>• 10 Mm PIPES</li> <li>• 100 Mm NaCl</li> <li>• 300 mM sucrose</li> <li>• 3 Mm MgCl<sub>2</sub></li> <li>• +0,7% (v/v) Trit-X-100</li> </ul>	CSK	-4
Dumbecco's Modified Eagle Medium	Sigma-Aldrich, s.r.o. [D6429-500ML]	DMEM	-4
fetal bovine serum	Gibco [10270]	FBS	-20°C
Minimum Essential Medium Eagle, no glutamine	Gibco [21090002]	MEM	-4
Opti-MEM Reduced Serum Medium	Gibco [11058-021]	Opti-MEM	
Phosphate-buffered saline	NaH <sub>2</sub> PO <sub>4</sub> × 12 H <sub>2</sub> O, KH <sub>2</sub> PO <sub>4</sub> (or Na <sub>2</sub> HPO <sub>4</sub> × 2 H <sub>2</sub> O) + dH <sub>2</sub> O Gibco [10010031] or provided by IMG	PBS	-4
running buffer 10x	<ul style="list-style-type: none"> <li>• 30,3 g Tris</li> <li>• 144 g Glycine</li> <li>• 10 g SDS</li> <li>• 1 l ddH<sub>2</sub>O</li> </ul>	-	RT
SDS sample buffer	<ul style="list-style-type: none"> <li>• 2.0 ml 1M Tris-HCl pH 6.8</li> <li>• 0.8 g SDS</li> <li>• 4.0 ml 100% glycerol</li> <li>• 0.4 ml 14.7 M β-mercaptoethanol</li> <li>• 1.0 ml 0.5 M EDTA</li> <li>• 8 mg bromophenol Blue</li> </ul>	SB	-20°C
transfer buffer 10x	<ul style="list-style-type: none"> <li>• 30,3 g Tris</li> <li>• 144 g Glycin</li> <li>• 1 l ddH<sub>2</sub>O</li> </ul>	-	RT



### 3.2 Commercial molecular biology assay kits

Kit	Company	Method
Pierce™ BCA Assay Kit	Thermo Fisher Scientific, cat. no. 23227	Protein quantification
Click-iT® RNA Alexa Fluor™ 488 Imaging Kit	Invitrogen, cat. no. C10329	EdU direct immunostaining
Amersham ECL Prime Western Blotting Detection Reagent	GE Healthcare Life Sciences, cat.no. RPN2232	Western blotting

### 3.3 Cell lines, vectors and siRNA

All cells were tested for mycoplasma and the result was negative.

Cell line	Cell type	Description	Source
1BR3	Human primary skin fibroblasts	Control fibroblasts obtained with permission from a healthy individual. For simplicity, in text depicted as 1BR.	Kindly provided by Keith Caldecott's laboratory (Genome Damage and Stability Centre at the University of Sussex, UK)
XD1	<i>XRCC1</i> -mutated fibroblasts	Patient-derived fibroblasts with heterozygous mutation in <i>XRCC1</i>	
#428	<i>XRCC1</i> -mutated fibroblasts	Patient-derived fibroblasts with homozygous mutation in <i>XRCC1</i>	
U2OS	Human bone osteosarcoma cells	Control human cells from ATCC®.	(U-2 OS ATCC® HTB-96™).
<i>XRCC1</i> <sup>-/-</sup> U2OS	CRISPR-Cas9 gene edited human bone osteosarcoma cells	<i>XRCC1</i> -deleted U2OS cells.	(Polo et al., 2019a)

Crispr-Cas9 edited U2OS cell lines	Expression constructs
<i>XRCC1</i> <sup>-/-</sup> U2OS	-
U2OS EV	pCD2E-empty vector
U2OS M3#9	pCD2E-XRCC1-His(WT)
U2OS M165#14	pCD2E-XRCC1-His <sup>R335A/K369A</sup>
U2OS M73#2	pCD2E-XRCC1-His <sup>S518A/T519A/T523A</sup>

All Crispr-Cas9 edited *XRCC1*<sup>-/-</sup> U2OS clones were obtained from Keith Caldecott's laboratory (Genome Damage and Stability Centre at the University of Sussex, UK) and prepared by Marek Adamowicz as following (unpublished):

*XRCC1*<sup>-/-</sup> U2OS cells (Polo et al., 2019a) stably complemented with the XRCC1 expression constructs: pCD2E-XRCC1-His(WT); pCD2E-XRCC1-His<sup>S518A/T519A/T523A</sup>; pCD2E-XRCC1-His<sup>R335A/K369A</sup> were generated by co-transfection of the indicated constructs or empty vector (pCD2E) with a plasmid encoding resistance to puromycin (pCI-puro). Stably transfected cells were selected with puromycin (2µg/ml) and, after one week, single colonies were isolated, amplified, and verified by western blotting and immunofluorescence.

Control non-targeting siRNA and siXRCC1 were purchased from Dharmacon (ON-TARGETplus Non-targeting Control Pool, catalog number D-001810-10; ON-TARGETplus Human XRCC1 siRNA, catalog number L-009394-00-0005). Concentrations were used as described in manufacturer's protocol.

### 3.4 Cell culture, cryopreservation and storage

1BR3 (normal human skin fibroblasts, abbr. 1BR), derived from a skin biopsy of a normal adult doner, and XRCC1-patients' fibroblasts were kindly provided by Keith Caldecott's laboratory (Genome Damage and Stability Centre at the University of Sussex, UK) and cultured under stable conditions in Modified Eagle's Medium (MEM) supplemented with 15% (v/v) fetal bovine serum (FBS), 1% (v/v) L-glutamin and 1% (v/v) antibiotics penicillin/streptomycin (P/S).

U2OS (human osteosarcoma cells) obtained from ATCC® (U-2 OS ATCC® HTB-96™). *XRCC1*<sup>-/-</sup> U2OS and CRISPR-Cas9 gene-edited *XRCC1*<sup>-/-</sup> U2OS obtained from Keith Caldecott's laboratory (Genome Damage and Stability Centre at the University of Sussex, UK).

All U2OS cells were cultured under stable conditions (5% O<sub>2</sub>, 5% CO<sub>2</sub>, 37°C) in Dulbecco's Modified Eagle's Medium (DMEM) supplemented with 10% (v/v) FBS and 1% (v/v) antibiotics P/S.

Aliquoted cells were stored at -180°C in liquid nitrogen. Aliquots were prepared as following. Cells in flask (80-90% confluence) were trypsinized and then centrifuged (Centrifuge 5702, Eppendorf) at 1400 rpm for 3,5 minutes. Pellet was resuspended in cryomedium (fibroblasts: FBS with 10% v/v DMSO (Serva); U2OS: DMEM complete with 10% DMSO), placed to plastic eppendorf tubes and then slowly cooled to -80°C. After one day, tubes were placed to liquid nitrogen tanks.

For using stored cells, aliquots were thawed, and tubes' content was quickly transferred to test-tubes with suitable medium, then centrifuged (Centrifuge 5702, Eppendorf) at 1400 rpm for 3,5 minutes. Pellets were then carefully resuspended in suitable medium and placed into a flask.

### 3.5 RNA interference

Knock-down of XRCC1 protein was performed via reverse siRNA transfection using non-targeting siRNA SMARTPOOL and siXRCC1 SMARTpool (Dharmacon; D-001810-10 and L-009394-00-0005, respectively). Cells were seeded from 80% cell confluent 75 mm flask to glass coverslips in 6well plate. Then transfected with siRNA using Lipofectamine RNAiMAX Reagent (ThermoFisher Scientific; catalog number 13778-150) following the manufacturer's protocol and cultured in antibiotics (ATB)-free MEM for 1 day under stable conditions (5 % O<sub>2</sub>, 5 % CO<sub>2</sub>, 37°C). The ATB-free MEM was then changed for MEM<sup>c</sup> and cells were cultured 2 more days. Together, cells were assayed 72 hours after transfection, usually reaching 80-90% confluence on coverslips.

### 3.6 Preparation of cell lysates, protein concentration quantification

Cells were washed in PBS, lysed with 95°C sample buffer (SB) and scraped from the plate well (applied volume depending on well size and cell confluence percentage). Lysate was boiled for 10 minutes at 95°C and then 3x sonicated for 30 seconds with 30 seconds pauses (Bioruptor Sonicator System, version 2.1.).

Protein concentration in cell lysates was measured via BCA assay, using Pierce™ BCA Assay Kit (ThermoFisher Scientific; catalog number 23227) protocol provided by manufacturer. The lysates were loaded onto SDS-PAGE (30 µg protein/well).

### 3.7 SDS-PAGE, Western blotting, immunostaining and protein detection

Polyacrylamide (PAM) gel electrophoresis (PAGE) was run under stable conditions (constant current 25 mA per gel with maximum voltage 120 V). In 1 mm gels, PAM concentration was 10 %. As a marker for protein size determination PageRuler™ Prestained Protein Ladder (catalog number 26616, Thermo Scientific) was used.

Protein transfer to Nitrocellulose Blotting Membrane (Amersham™Protran™ 0.45 µm NC; catalog number 10600002) was run under stable conditions for 90 minutes (constant current 400 mA, maximum voltage 150 V) in 1x transfer buffer prepared from 10x solution (see 3.1 section Solutions). The loading and transfer precision was then checked by control staining as following. Membrane was placed into a suitable plastic box and incubated for one minute with Ponceau S, then one time washed with ddH<sub>2</sub>O and dried. As a proof of successful protein transfer and equally loaded amounts lysate, Ponceau S bound to the proteins was observed. Illustrative example of Ponceau S stained membrane (Fig. 17).

Membrane was then washed in PBS+Tween 20 to remove the control staining and blocked in 10% milk for at least 30 minutes. PBS-Tween 20 washing followed and finally, membrane was incubated with primary antibodies (diluted in 5% milk) for one hour (at room temperature on low speed See-saw rocker SSL4 (stuart®)). After the first antibody incubation, membrane was washed three times in PBS+Tween 20 and then incubated with secondary

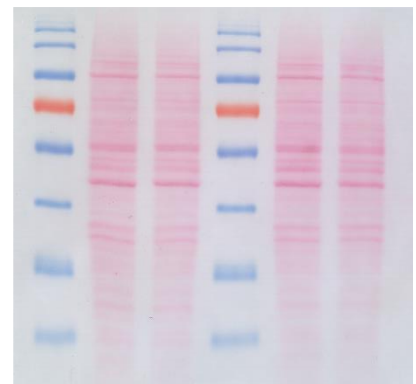


Figure 17: **Illustrative picture of protein detection on a membrane.** Stained with Ponceau S for protein detection.

antibodies (diluted in 5% milk) for an hour. Again, three times washing in PBS+Tween-20 followed.

For protein detection, the membrane was carefully dried and ECL™ Western Blotting Detection Reagents 1+2 (GE Healthcare, cat. n. RPN2209) kit was used as prescribed in manufacturer's protocol. Placed in cassette, a film was exposed to the membrane and after specific time period (chosen by practical experience with specific cell type, antibodies and other attributes), the film was developed using automated X-ray film processor machine OPTIMAX 2010 (PROTEC GmbH & Co. KG).

### 3.8 Cell pre-extraction and fixation

For measuring chromatin retention of proteins, pre-extraction was performed prior to fixation as follows: Cells on coverslips in 24well plastic plate were washed with 500 µl/well PBS. Then pre-extracted with 300 µl/well pre-extraction buffer for 2 minutes on ice (See-Saw rocker, 11 osc/min). For fibroblasts, pre-extraction buffer: cold 0,2% Triton™ X-100 (cat. n. X100-1L) was used. For U2OS cells, CSK pre-extraction buffer (see 3.1 section Solutions) was used.

For fixation, pre-extraction buffer was removed and replaced with 300 µl/well formaldehyde (FA) (VWR™; cat. n. 5167.1000) for 10 minutes at RT (See-Saw rocker, 11 osc/min). After fixation, cells were washed with 400 µl/well PBS and then stored in 4°C in 0,1 % azide solution in PBS (500 µl/well) for one day.

### 3.9 Immunofluorescence

Fixed cells on coverslips were permeabilized with 300 µl/well cold methanol:acetone (1:1) for 10 minutes at RT (See-Saw rocker (11 osc/min)), then 2x washed with 500 µl/well PBS and blocked for 30 minutes in 400 µl/well 10% FBS on RT. Following rising in PBS, coverslips were incubated with 80 µl/coverslip primary antibody solution for one hour at RT.

After this, cells were washed 3x with 200 µl/coverslip PBS and incubated with 80 µl/coverslip secondary antibody solution for one hour at RT. Finally, cells were washed 3x with 200 µl/coverslip PBS, nuclei were stained with DAPI (1 µg/ml in water, 2 min; Acros, cat. n. 202710100) solution 80 µl/coverslip for 2 minutes and coverslips were then mounted using antifade mounting medium (VECTASHIELD®, Vector Laboratories, SKU: H-1000-10).

To preserve poly(ADP-ribose) modification as a marker of single-strand breaks in DNA, cells were treated with 10  $\mu\text{M}$  PARGi for one hour prior to lyse (for detailed reasoning see chapter 1.2.3 Regulation of poly-ADP-ribosylation). Cell lysates and cells on coverslips were processed regularly, as described before (see previous chapter).

For studying endogenous single-strand breaks in the nucleic DNA: inhibition of PARG allows retaining of the PARylation at the site of SSBs, therefore, PAR-specific antibody may bound and specific secondary antibody with fluorescent dye can be used. Visual result is then observed on ScanR microscope and further analysis can reveal the intensity of fluorescence in the nucleus of the cell. Intensity of fluorescence represents the level of PARylation (molecular mechanism simplified in Fig. 15).

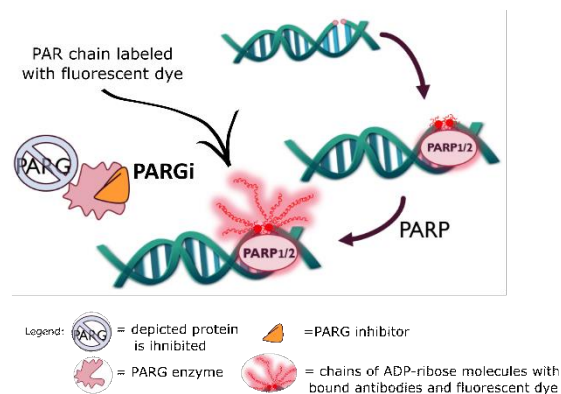


Figure 18: Schematic model of visualization of SSBs via PARG inhibition. Legend is depicted in the picture.

### 3.10 Click-iT EdU Proliferation Assay

Proliferation assay (EdU labelling) was performed using Click-iT™ EdU Cell Proliferation Kit for Imaging protocol and Alexa Fluor™ 488 dye (ThermoFisher, catalog number C10337). After cell fixation, coverslips with cells were placed on parafilm and washed with 200  $\mu\text{l}$ /coverslip PBS, then replaced upside down onto a drop (19  $\mu\text{l}$ /coverslip) of Click-iT® reaction cocktails for 30 minutes. After the treatment, cells were washed 3 times with 200  $\mu\text{l}$ /coverslip PBS.

Click-iT™ EdU Cell Proliferation Kit for Imaging protocol was adjusted in reaction cocktail component Alexa Fluor™ 488 dye as following. Original volume: 1,5  $\mu\text{l}$ /coverslip, adjusted volume: 1,8  $\mu\text{l}$ /coverslip.

### 3.11 Microscopy and Scan-R cell analysis system

Light microscopy (Primovert microscope, Zeiss) was used for live observation and fluorescent microscopy (Eclipse E400 Microscope, Nikon) was used for observation of fixed cells.

Imaging of fixed material was carried out on the automatic high-content screening platform Olympus scanR 3.1., OLYMPUS. High-resolution pictures were acquired by automated wide-field image acquisition using Olympus ScanR high-content screening station equipped with a motorized stage and UPLSAPO 40x/0.95 DRY CORR; FWD 0.18 (CG 0.11 – 0.2) objective and sCMOS camera Hammamatsu ORCA-Flash4.0 V2 – 6,5  $\mu\text{m}$  pixel. From each sample, 225 images were taken with the average cell number per position  $\sim 2$  in case of patient-derived cells, and  $\sim 4$  for U2OS and *XRCCI*<sup>-/-</sup>U2OS cell lines.

Using dot blots, histograms and gating settings nuclei were identified and counted (Fig. 19). Then, cells were gated according to the amount of DNA in the nucleus and EdU incorporation (Total intensity DAPI and Total intensity A488, respectively) (Figure 20).

Quantification was done by ScanR Analysis Software. At least 500 or 1000 nuclei per sample were counted per condition<sup>4</sup>. Data from ScanR analysis were processed in Microsoft Excel and PRIMUS. In graphs, data are represented as mean  $\pm$  SEM.

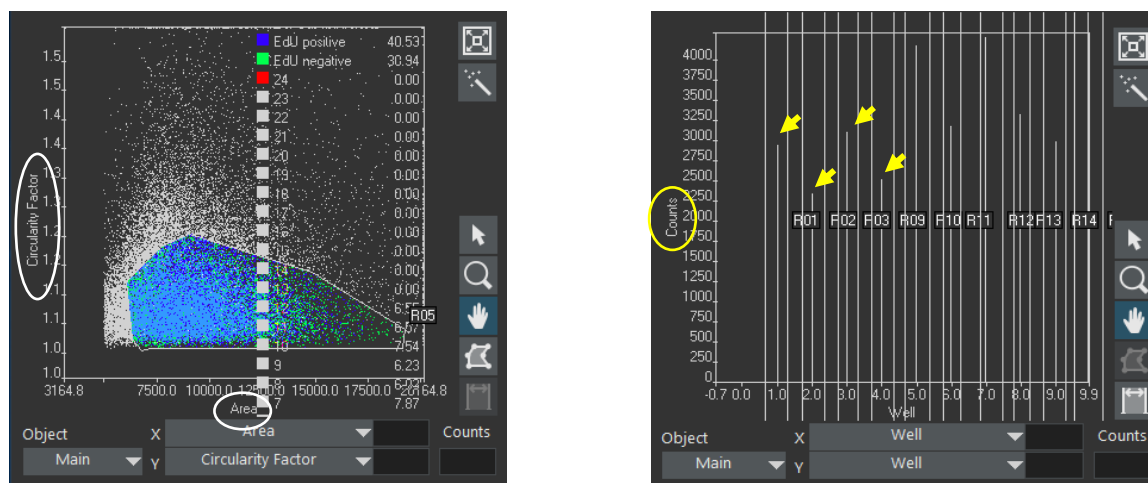


Figure 19: **Illustrative picture of ScanR analysis software environment.** Dot blot with detected objects depicted as dots, based on cell nucleus attributes highlighted in white ellipses) (left), histogram with cell numbers per analysed sample (right).

<sup>4</sup> unless otherwise stated in graph description

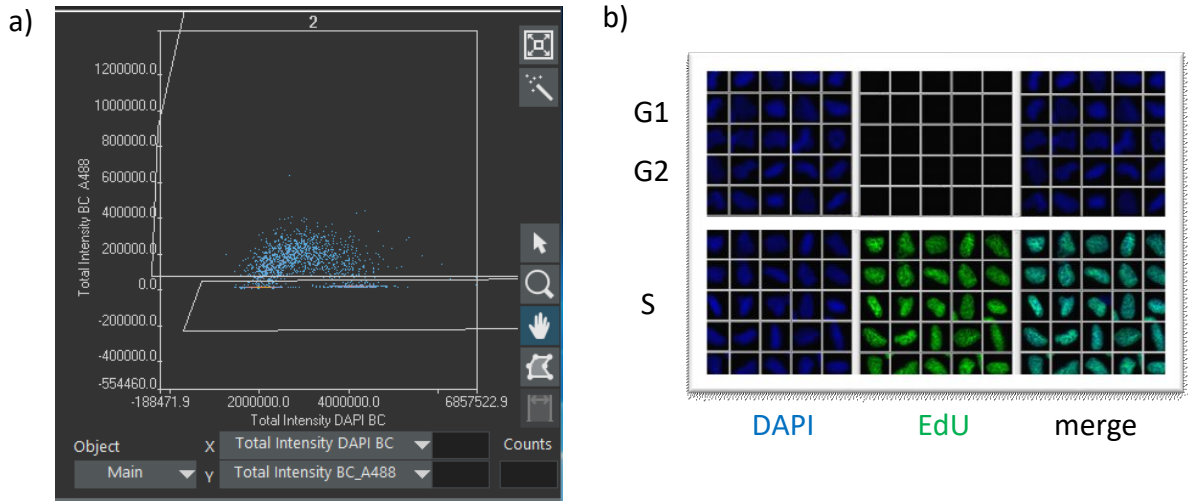


Figure 20: **Illustrative picture of ScanR analysis software environment (a) and representative images of gated cells (b).** Objects depicted as dots, gating based on the amount of DNA in the nucleus (Total Intensity DAPI BC) and EdU incorporation (Total Intensity BC 488) (a). Representative images of 25 randomly selected cells from a sample, gated according to EdU labelling

### 3.12 Data analysis and statistics

Experimental data were analysed using ScanR analysis software (described in previous chapter), and Microsoft Excel programme. Number of experimental repeats are indicated in figures' legends. In case of single experiment data, minimum number of cells in samples are also indicated in figures' legends. In charts with multiple experimental repeats, standard error of the mean (SEM) was calculated as following:

$$SEM = \frac{SD}{\sqrt{n}} \quad SD = \sqrt{\frac{\sum(y_i - y_{mean})^2}{n-1}}$$

n=sample size; SEM=standard error of the mean; SD= standard deviation;  $y_i$ =value;  $y_{mean}$ =average value

Statistical tests were conducted using Prism and MatLab programme. Relevant statistical methods are also indicated in figures' legends, either F- test for determination of variance and suitable *t*- test (for the comparison of two independent samples) or a combination of one-way ANOVA test followed by Tukey's range test.

Quantification of protein amounts in blots was conducted after a film was developed and scanned via in Image J Lite software.



### 3.13 Graphic

Pictures and schemes without a source citation were drawn in Inkscape and Microsoft PowerPoint. Figures adapted from various authors were edited in Inkscape.

## 4 Results

Defects in a critical single-strand break repair protein XRCC1 have been associated with ocular motor apraxia, axonal neuropathy and progressive cerebellar ataxia demonstrating that this protein is neuroprotective in humans (Hoch et al., 2017; O'Connor et al., 2018)

To investigate the nature of the endogenous DNA lesions that trigger such neurodegeneration in humans, I have employed primary fibroblasts derived from different *XRCC1*-mutated patients harbouring the biallelic heterozygous mutations K431N and Q465\* (denoted here as XD1) or homozygous mutations K431N (denoted here as #428) (for detailed description see chapter 1.3.1.) and from one unaffected individual (denoted here as 1BR). As an additional control, I also used U2OS cell lines in which *XRCC1* was inactivated by CRISPR/Cas9 gene editing (denoted here as *XRCC1*<sup>-/-</sup>) (Polo et al., 2019a). I describe XRCC1 protein levels in those cells, and I focus on ADP-ribosylation in response to endogenous and exogenous stress and the origin of endogenous DNA single-strand breaks.

### 4.1 Reduced XRCC1 protein levels in *XRCC1*-mutated patient fibroblasts

First of all, in order to estimate the levels of XRCC1 protein in patient-derived fibroblasts (XD1 and #428). Western blotting of total cell lysates, using control primary human fibroblasts from an unaffected individual (1BR) as a positive control, was performed. This experiment showed that both XD1 and #428 cells have greatly reduced levels of XRCC1 protein, as detected by anti-XRCC1 antibody, but still possess some small residual amount when compared to 1BR control cells (Fig. 21, left). To confirm the specificity of anti-XRCC1 antibody, I also examined U2OS cells in which *XRCC1* was inactivated by CRISPR/Cas9 gene editing. As expected, the *XRCC1*<sup>-/-</sup> U2OS cells lacked detectable levels of XRCC1 protein (Fig. 21, right).



**Figure 21: XRCC1 protein levels in *XRCC1*-defective cells.** XRCC1 protein levels in lysates of the indicated *XRCC1*-mutated patient-derived fibroblasts (left) and wild type (WT) and *XRCC1*<sup>-/-</sup> U2OS cells (right) were measured by Western blotting. Ponceau S or α-tubulin were used as a loading control.

Further quantification of blot revealed approximate percentage of the residual XRCC1 in XD1 patient-derived fibroblasts to be ~ 5-10 % as that of the 1BR control (as measured by an imaging software Image J Lite and is consistent with the previous data (Hoch et al., 2017). Such residual amount of XRCC1 protein in the cell lysate is a consequence of XD1 patient's mutations, which alters splicing efficiency of *XRCC1* (p. K431N) or results in truncated protein (p. Q465\*).

As predicted, due to biallelic homozygous mutation K431N in #428 patient-derived cells, the level of XRCC1 in the cell lysate was notably higher than in XD1 patient and was ~ 15-20 % of that of the 1BR control (Fig. 21, left).

#### 4.2 ADP-ribosylation in *XRCC1*-mutated patient fibroblasts is detected primarily during S phase

It was previously described that *XRCC1*-defective cells show reduced ability to repair SSBs and are sensitive to DNA damaging reagent such as alkylating agents, camptothecin (CPT), hydrogen peroxide (H<sub>2</sub>O<sub>2</sub>) or to ionizing radiation (summarized in Caldecott, 2019)

Endogenous DNA single-strand breaks can originate from products of abortive TOP1 activity, intermediates during the BER pathway, oxidative stress and/or replicative errors and are rapidly detected by PARP enzymes. Activated PARPs enable labelling of SSBs with the chains of ADP-ribose molecules that are subsequently removed by PARG hydrolase. This process is very fast and transient and direct immunofluorescence staining of ADP-ribosylation at the site of SSB is technically impracticable. To circumvent this problem, I use PARG inhibitor (PARGi) to inhibit the ADP-ribose removal process which allows capturing of ADP-ribose molecules at the site of endogenous DNA damage.

Considering the nature of neurons, which are negatively affected by *XRCC1* mutations, in further experiments I performed a proliferation assay using Click-iT™ EdU Cell Proliferation Kit for Imaging (for more detailed information see 3.10) to distinguish the ADP-ribosylation in EdU positive cell populations (cells in S phase) from EdU negative cell populations (cells in G1 or G2 phases).

I examined ADP-ribose levels in the chromatin of *XRCC1*-mutated patient-derived fibroblasts in response to one hour of PARGi treatment, using 1BR cells as a negative control. After one hour of incubation with PARGi under standard cultivation conditions, both the XD1

and #428 patient cells divulged a significantly increased level of ADP-ribose in the EdU positive cell population (Fig. 22). Surprisingly, in the EdU negative population after one hour of PARGi treatment, only the XD1 cells mean ADP-ribose level was slightly increased, whereas, in the #428 cells, the mean ADP-ribose level remained as low as in the 1BR control cells (Fig. 22).

In contrast, in the case of the U2OS cells in which *XRCC1* was deleted (*XRCC1*<sup>-/-</sup>) (see section 3.3. Cell lines, vectors and siRNA), one hour of PARGi treatment resulted in an increased ADP-ribose chromatin levels in both the EdU negative and the EdU positive cell populations (Fig. 23). The increase in ADP-ribosylation in the *XRCC1*<sup>-/-</sup> cells after one hour of PARGi treatment was about double that of the wild type U2OS (WT) after the same treatment (Fig. 23).

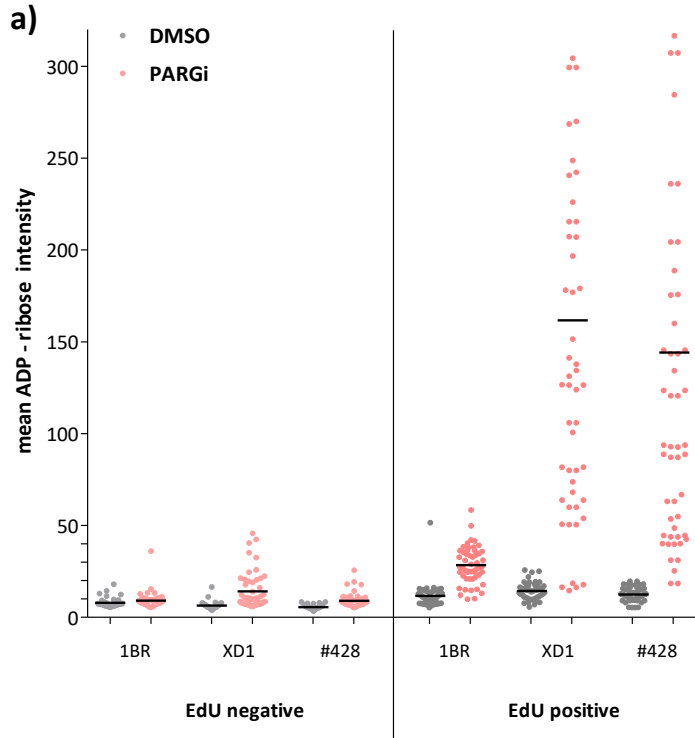
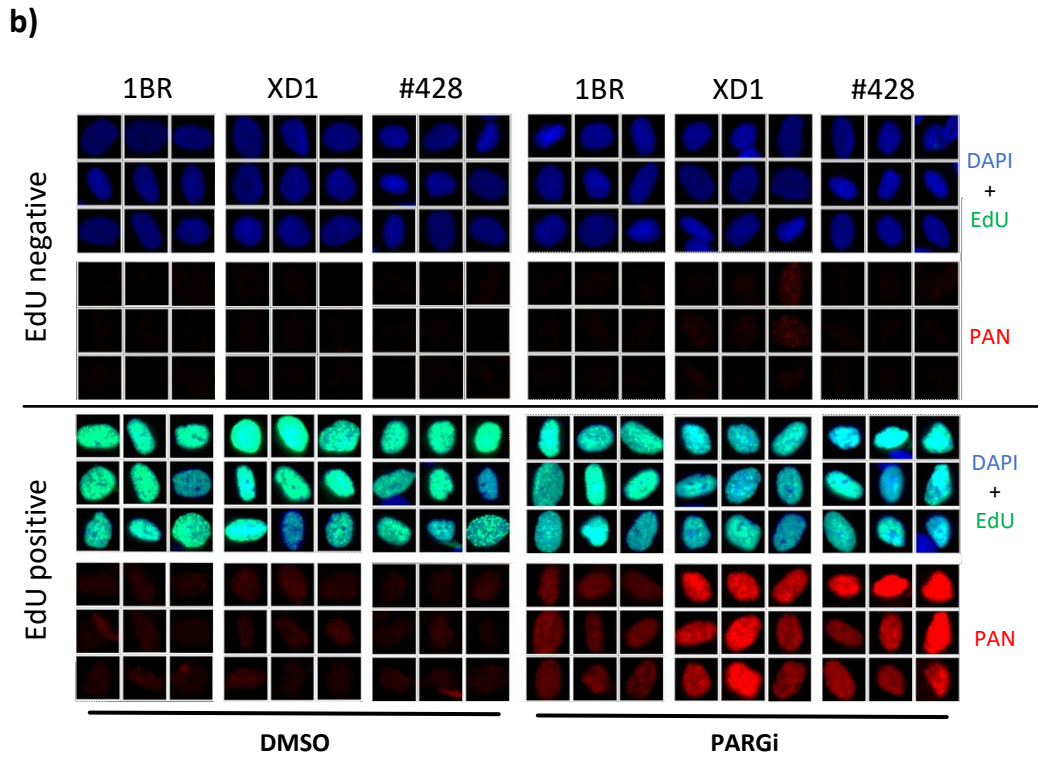
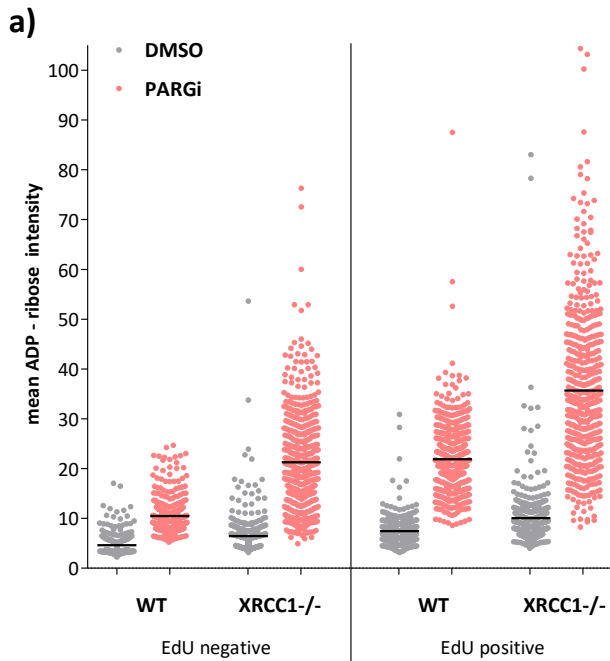
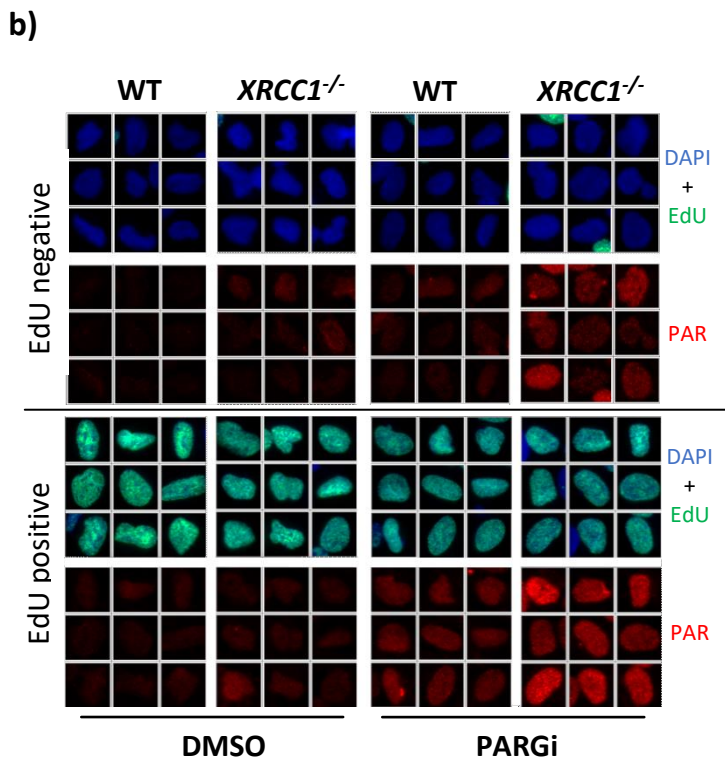


Figure 22: **ADP-ribose levels after one hour of 10  $\mu$ M PARGi exposure in *XRCC1*-defective cells.** 1BR wild type human primary fibroblasts were used as the negative control for XD1 and #428 patient-derived fibroblasts. EdU negative and EdU positive cell populations were gated according to EdU incorporation (based on ScanR analysis). Values and means are based on ScanR and GraphPad PRISM analysis. Quantification (a) and representative images (b) are shown. 7 data points are outside the axis limits; n=1





**Figure 23: ADP-ribose levels after one hour of 10  $\mu$ M PARGi exposure in *XRCC1*<sup>-/-</sup> U2OS cells.** U2OS wild type cells were used as the negative control for *XRCC1*<sup>-/-</sup> U2OS cells. EdU negative and EdU positive cell populations were gated according to EdU incorporation (based on ScanR analysis). Values and means are based on ScanR and GraphPad PRISM analysis. Quantification (a) and representative images (b) are shown. n=1



#### 4.2.1 The level of ADP-ribosylation in G1/G2 cells correlates with the amount of the remaining XRCC1 protein

To further reduce the remaining levels of XRCC1 protein in *XRCC1*-mutated patient-derived fibroblasts, I performed siRNA knock-down of XRCC1 and evaluated the successful siRNA interference by Western blotting (Fig. 24).

Quantification of blots by Image J Lite software confirmed at least ~50% decrease in XRCC1 levels upon siXRCC1 treatment in the 1BR control cells. The XRCC1 level in all samples was normalized to siNT treated control human primary fibroblasts (1BR).

The amount of XRCC1 in XD1 and #428 patient-derived cells treated with siNT (~10 % and ~20%, respectively) confirmed previously measured low XRCC1 levels (Fig. 24). In patient-derived fibroblast, already low levels of the protein were successfully reduced further to 1-3 % (Fig. 24).

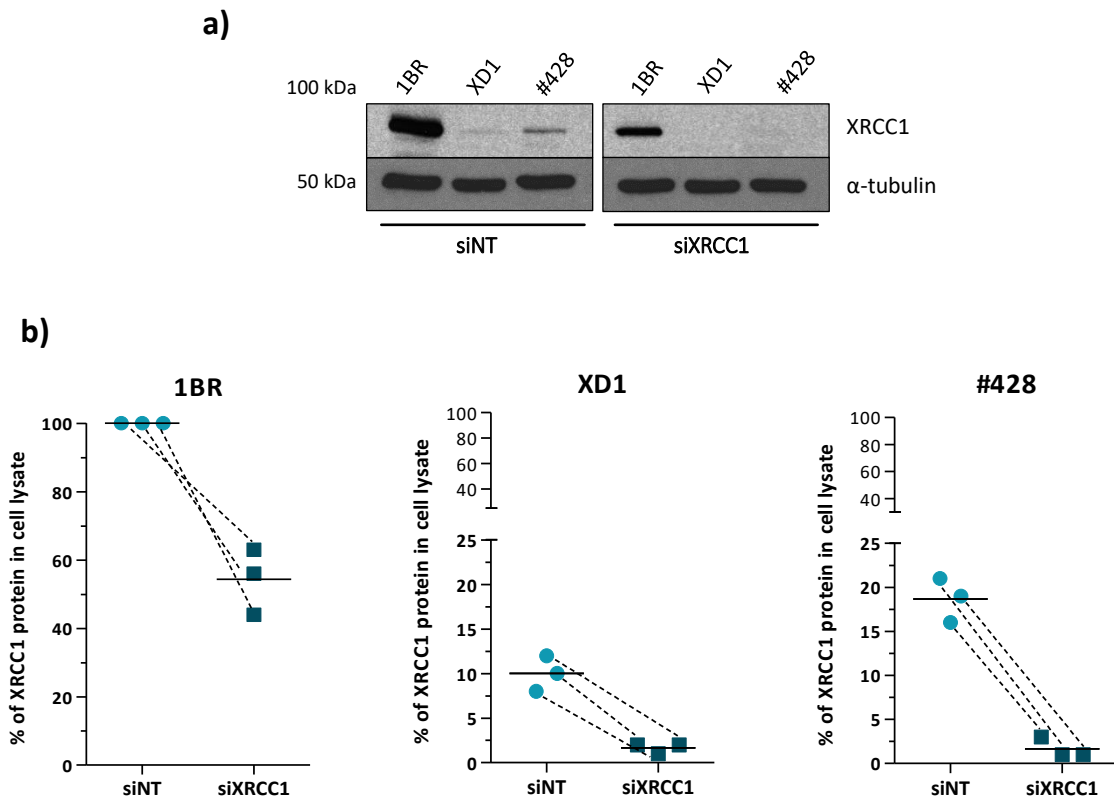


Figure 24: **XRCC1 protein level in *XRCC1*-mutated patient-derived fibroblasts after siRNA knock-down.** Cells treated with siNT and siXRCC1. Human primary fibroblast from an unaffected individual (1BR) were used as control. Blots stained for XRCC1 protein (**a**) and quantification of blots (**b**) are shown. XRCC1-mutated patient-derived fibroblasts and 1BR control cells before (siNT; light blue dots) and after XRCC1 knock-down (siXRCC1; dark blue squares). 3 independent experiments were quantified using Image J Lite imaging software. Amount of the protein in siRNA non-treated control cells was normalized to 100 %.

The patient-derived fibroblasts exposed to siXRCC1 basically stop to proliferate. Due to this toxicity of siXRCC1 treatment (as revealed by performed EdU labelling (for detailed information see chapter 3.10), and with respect to AOA-XRCC1 phenotype where mainly neurons (non-proliferating cells) are affected, I decided to further focus on G1/G2 cell populations (populations were gated based on the EdU incorporation as previously described).

Firstly, I decided to treat the *XRCC1*-mutated cells of the XD1 and #428 patients, in which XRCC1 was depleted via siRNA interference, with camptothecin (CPT) as a control evaluation experiment. CPT is a known topoisomerase I (TOP1) inhibitor and induction of DNA damage by CPT activates PARP1 (as was shown by Caldecott's research group (Hoch et al., 2017), therefore, enables the recruitment of XRCC1 to the damage site (M. Li et al., 2013; Polo et al., 2019b).

In the control cells, TOP1-cc were repaired by SSBR pathway using XRCC1 protein. In the XD1 patient's cells, treated with CPT for one hour, the mean ADP-ribose levels significantly increased in both siNT and siXRCC1 treated XD1 cells, compared to siNT treated and siXRCC1 treated 1BR control cells, respectively (Fig. 25). Interestingly, in the siNT treated #428 patient fibroblasts exposed for one hour to CPT treatment, there was no significant increase in mean ADP-ribose levels, compared to the siNT 1BR control cells (Fig. 25).

On the other hand, depletion of XRCC1 protein in these (#428 patient-derived) cells via siRNA interference resulted in an elevated ADP-ribosylation after one hour of CPT treatment (Fig. 25). This confirms that stable ternary complex of CPT, DNA and TOP1 in cells with defective SSBR results in an elevated ADP-ribosylation.

Successful knock-down of XRCC1 protein in both XD1 and patient-derived fibroblasts led to more than doubled mean ADP-ribose levels compared to that of siNT treated XD1 and #428 cells, respectively (Fig. 25). Noteworthy, the ADP-ribose level in XRCC1 depleted #428 cells<sup>5</sup> was increased to the extent of that of the siNT treated XD1 cells (where the amount of XRCC1 is about 10 % of that of 1BR control cells).

---

<sup>5</sup> where the XRCC1 protein level was reduced to less than 50 % of that of siNT #428 cells



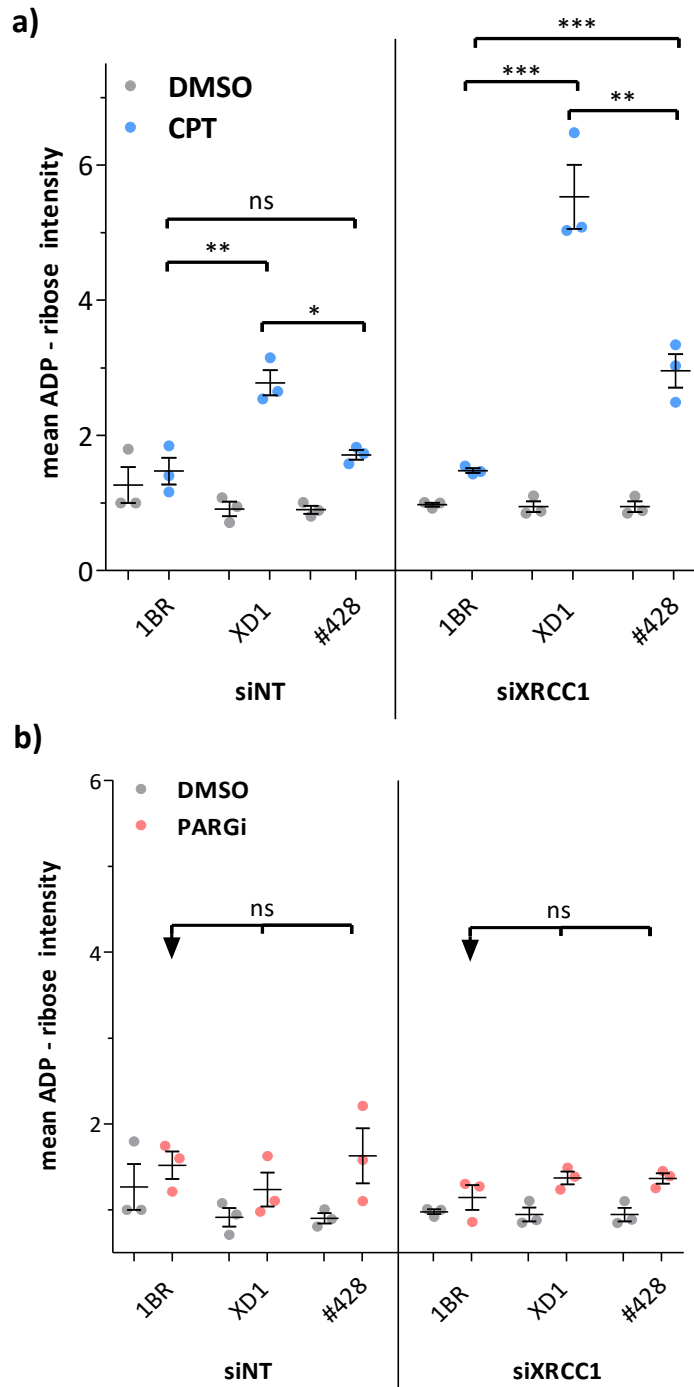
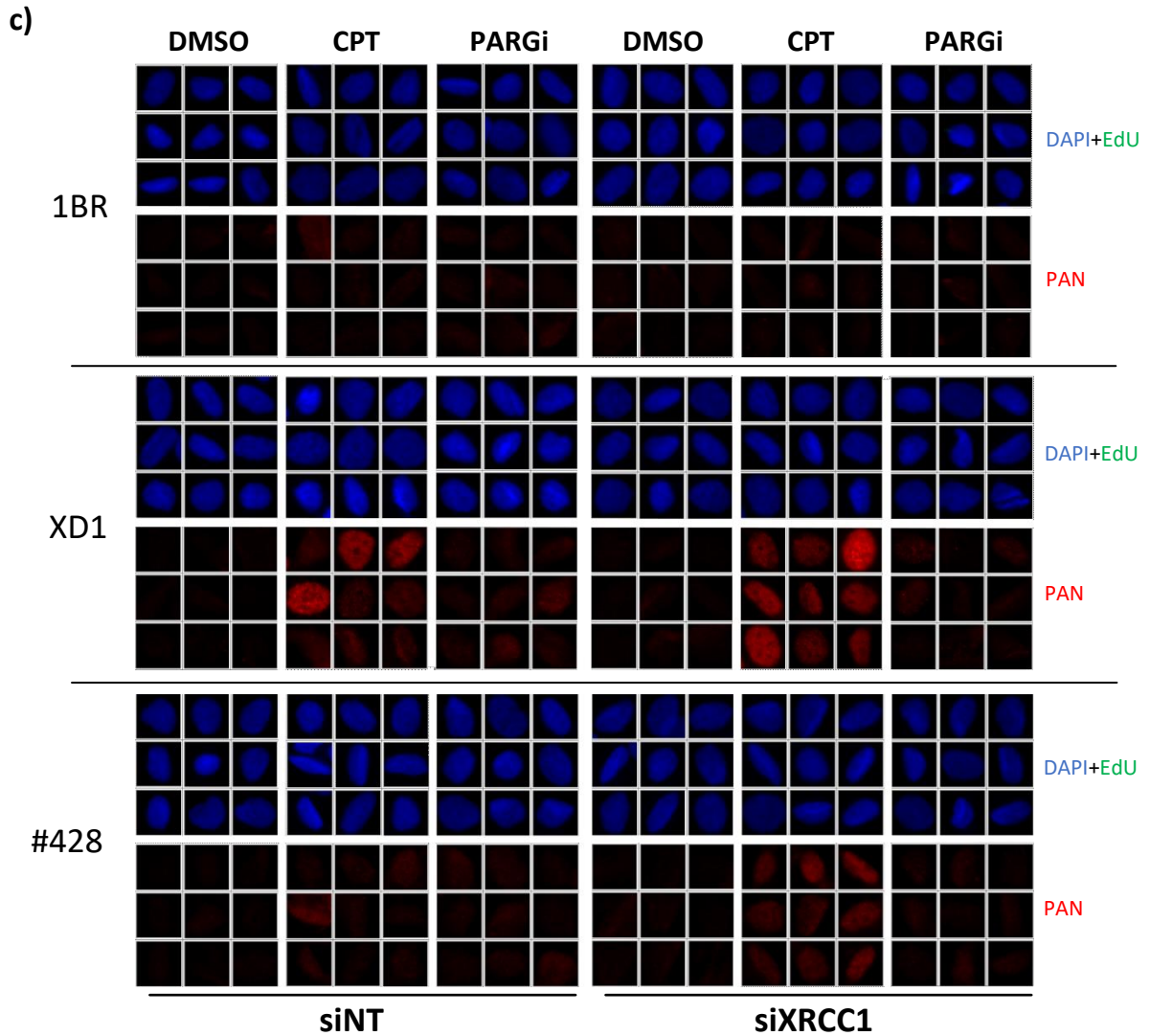


Figure 25: ADP-ribose levels after one hour of 10  $\mu$ M CPT (a) or 10  $\mu$ M PARGi (b) exposure in EdU negative *XRCC1*-defective cells with (siXRCC1) or without (siNT) depleted *XRCC1*. 1BR wild type human primary fibroblasts were used as the negative control for XD1 and #428 patient-derived fibroblasts. Negative control samples for siXRCC1 treated cells (right panel) were treated with siNT (left panel). EdU negative cells were gated according to EdU incorporation (based on ScanR analysis). Values and means are based on ScanR and GraphPad PRISM analysis. Quantification (a, b) and representative ScanR images (c) are shown. n=3. ns =  $P > 0.05$ , \* =  $P \leq 0.05$ , \*\* =  $P \leq 0.01$ , \*\*\* =  $P \leq 0.001$ .



Simultaneously with the one hour of CPT exposure experiments described in the previous paragraphs, I performed one hour of PARGi exposure experiments to reveal the endogenous ADP-ribose levels in context of XRCC1-defective cells.

After one hour of PARGi treatment in both XD1 and #428 patient cells, independently of the siRNA transfection (Fig. 25), I generally observed lower than average mean ADP-ribose levels (Fig. 25, Y axis scale) compared to one hour of CPT treatment (Fig. 25, Y axis scale). Also, surprisingly, successful XRCC1 knock-down did not lead to a significant increase in ADP-ribose levels in either patients' fibroblasts compared to siNT treated patients' cells (Fig. 25).

To confirm whether CPT-induced increase in ADP-ribose levels is dependent on the amount of the XRCC1 protein, the ADP-ribose level after one hour of CPT treatment was also measured in *XRCC1*<sup>-/-</sup> U2OS cells, in which XRCC1 was deleted as previously described. I also performed EdU labelling using Click-iT™ EdU Cell Proliferation Kit for Imaging to distinguish the EdU positive (S phase) and EdU negative (G1/G2 phase) cell populations.

After one hour of CPT treatment, the mean ADP-ribose levels in these cells was significantly increased (~ 2.6-fold in EdU negative populations) compared to U2OS wild type control cells (Fig. 26).

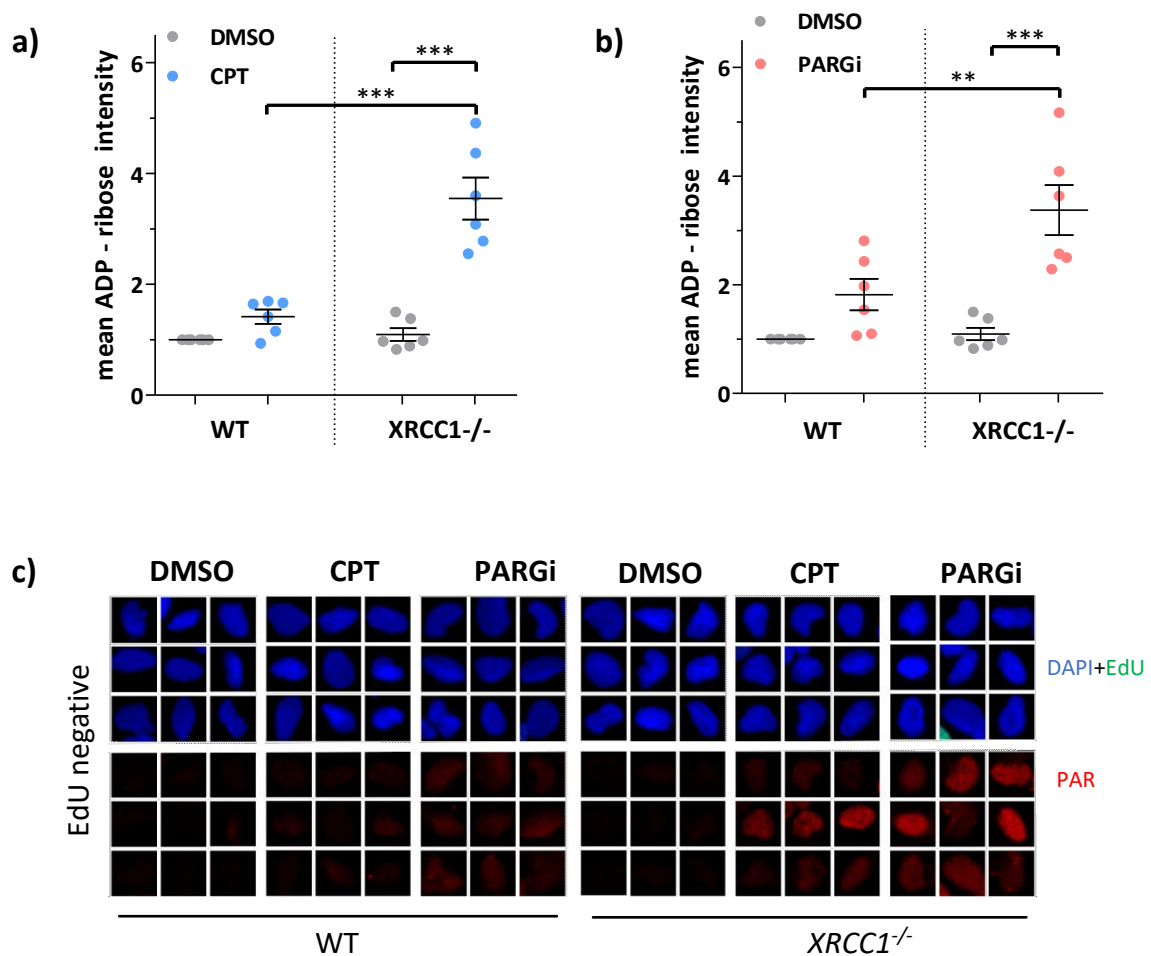


Figure 26: ADP-ribose levels after one hour of 10  $\mu$ M CPT (left graph) or 10  $\mu$ M PARGi (right graph) exposure in EdU negative *XRCC1*<sup>-/-</sup> U2OS cells. U2OS wild type cells were used as the negative control for *XRCC1*<sup>-/-</sup> U2OS cells. EdU negative cell populations were gated according to EdU incorporation (based on ScanR analysis). Values and means are based on ScanR and GraphPad PRISM analysis. Quantification (a, b) and representative ScanR images (c) are shown. n=6. \*\*=  $P \leq 0.01$ , \*\*\* =  $P \leq 0.001$ .

This confirms that XRCC1 protein is important for the repair of stalled TOP1-cc-induced SSBs in G1/G2 phase. Unlike in the patients' cells, in EdU negative population of *XRCC1*<sup>-/-</sup> U2OS, one hour of PARGi treatment led to an elevated endogenous ADP-ribosylation (~1.8-fold) (Fig. 26).

Considering the effectivity of siRNA interference in the patient-derived fibroblasts, we would expect elevated endogenous ADP-ribose levels in the G1/G2 cell cycle phase, as it is with CRISPR/Cas9 *XRCC1*-deleted cells. It is probable that the remaining, although extremely reduced, level of the XRCC1 protein in siXRCC1 treated patients' cells is still enough for the regulation of endogenous DNA damage repair in the G1/G2 cell cycle phases.

### 4.3 Abortive human DNA topoisomerase I activity is not responsible for elevated endogenous ADP-ribosylation in *XRCC1*-deleted cells

Since endogenous SSBs in DNA may arise from various sources and I observed elevated endogenous ADP-ribosylation during G1/G2 only in *XRCC1*-deleted U2OS cells, I decided to test potential sources of endogenous DNA damage *XRCC1*<sup>-/-</sup> cells. Firstly, considering previous data, which show that XRCC1 is involved in the repair of stalled TOP1-cc, I performed following experiments.

As was previously mentioned, formation of TOP1-cleavage complex (TOP1-cc) under standard conditions activates the ubiquitin-26S proteasome pathway, which leads to a partial cleavage of TOP1. Then, hydrolysis of the phosphodiester bond between 3' end of DNA and TOP1 enables ADP-ribosylation of the remaining peptide (at the site of TOP1-induced DNA single-strand break) by PARP enzymes. Chains of ADP-ribose molecules then serve as a DNA damage label, which ensures recognition of such breaks and, therefore, activation of the SSBR pathways (Pommier et al., 2006). Obviously, as was shown in Figure 25, cells in G1/G2 phases expressing XRCC1 are able to deal with SSBs induced by CPT.

I decided to test, whether the active ubiquitin-26S proteasome pathway is the mechanism co-operating with XRCC1-dependent repair pathway, utilized in cells for the repair of CPT-induced SSBs, using a proteasome inhibitor MG132.

MG132 inhibits the degradation of TOP1 and thus block the cleavage by TDP1. In MG132 inhibitor treated cells, TOP1 is not ubiquitinated and, therefore, is not degraded by the

proteasome. Uncleaved stalled TOP1-cc disables exposure of the DNA nick and its recognition by the PARP enzymes. Such single-strand breaks in DNA cannot be recognized, and as a consequence, the DNA is not ADP-ribose labelled. Basically, since there is no PARylation which would recruit XRCC1, the SSB remains and cannot be repaired via XRCC1 (Desai et al., 2001).

Firstly, I performed a rescue experiment with the previously described TOP1 inhibitor camptothecin (CPT) and the proteasome inhibitor MG132. I treated *XRCC1*<sup>-/-</sup> U2OS cells with CPT for one hour, with or without addition of MG132, using wild type U2OS (WT) as a negative control. To avoid false results, I ensured that the solvent DMSO or MG132 inhibitor does not affect the cells via two control samples (DMSO only for one hour and MG132 only for one hour (light grey, dark grey, respectively; Fig. 27). Again, in the following experiment, I performed EdU labelling as previously described and I gated the G1/G2 and the S phase cell populations. Here, I show the G1/G2 as well as the S phase cell populations (denoted as EdU positive), because the cell cycle proliferation was not affected<sup>6</sup>.

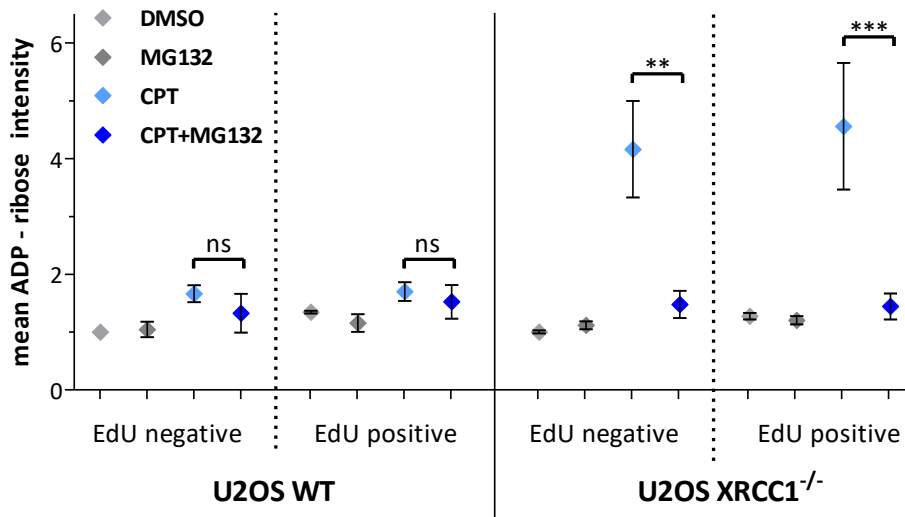
As expected (and consistent with the previous results), following one hour of CPT treatment without MG132, EdU negative *XRCC1*<sup>-/-</sup> U2OS cells show increased ADP-ribose levels compared to EdU negative CPT treated U2OS WT control cells (Fig. 27). Exposure of *XRCC1*<sup>-/-</sup>U2OS cells to CPT and MG132 for one hour at the same time led to a significant decrease in ADP-ribose levels in those cells (Fig. 27). MG132 completely reversed the subsequent activation of SSB pathway by CPT inhibition of TOP1 in G1/G2 population as well as in S phase cell population (Fig. 27).

Proteasome and XRCC1 seem to be necessary for the repair of SSB at the site of CPT-inhibited Top1-cc. Therefore, to investigate whether high endogenous ADP-ribosylation in *XRCC1*-deleted cells is caused by TOP1 activity, I treated *XRCC1*<sup>-/-</sup> U2OS cells with PARGi for one hour with (red; Fig. 27) or without (pink; Fig. 27) addition of MG132, using U2OS wild type (U2OS WT) as a negative control. Once again, in the following experiment, I performed EdU labelling as previously described and EdU positive and EdU negative cell populations were gated.

---

<sup>6</sup> based on ScanR analysis, where the numbers of EdU positive cells per sample was not affected by any of the used treatment

a)



b)

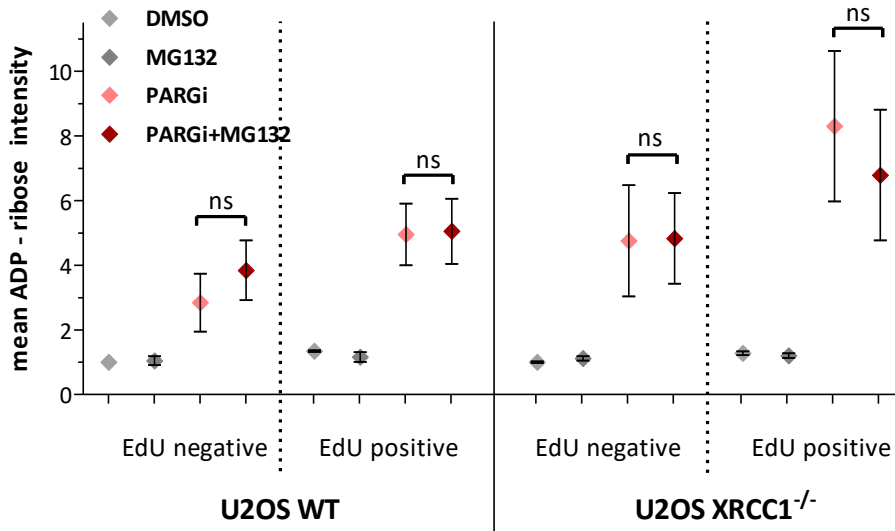
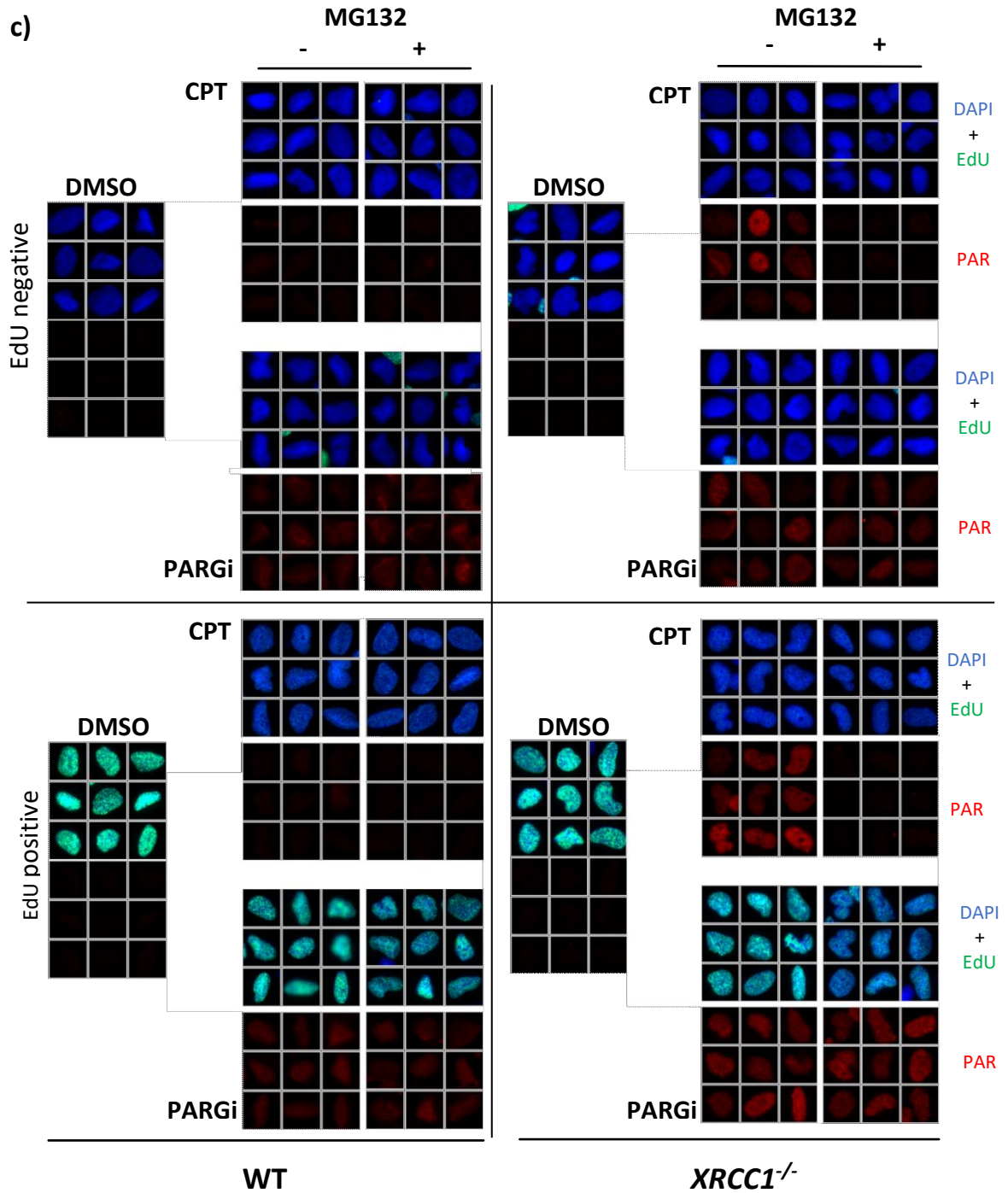


Figure 27: ADP-ribose levels after one hour of 10  $\mu$ M CPT (a) or 10  $\mu$ M PARGi (b) treatment with (dark blue/dark red) or without (light blue/pink) addition of 10  $\mu$ M MG132 proteasome inhibitor in *XRCC1*<sup>-/-</sup> U2OS cells. U2OS wild type cells were used as a control. DMSO (10  $\mu$ M) and MG132 (10  $\mu$ M) treated samples were used as a negative treatment control. EdU negative (left in each panel) and EdU positive (right in each panel) were gated according to EdU incorporation (based on ScanR analysis). Values and means are based on ScanR and GraphPad PRISM analysis. Quantification (a, b) and representative ScanR images (c) are shown. n=3. ns = P>0.05, \*\* = P<0.01, \*\*\* = P<0.001.



Thus, I visualized only endogenous SSBs using PARG inhibitor. Compared to DMSO and MG132 only controls, I observed elevated ADP-ribosylation in the S phase cell populations of U2OS WT and in the S phase populations of *XRCC1*<sup>-/-</sup> U2OS as well (S phase depicted as EdU

positive in Fig. 27). This is an expected result, considering the S phase cellular processes (e.g. replication stress and formation of Okazaki fragments).

In the G1/G2 phase cell populations (in charts depicted as EdU negative) after one hour of PARGi treatment, ADP-ribose level significantly increased in *XRCC1*<sup>-/-</sup> U2OS, compared to PARGi treated U2OS WT control (significance confirmed by one-way ANOVA and Tukey's comparison test in PRISM software, for simplicity of relevant charts not shown) (Fig. 27, pink rhombuses). Addition of MG132 inhibitor although, had no effect on the PARylation of the endogenous SSB lesions in either WT U2OS WT or *XRCC1*<sup>-/-</sup> U2OS (Fig. 27, red rhombuses in each panel), which suggest that the source of the endogenous SSB lesions is presumable some other DNA damaging agent. Although there is many options such as oxidation, alkylation and other, many DNA-damage causing agents result in SSBs repaired via SSBR which utilize the PNKP end-processing enzyme.

#### 4.4 XRCC1 interaction with PNKP is not essential for SSBR of endogenous BER-induced lesions in *XRCC1*-mutated U2OS cells

To investigate whether the endogenous ADP-ribosylation in the nucleus is caused by BER-induced or oxidative stress-induced SSBs, I decided to examine selected CRISPR/Cas9 gene edited *XRCC1*<sup>-/-</sup>U2OS cell lines (for detailed description see Material and Methods). In the following experiments, the following cell lines were used (Table 1).

Table 1: U2OS cell lines with genetic and function description.

Cell type	Cell line	Plasmid	Denoted as	Disrupted function
U2OS	wild type	-	WT	-
	<i>XRCC1</i> <sup>-/-</sup>	pCD2E-XH	KO <sup>XRCC1 WT</sup>	-
	<i>XRCC1</i> <sup>-/-</sup>	-	KO	scaffolding
	<i>XRCC1</i> <sup>-/-</sup>	pCD2E-empty vector	KO <sup>EV</sup>	scaffolding
	<i>XRCC1</i> <sup>-/-</sup>	pCD2E-XH <sup>R335A, K369A</sup>	KO <sup>XRCC1 RK</sup>	PAR/PARP1 binding
	<i>XRCC1</i> <sup>-/-</sup>	pCD2E-XH <sup>S518A, T519A, T523A</sup>	KO <sup>XRCC1 PNKP mut</sup>	PNKP binding



As *XRCC1*<sup>-/-</sup> transfected with an empty vector pCD2E show non-measurable amounts of the XRCC1 protein in the cell lysates (Fig. 28, confirmed by immunofluorescence assay Fig. 29), in the following experiments, KO<sup>EV</sup> serves as a control. As a negative control, I used wild type U2OS (WT) and *XRCC1*<sup>-/-</sup> U2OS complemented with full length human XRCC1<sup>WT</sup> (for the protocol description see Materials and Methods).

The U2OS KO<sup>XRCC1 RK</sup> cells encode the full length human XRCC1 protein mutated in the highly conserved BRCT1 domain, which binds to poly(ADP-ribose) (PAR). Such affinity to PAR enables the SSB recognition by XRCC1 protein and promotes its function (Breslin et al., 2015a). Disruption of such affinity causes a delay in SSB kinetics of H<sub>2</sub>O<sub>2</sub>-induced SSBs (Hoch et al., 2017), which mimics the physiological oxidative stress in cells.

In the KO<sup>XRCC1 PNKP mut</sup> cells encoding the full length human XRCC1-His protein, the high-affinity PNKP binding site is mutated at S518A, T519A and T523A. PNKP is one of the important enzymes in the SSB pathway of BER pathway-induced SSBs. After Western blotting and immunostaining the gel for XRCC1 protein, I observed slightly thicker band in all three U2OS cell lines expressing *XRCC1* (KO<sup>XRCC1 WT</sup>, KO<sup>XRCC1 RK</sup>, KO<sup>XRCC1 PNKP mut</sup>), compared to the U2OS WT (the amount of input cell lysate was corrected based the relevant loading control) (Fig. 28).

The overexpression of XRCC1 in those cells was confirmed by immunofluorescence and ScanR analysis (Fig. 29), but the level of XRCC1 protein did not differ throughout the cell cycle phases in any of measured cell lines (based on ScanR analysis; Fig. 29).

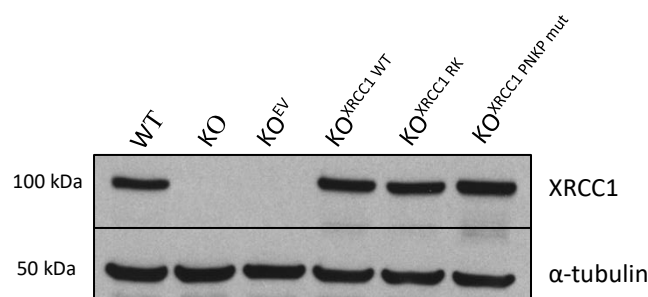
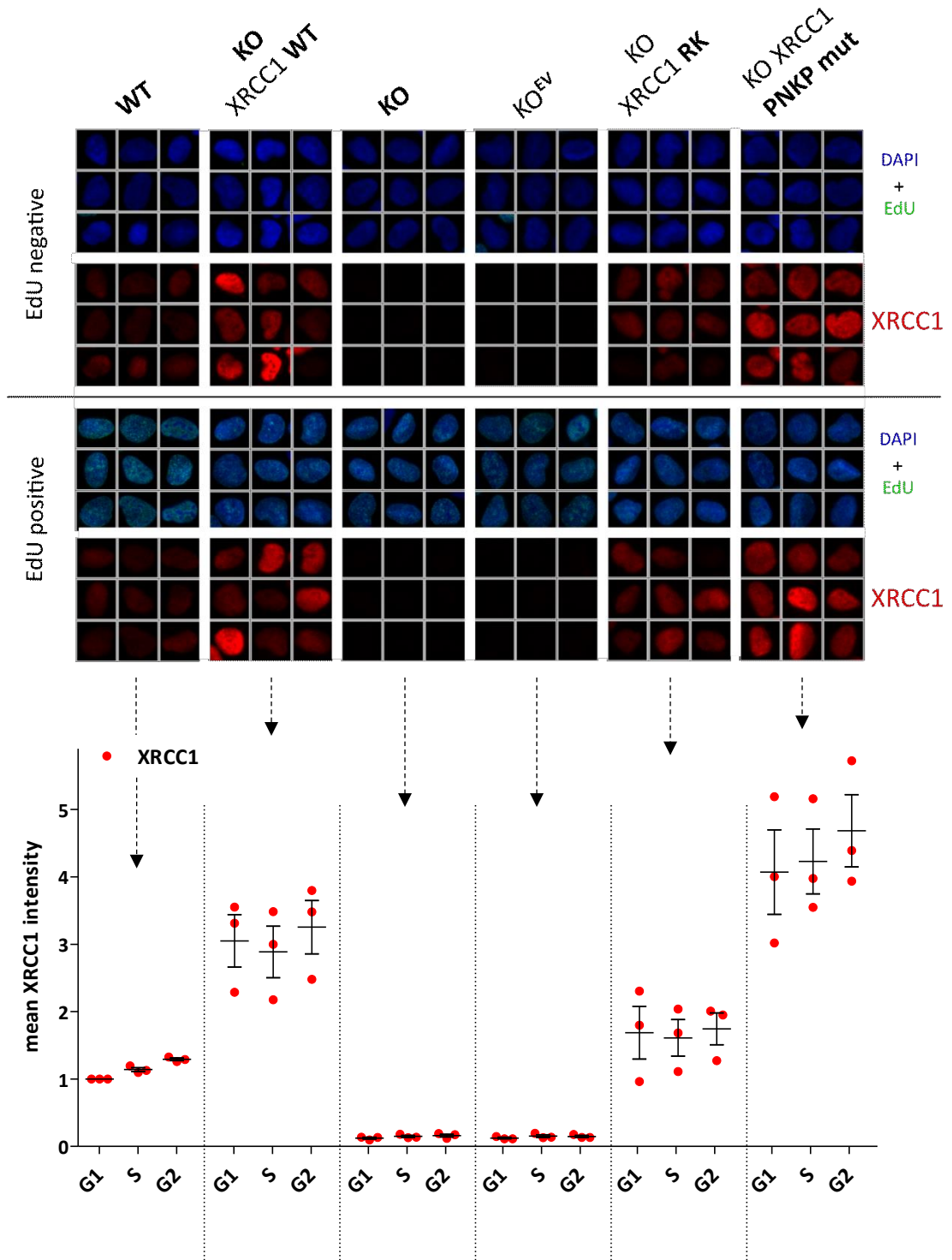


Figure 28: Amount of XRCC1 protein in U2OS wild type (WT) and CRISPR/Cas9 gene edited *XRCC1*<sup>-/-</sup> U2OS cell lines encoding different variants of XRCC1. *XRCC1*<sup>-/-</sup> U2OS depicted as “KO”. *XRCC1*<sup>-/-</sup> U2OS transfected with empty vector depicted as “EV”. Expressed protein variants denoted as “XRCC1 WT”, “XRCC1 RK” and “XRCC1 PNKP mut” (for more detailed description see Table 1).



**Figure 29: XRCC1 levels in selected U2OS cell lines (bottom) with representative images from ScanR (top).** Levels of the XRCC1 protein in the *XRCC1*-mutated U2OS cell lines. U2OS wild type (WT) as a positive control. *XRCC1*<sup>-/-</sup> U2OS depicted as “KO”. *XRCC1*<sup>-/-</sup> U2OS transfected with empty vector depicted as “KO<sup>EV</sup>”. Expressed protein variants denoted as “XRCC1 WT”, “XRCC1 RK” and “XRCC1 PNKP mut”; for more detailed description see chapter 3.3). Samples were prepared without pre-extraction. G1, G2 and S phases of the cell cycle were gated according to EdU incorporation, based on ScanR analysis. EdU negative images represent G1/G2 populations. Values and means based on ScanR and PRISM analysis. DAPI (blue), EdU (green, XRCC1 (red). n=3

Since proliferation of the cells in the following experiments was not affected by either of the used (CPT and PARGi) inhibitors<sup>7</sup>, in following experiments I show the EdU negative as well as the EdU positive gated cell populations (based on ScanR analysis).

Firstly, I performed an evaluation control experiment as following. I treated selected cell lines with CPT for one hour and measured levels of ADP-ribosylation on ScanR Olympus. As expected, the mean ADP-ribose levels after such treatment in U2OS KO<sup>XRCC1 WT</sup> cells expressing full length XRCC1 were comparable to that of U2OS WT control. Opposed to the U2OS KO<sup>XRCC1 WT</sup> cells, one hour of CPT treatment in U2OS KO cells transfected with empty vector (KO<sup>EV</sup>) and U2OS KO cells expressing either XRCC1<sup>RK</sup> or XRCC1<sup>PNKP mut</sup> resulted in significantly increased mean ADP-ribose levels in all mentioned (Fig. 30). Indeed, this was observed in both EdU negative and EdU positive populations (Fig. 30; for relevant P values see Table 2).

Table 2: Statistics corresponding to the results of CPT treatment in Figure 30.

control cells	P values				CPT treated cells
	EdU negative		EdU positive		
U2OS WT	0.0861	ns	0.0578	ns	U2OS KO <sup>XRCC1 WT</sup>
	0.0455	*	0.0100	**	U2OS KO <sup>EV</sup>
	0.0004	***	0.0002	***	U2OS KO <sup>XRCC1 RK</sup>
	0.0102	*	0.0063	**	U2OS KO <sup>XRCC1 PNKP mut</sup>

Secondly, in order to reveal the possible sources of the endogenous SSB lesions, I treated selected U2OS cell lines with PARGi for one hour. Compared to the control U2OS WT cells, in EdU positive cell populations in all following U2OS cell lines: KO<sup>XRCC1 WT</sup>, KO<sup>XRCC1 RK</sup>, KO<sup>EV</sup>, I observed significantly elevated endogenous ADP-ribosylation (Fig. 30; for relevant P values see Table 3). The slight increase in endogenous PARylation during the S phase, in case of *XRCC1*<sup>-/-</sup>U2OS cells expressing wild type XRCC1, might have been caused by the previous gene manipulation and cell cultivation. Such interventions, together with replication stress in S-

<sup>7</sup> based on EdU labelling performed as was described in previous experiments

phasic cells, might have caused some DDR perturbation that would result in elevated ADP-ribose levels.

Interestingly, in EdU negative cell populations, significant increase in the ADP-ribose levels was observed only in the U2OS KO<sup>EV</sup> cells and *XRCC1*<sup>-/-</sup> cells expressing XRCC1<sup>RK</sup> (Fig. 30; for relevant P values see Table 3).

Table 3: Statistics corresponding to the results of PARGi treatment in Figure 30.

control cells	P values				CPT treated cells
	EdU negative		EdU positive		
U2OS WT	0.2154	ns	0,0427	*	U2OS KO <sup>XRCC1 WT</sup>
	0.0268	*	0.0002	***	U2OS KO <sup>EV</sup>
	0.0125	*	0.0061	**	U2OS KO <sup>XRCC1 RK</sup>
	0.1624	ns	0.2047	ns	U2OS KO <sup>XRCC1 PNKP mut</sup>

As the endogenous ADP-ribose levels of the examined KO<sup>XRCC1 PNKP mut</sup> cells remained comparable to that of the negative control cells (U2OS WT and KO<sup>XRCC1 WT</sup>) (Fig. 30), it is unlikely that the endogenous SSBs are caused by lesions processed via the PNKP enzyme. Thus, the *XRCC1*-defective phenotype must be connected to alkylating or oxidative lesions and the revelation of the true origin of endogenous ADP-ribosylation in nonreplicating cells should be further studied. Hypothetical experiments and the reasoning for such is discussed in next chapter.

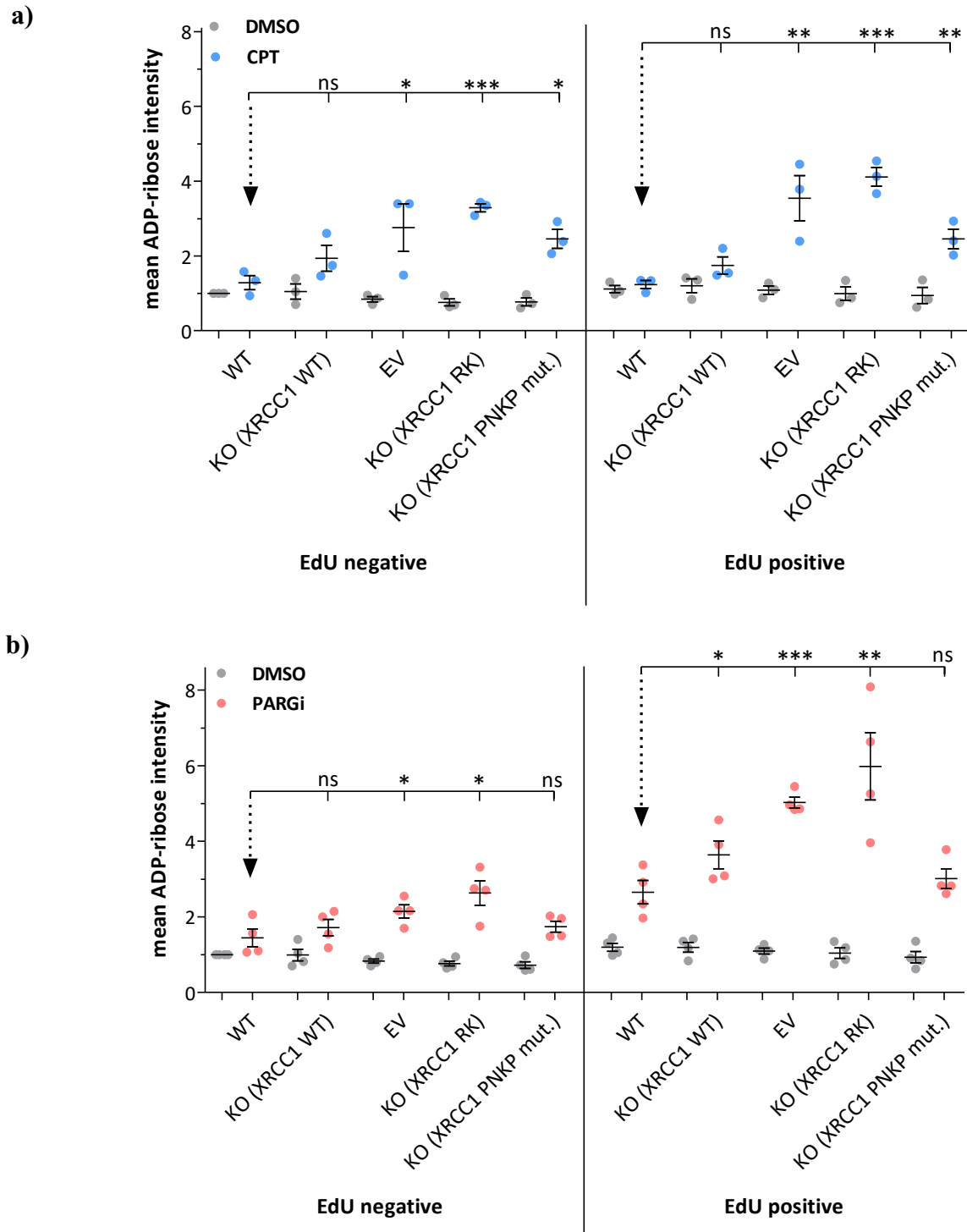
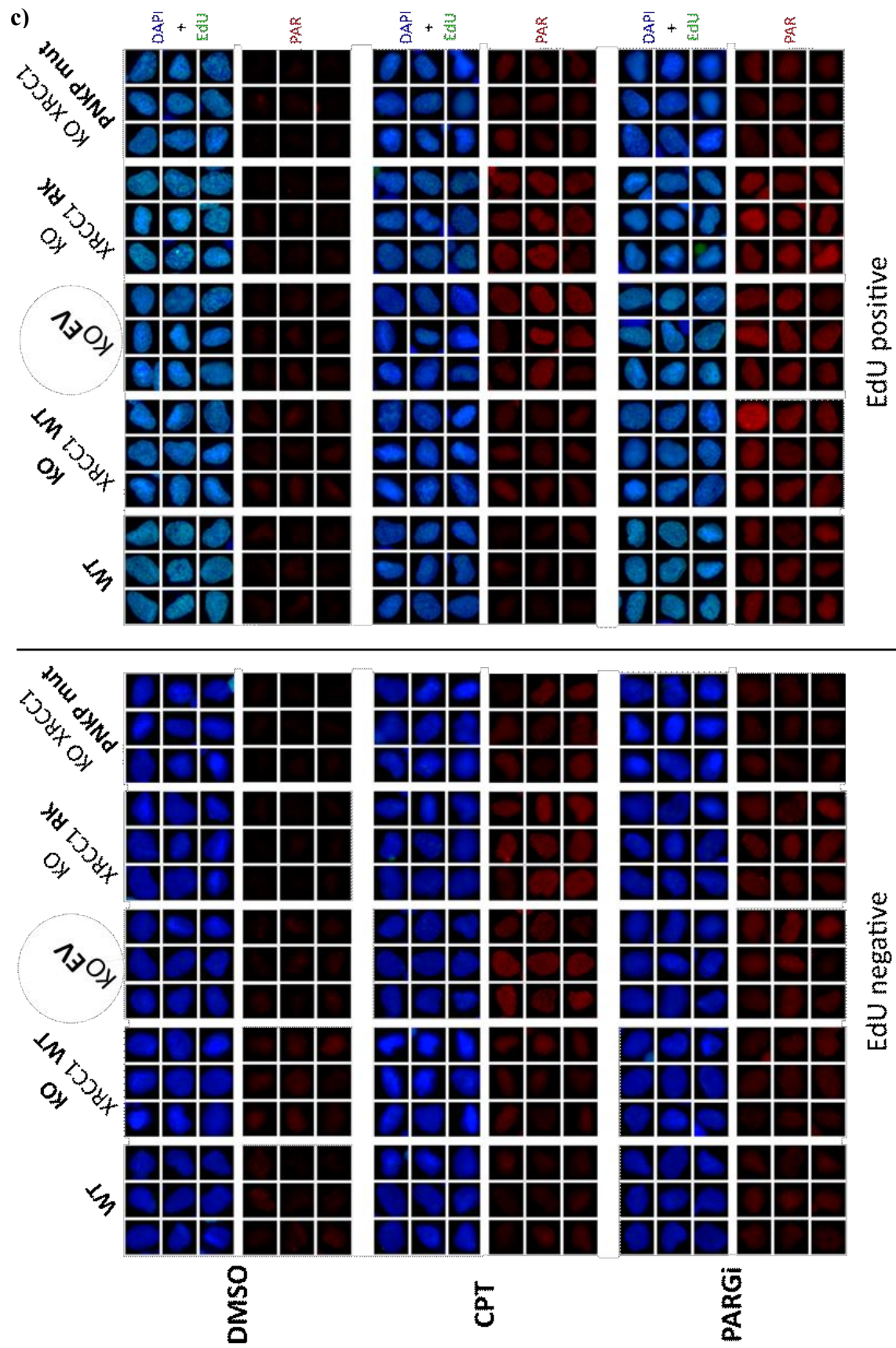


Figure 30: ADP-ribose levels after one hour of 10  $\mu$ M CPT (a) or 10  $\mu$ M PARGi (b) exposure in *XRCC1*-mutated U2OS cells. U2OS wild type (WT) cells were used as the negative control. EdU negative and EdU positive cell populations were gated according to EdU incorporation (based on ScanR analysis). Values and means are based on ScanR and GraphPad PRISM analysis. Quantification (a, b) and representative ScanR images (c) are shown. n=3. ns =  $P > 0.05$ , \* =  $P \leq 0.05$ , \*\* =  $P \leq 0.01$ , \*\*\* =  $P \leq 0.001$ .



## 5 Discussion

Mutations in the *XRCC1* gene lead to a disease called *Spinocerebellar Ataxia Autosomal recessive 26 (SCAR26)*, here referred to as ataxia oculomotor apraxia-XRCC1 (AOA-XRCC1). There are so far three described patients (Hoch et al., 2017; O'Connor et al., 2018) diagnosed with AOA-XRCC1.

The first described patient (hereinafter referred to as XD1 patient) has a heterozygous mutation in *XRCC1*<sup>8</sup> which causes an altered expression resulting in only about ~10 % of the total full length XRCC1 amount in cells<sup>9</sup>. The two more recently identified patients carry an identical biallelic homozygous<sup>10</sup> mutation in the *XRCC1* gene (O'Connor et al., 2018). The patients' phenotype involves progressive cerebellar atrophy and ataxic symptoms such as ataxic gait, difficulties to speak and swallow, worsened proprioception and lateral gaze nystagmus. In the patient with heterozygous mutation, it was described that following the induction of SSBs by oxidative stress and by topoisomerase I inhibitor, the patient's cells show greatly reduced XRCC1 protein levels accompanied by a massive increase in poly(ADP-ribose) levels disrupted SSBR kinetic and, respectively. Therefore, XRCC1 protein was shown to be necessary for the repair of SSBs caused by exogenous agents.

Moreover, a robust endogenous ADP-ribosylation is detectable at the replication sites during normal human S phase and is the result of unligated Okazaki fragments. XRCC1 was shown to be important in the non-canonical "back-up" pathway for the ligation of the fragments. Interestingly, in *XRCC1*-deleted cells, the elevated ADP-ribose levels are detectable in the S phase and, also in the G1 and G2 cell cycle phases (Hanzlikova et al., 2018), which gives rise to at least two important questions. How much of the full length XRCC1 protein is in the *XRCC1*-mutated patients' cells and does it affect the level of ADP-ribosylation?

In order to answer these questions, I first of all measured the remaining levels of XRCC1 protein in the patient-derived cells and compared them to the XRCC1 protein levels in normal cells. Western blotting confirmed that the level of XRCC1 protein in *XRCC1*-mutated patient (XD1) cells is greatly reduced in comparison to the healthy individual-derived cells. I also

---

<sup>8</sup> c. 1293G>C (p.K431N) and c. 1393C>T (p.Q465\*)

<sup>9</sup> Compared to the cells from an unaffected individual.

<sup>10</sup> c. 1293G>C (p.K431N) and c. 1293G>C (p.K431N)

examined one of the two more recently identified patients (hereinafter referred to as #428 patient). Western blotting revealed that the XRCC1 protein levels in the homozygous patient-derived cells are also greatly reduced in comparison to its healthy counterpart. We noticed a slight difference between the two examined patients (approximately 2 to 2.5-fold higher amount of XRCC1 protein in the homozygous patient-derived cells<sup>11</sup>), presumably caused by the different consequences of the homozygous and heterozygous patients' mutations.

We did not detect any truncated XRCC1 protein in XD1 patient-derived cells, suggesting that premature stop codon (p.Q465\*) caused by the 1393C>T mutation results in non-stable mRNA<sup>12</sup>, the *XRCC1* missense mutation c. 1293G>C (p.K431N) resulted in about 10 % of correctly spliced XRCC1 mRNA.

This is an interesting, but not unexpected result, because the mutation is located at exon 11, within the 5' donor splice site of intron 11 (Fig. 31) and thus, the pre-mature XRCC1 mRNA splicing is in most cases aberrant and results in an intron inclusion and mRNA degradation.

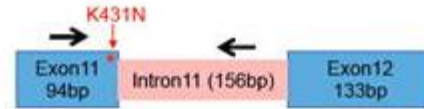


Figure 31: The position of the mutation in XRCC1 gene in relation to pre-mRNA splicing. Adapted from (Hoch et al., 2017).

Given the heterozygosity of XD1 patient and the difference between the XRCC1 protein amounts in the XD1 and #428 patient-derived cells, we can hypothesize that the biallelic homozygous mutation c. 1293G>C (p.K431N) provides ~2 times higher probability of correctly spliced XRCC1 variant than the heterozygous mutation.

As I showed that *XRCC1*-mutated patients have greatly reduced XRCC1 levels, next, I focused on the endogenous levels of ADP-ribose in these cells. The investigation showed that XRCC1 is DNA-protective during the S phase, as the endogenous ADP-ribosylation in S phase populations of *XRCC1*-mutated cells was greatly increased in comparison to the wild type cells. This was expected, because cells lacking *XRCC1* completely show elevated ADP-ribose levels during the S phase as well (Hanzlikova et al., 2018b).

<sup>11</sup> Calculated from a single experiment without any intervention and three independent experiments, where patient-derived fibroblasts were treated with non-target siRNA, using Image J Lite software; see chapter 4.2.1 .

<sup>12</sup> which is subsequently degraded and, therefore, not translated into a functional protein



What was surprising is that, in contrast to the elevated DNA damage rate<sup>13</sup> in the G1 and G2 phases in *XRCC1*-deleted cells, in the patients' cells, the G1/G2 ADP-ribose levels remained low, comparable to that of the normal cells. I must note that this does not imply that the endogenous SSBs are not present in the G1 and G2 phases. More probably, these endogenous SSBs in G1/G2 patients' cells are repaired by the XRCC1 protein residuum in these cells.

Given the above described observations and given the fact that XRCC1 knock-out is embryonically lethal (Tebbs et al., 1999), we decided to test the hypothesis that the residual protein level of XRCC1 in the patients is sufficient for the repair of endogenous SSBs in G1 and G2 cell cycle phases. To do so, I decided to reduce the remaining XRCC1 levels in the patients' cells and answer the question whether the XRCC1 residuum in these cells is really the necessary minimum for sufficient SSBR in non-replicating cells.

I depleted the XRCC1 protein via RNA interference. Such manipulation of the patient-derived cells revealed a lesser number of proliferating cells than in the control samples. To the point where any statistics from the population would not be a representative sample for disclosure. This problem was probably caused by the toxicity of the siXRCC1 treatment and the higher sensitivity of the patient-derived cells. Luckily, due to the cell type affected in the examined patients and the AOA-XRCC1 phenotype, this complication did not limit the exploration of the G1/G2 cell populations, which is the relevant one in the context of neurodegeneration. However, in the G1/G2 cell populations, the depletion of XRCC1 via siRNA interference in patient-derived cell did not change the endogenous ADP-ribose levels.

Although this was unexpected, considering the previously described phenotype of *XRCC1*-deleted cells, where the G1/G2 endogenous ADP-ribose levels are increased, the sufficient SSBR repair in G1/G2 cell populations of the XRCC1-depleted patients' cell can be explained. The siRNA knock-down is not a 100 % efficient method, and after the *siXRCC1* treatment, there was still some detectable amount of XRCC1 protein remaining in the cells (1-3 % of that of the wild type controls). Therefore, the threshold of XRCC1 protein amount, which would cause a significant increase in ADP-ribosylation, must be very low.

---

<sup>13</sup> DNA damage rate correlates to the endogenous levels of ADP-ribose in the nucleus of the cell.

I must note that there are ongoing experiments which confirm that although a minimum of about 3 % of XRCC1 protein in cells might be sufficient for rapid<sup>14</sup> SSB, over a longer period of time, the patients' XRCC1 protein level is no longer sufficient for the SSB in the G1/G2 cell populations. To be specific, patient cells treated with PARG inhibitor for 1, 2, 4, 6 and 8 hours revealed massively elevated endogenous PARylation after 8 hours (data not shown).

Together, these results suggest that XRCC1 residuum in patient-derived fibroblasts (approximately 10-20 % of the protein amount in unaffected cells) is sufficient and necessary for the rapid DNA single-strand break repair in the G1/G2 phase.

Taking into account that:

- siRNA knock-down is not efficient for a complete depletion of the XRCC1 protein;
- siXRCC1 treatment in human fibroblasts is toxic and causes decrease in the number of proliferating cells; and
- XRCC1-deleted cells show elevated endogenous ADP-ribosylation in G1/G2,

we further decided that for the purpose of mechanistic research of the origin of endogenous ADP-ribosylation in cells, human fibroblasts are not a suitable model, therefore, we use *XRCC1*<sup>-/-</sup> U2OS as a model system. However, in parallel with our investigations, in our Sussex research group, there is an ongoing effort to cultivate neural cells extracted from neural specific conditional *Xrcc1*<sup>Nes-Cre</sup> knock-out mice (Lee et al., 2009). These cells would be more accurate model in the future investigation of the source of endogenous DNA damage in non-proliferating neural cells. Utilizing the neural cells extracted from the AOA-XRCC1 murine model, we could focus on specific brain regions (unpublished data in Komulainen et al., 2020).

There are several options, where the SSBs in the G1/G2 phases might be coming from. In general, these options include direct sugar disintegration done by reactive oxygen species and indirectly caused SSB lesions. Among the indirect causes we find errantly incorporated ribonucleotides (rNTPs) in the DNA and their repair, damaged bases (alkylated or oxidized) and

---

<sup>14</sup> where rapid is defined as within a period of one hour after an endogenous SSB was induced

their repair via base excision repair pathway and SSB lesions caused by aberrant topoisomerase I activity.

As TOP1 is an enzyme able to perform an incision of the DNA, its stalling by camptothecin induces SSBs, which can be repaired via SSBR, if functional XRCC1 protein is present. We confirmed this in XRCC1 patient-derived cells and *XRCC1*-deleted cells, where TOP1 inhibition by CPT cause elevated ADP-ribosylation, a sign of unrepaired single-strand breaks. Moreover, the amount of XRCC1 protein negatively correlates with the abundance of SSBs in the DNA.

Considering these results, we can conclude that XRCC1, in the amount of at least 10 % of that of the protein amount in unaffected cells, is required for the rapid repair of DNA damage caused by the stalled TOP1 enzyme.

The hypothesis that the endogenous SSBs, which stand behind the AOA-XRCC1 patients' phenotype, are caused by aberrant TOP1 activity was examined in suitable model cells (lacking XRCC1 protein completely). As expected, based on data published by Desai et al. (2001), the effect of CPT (CPT-induced single-strand breaks in DNA) was completely reversed by addition of proteasome inhibitor MG132. This was not true in the case of endogenous SSBs, showing that aberrant TOP1 activity, clearly, do not represent the main source of the endogenous SSBs.

However, TOP1 does not work only as a torsion stress reliever. In yeast, it has been shown that, in the absence of RNase H2 (when the RER pathway is disrupted), the previously errantly incorporated rNTPs by DNA polymerases can be recognized and excised by Top1. In DDR-deficient cells, this can subsequently result in double-strand breaks and possibly cell death (Kim et al., 2011; Cristini et al., 2019). DNA polymerases provide the DNA synthesis and ensure very efficient proofreading and detection of mismatched bases in a newly synthesized DNA strand, (mismatch repair, MMR; reviewed in Li, 2008).

During replication, these enzymes are very active and, as a substrate, they can use rNTPs as well as dNTPs (Abbotts & Wilson, 2014). The quite frequent incorporation of rNTP is probably caused by the imbalance in the rNTP/dNTP pool at the replication fork (Yao et al., 2013). Unfortunately, the detection of errantly incorporated rNTPs requires a finer system which engages endoribonuclease RNase H2 (see Fig. 33) for a pathway called the ribonucleotide excision repair pathway (RER) (Sparks et al., 2012), and presumably also engages TOP1 (Fig. 32).

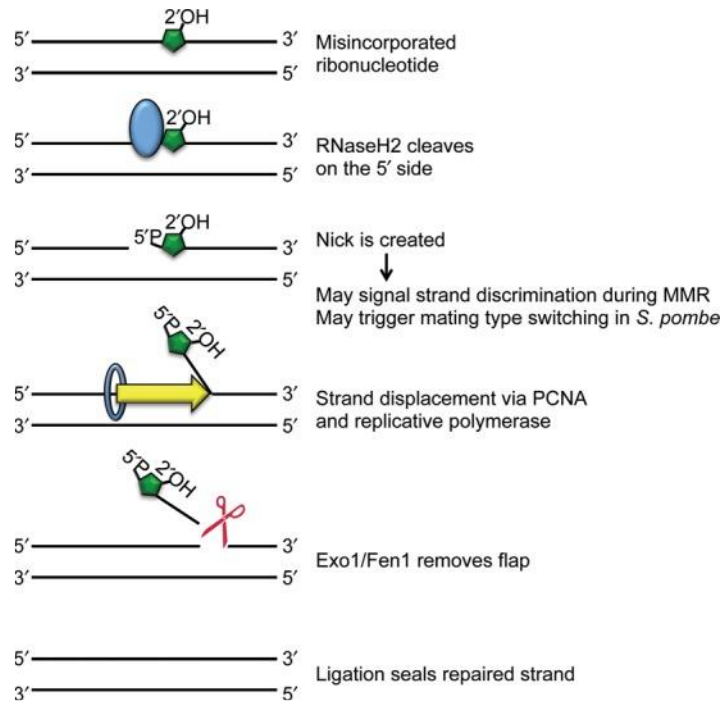


Figure 32: **Ribonucleotide excision repair mechanism.** Source: Potenski CJ, Klein HL. How the misincorporation of ribonucleotides into genomic DNA can be both harmful and helpful to cells. *Nucleic Acids Res.* 2014;42(16):10226-10234.

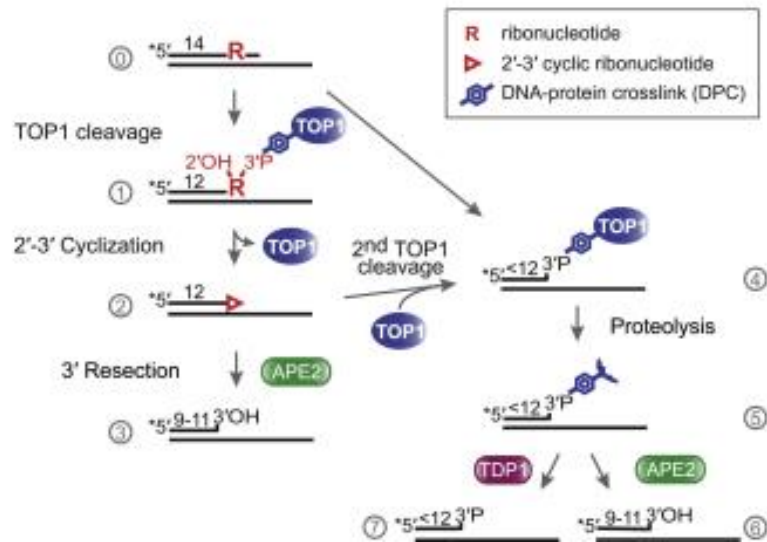


Figure 33: **Model of rNTP excision by TOP1.** Adapted from (Álvarez-Quilón et al., 2020).

The contribution of TOP1 to the controlling of misincorporated rNTPs and their repair has not been estimated yet, but given the observation that stalled TOP1-cleavage complexes in *XRCC1*-defective cells is not the main source of endogenous SSBs, we can hypothesize that neither the TOP1 excision of rNTPs is responsible for such endogenous DNA damage.

Taking into account the phenotype similarity between AOA-*XRCC1* and AOA4 diseases (caused by mutations in *XRCC1* or *PNKP*, respectively), the lesions whose repair require the *PNKP* enzyme were suspected to be the origin of the unrepaired endogenous SSBs in the G1/G2 cell cycle phases. Thus, lesions, which activate the DNA-repair pathway requiring the *PNKP* activity, were examined.

Examination of cells with disrupted *PNKP* activity in SSBR revealed that these cells do not show elevated endogenous levels of ADP-ribose in G2/G2. Considering this data in full, it seems that *XRCC1/PNKP* interaction, thus, *PNKP* recruitment and activity is not relevant in *XRCC1*-mutated patients- and AOA1-*XRCC1*- phenotype. To prove this, we could also submit the cells to the methylating agent methyl methanesulfonate (MMS). DNA damage caused by this chemical compound is repaired via a pathway which does not utilize the *PNKP* enzyme. Therefore, the treatment should not affect the ADP-ribose levels in cell expressing the mutant variant of *XRCC1*, which is unable to bind the *PNKP*.

In the context of the aforementioned observations, therefore, excluding the TOP1 lesions and *XRCC1/PNKP* repaired lesions as the main source of endogenous SSBs for now, there are two players left (Fig. 34):

- 1) alkylation, caused by methylation on N- atoms, which represent most of the alkylations, or O-atoms in DNA bases (examples is Fig. 3); and
- 2) oxidative lesions (some of which are also listed in Fig. 3), recognized by and repaired, in close cooperation with AP endonucleases, by DNA glycosylases (DGs).

A neuron's life span is unusually long and their consumption of O<sub>2</sub> is extreme due to the high number of mitochondria and the reactive oxygen species (ROS) pose one of the most common deleterious agents in the cell. The DNA is attacked by the derivatives of oxygen called free radicals (e.g. hydroxyl radical, superoxide radical, peroxy, alkoxy) and oxidizing agents

(hydrogen peroxide (H<sub>2</sub>O<sub>2</sub>) and singlet oxygen) causing more than 20 different forms of damaged bases.

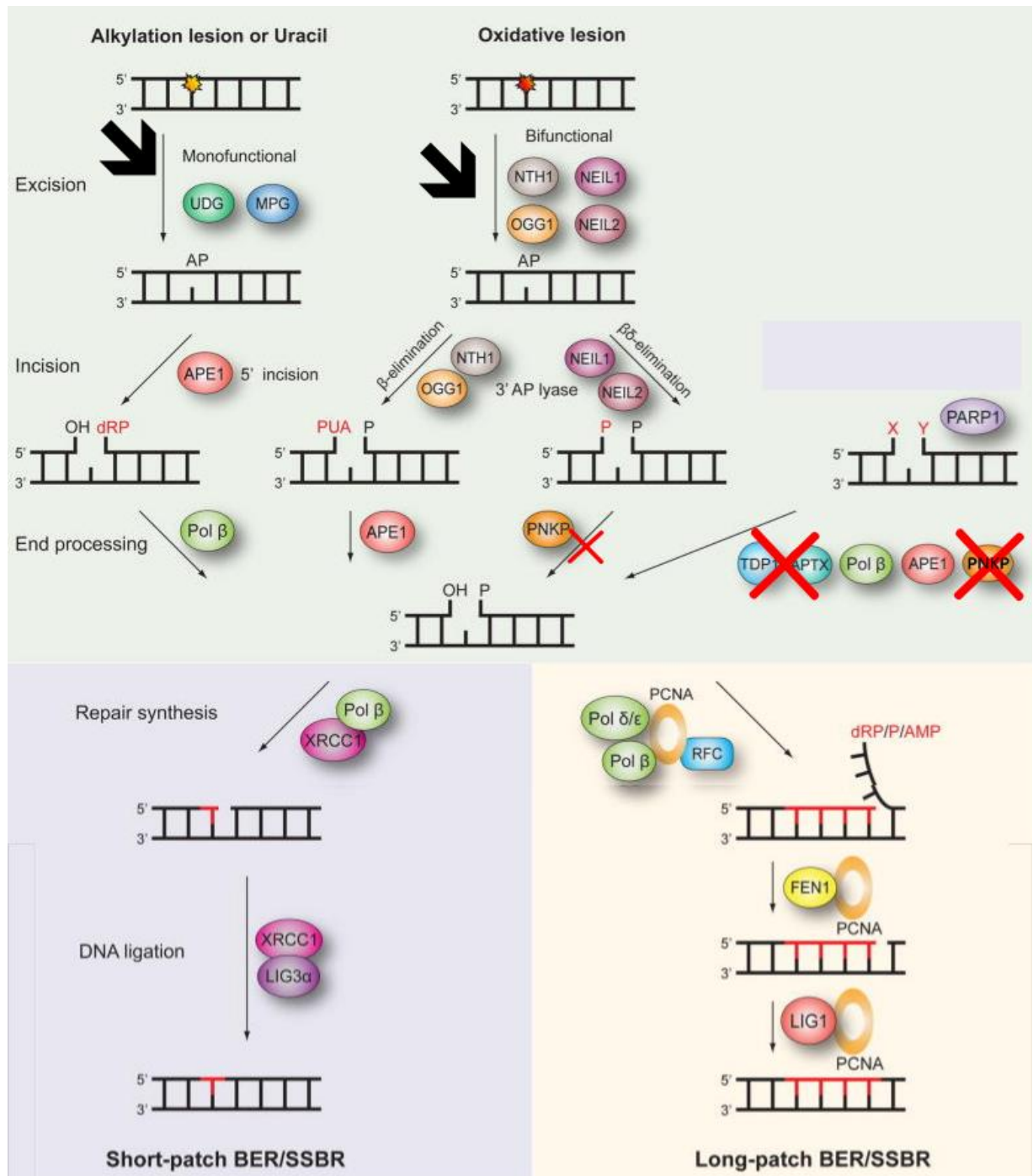


Figure 34: **Connection between SSBR, BER pathway and DNA glycosylases.** Excluded protein are labelled with red crosses, possible sources of the endogenous SSBs are highlighted with black arrows Adapted from (Jeppesen et al., 2011).

Since the etiology of, unfortunately very common, neurological diseases such as amyotrophic lateral sclerosis (ALS), Alzheimer's, Parkinson's and Huntington's disease (AD, PD and HD, respectively) is linked to oxidative stress<sup>15</sup> (Aguirre et al., 2005; Lyras et al., 1997; Yasuhara et al., 2007; Zheng et al., 2018, respectively), we should consider the ROS-induced lesions as the main source of PARylated endogenous lesions which subsequently cause neurodegeneration in SSBR-defective patients.

Given these neural attributes, I do not discuss alkylation lesions in great detail. Although such lesions are strongly linked to NER and MMR (Kondo et al., 2010), they should not be overlooked, because methylation of the DNA is a crucial chemical modification in epigenetics, which overlap with neurodevelopment and synaptic plasticity (B. Yao & Jin, 2014).

Oxidative lesions (most often AP sites, 8-oxoG and TG) are repaired by DNA glycosylases. This family of enzymes consists of two sub-classes: monofunctional and bifunctional glycosylases (examples of class members and substrates are listed in Table 4). The monofunctional glycosylases generate highly mutagenic AP sites, but do not possess an endonuclease activity. Therefore, the downstream repair of the lesion is dependent on the processing by APE1<sup>16</sup>.

The bifunctional glycosylases, as their name suggest, are capable of both steps (removal of the damaged base via  $\beta$  or  $\beta\delta$  elimination and cleavage of the phosphodiester backbone at the AP site). The difference between  $\beta$  or  $\beta\delta$  elimination is in the form of damaged DNA ends, which are left at the site of incision (3'-PUA and 5'-P in case of the former, 3'-P and 5'-P in case of the latter) and their further processing (Fig. 34).

The above discussed results imply that the  $\beta\delta$  elimination (recognition and excision of oxidized pyrimidines and FapyG) by NEILs and subsequent processing by PNKP is a DNA repair pathway resolving less important lesions, or that its function is redundant with some of the other mechanisms. Also, in rat brains, the differentiation of neurons is accompanied by a decrease in NEIL1/2 protein levels and decreased activity of NTH1, Pol $\beta$  and other proteins involved in the repair of replication-induced lesions. Importantly, the activity of OGG1

---

<sup>15</sup> There is an interesting connection between reactive iron and age-related neurodegeneration reviewed in (Zecca et al., 2004).

<sup>16</sup> which function is to incise the DNA causing an SSB, which must be subsequently repaired via XRCC1-dependent SSBR

glycosylase in adult brains was shown to be also reduced, compared to other tissues (Wilson & McNeill, 2007).

Together with this data, Wilson & McNeill (2007) also described altered *Xrcc1* and *Lig3 $\alpha$*  expression, supporting the suspicion that the origin of DNA lesions which cause neurodegeneration in *XRCC1*-defective patients are 8-oxoG, excised via *OGG1* (requiring high expression rate of *XRCC1* in aged brains). The 8-oxoG pairs with A, which is from the 8-oxoG:A pair excised by the monofunctional DNA glycosylase MutY homolog DNA glycosylase causing an AP site, which is then resolved by *APE1*. In addition, *Mutyh*<sup>-/-</sup> mice exposed to 3-nitropropionic acid (inhibitor of mitochondrial complex II, neurotoxic compound (Szabó et al., n.d.)) show reduced accumulation of single-strand DNA, compared to *Ogg1*<sup>-/-</sup> mice. Also, *Mutyh*<sup>-/-</sup> *Ogg1*<sup>-/-</sup> mice exposed to the mitochondrial toxin exhibited improved motor function (compared to the *Ogg1*<sup>-/-</sup> mice).

Table 4: **Substrates of monofunctional and bifunctional DNA glycosylases.** Abbreviations: uracil-DNA glycosylase (UNG), thymine-DNA glycosylase (TDG), single-strand-specific monofunctional uracil DNA glycosylase 1 (SMUG1), MutY homolog DNA glycosylase (MUTYH), human 8-oxoguanine DNA glycosylase (OGG1), endonuclease VIII-like 1, 2, 3 (NEIL1, 2, 3), endonuclease III-like protein 1 (NTH1), 5-hmU = 5-hydroxymethyl uracil, 5-OH-C = 5-hydroxycytidine, 5-OH-U = 5'-hydroxyuracil, 8-oxoG = 8-oxoguanosine, TG = thymine glycol, FapyG, FapyA = formamidopyrimidines, A = adenine, T = thymine, G = guanosine, C = cytosine.

DNA glycosylase					
Monofunctional			Bifunctional		
Name	Main substrate	Incision	Name	Main substrate	Incision
<b>MUTYH</b>	A in A:8-oxoG pair	APE1	<b>OGG1</b>	8-oxoG,	$\beta$ -elimination
<b>TDG</b>	T/U in T/U:G pair		<b>NTH1</b>	TG, FapyG, 5-OH-C, 5-OH-U	
<b>SMUG1</b>	5-hmU, uracil		<b>NEIL1</b>	TG, FapyG, FapyA, 8-oxoG, 5-OH-C, 5-OH-U	$\beta\delta$ -elimination
<b>UNG</b>	uracil		<b>NEIL2</b>	TG, FapyG, FapyA, 8-oxoG, 5-OH-C, 5-OH-U	
			<b>NEIL3</b>	FapyG, FapyA	



In order to distinguish whether the most common oxidative lesion 8-oxoG is the toxic lesion underpinning the *XRCC1*-defective phenotype (accumulation of SSBs and thus, elevated PARylation), we should investigate the pathway required for its repair. Knock-down or inhibition of the OGG1 in *XRCC1*-defective cells would divulge, if the toxicity of 8-oxoG comes from its processing. A different result would suggest that there is a connection with MUTYH- and APE1-processed A in the toxic 8-oxoG:A base pair.

Either way, in neurodegenerative diseases, oxidative stress is already proven to be a key modulator and further research and more accurate disease animal models are necessary to uncover the mechanistic cause of neurodegenerative diseases such as cerebellar ataxias. As the *XRCC1*-deletion is embryonically lethal (Tebbs et al., 1999) and only 10 % of the *XRCC1* protein in cells is required for normal neural development in mice (Tebbs et al., 2003), the future perspective of this thesis lies on a knock-in murine model carrying the same mutations as the homozygous AOA1-*XRCC1* patients, which is currently bred and, if the luck is with us, should be available soon. Such disease model would be more accurate and would broaden the research of the possibility to study the AOA-*XRCC1* mice brain during development as well as during the adult life.

## 6 Conclusions

The first aim of this thesis was to measure the levels of single-strand break repair (SSBR) protein XRCC1 in *XRCC1*-mutated patients. Such investigation revealed greatly reduced XRCC1 protein levels in AOA-XRCC1 patient-derived cells.

Fulfilling the next goal of the thesis, I described the relation between *XRCC1*-defectiveness and the endogenous levels of ADP-ribose throughout the cell cycle. The elevated endogenous chromatin ADP-ribose levels in the S, G1 and G2 cell cycle phase in *XRCC1*-defective cells represent the SSB lesions in the DNA, which convey a strong impression that XRCC1 protein is necessary for the repair of the endogenous DNA damage during S phase, as well as during the G1 and G2 cell cycle phases.

Further exploration of the molecular mechanism of SSB accumulation in *XRCC1*-defective cells gave us clear evidences that the main source of these DNA lesions in nonreplicating cells is neither an aberrant topoisomerase I (TOP1) activity, nor lesions, which would require the polynucleotide kinase phosphatase (PNKP) enzyme. Most likely, the findings imply that the the origin of the endogenous SSBs which arise during the G1 and G2 is oxidative or alkylating DNA damage.

## 7 References

- Abbotts, R., & Madhusudan, S. (2010). Human AP endonuclease 1 (APE1): From mechanistic insights to druggable target in cancer. In *Cancer Treatment Reviews* (Vol. 36, Issue 5, pp. 425–435). *Cancer Treat Rev.* <https://doi.org/10.1016/j.ctrv.2009.12.006>
- Abbotts, R., & Wilson, D. M. (2014). Ribonucleotides as nucleotide excision repair substrates. In *DNA Repair* (Vol. 13, Issue 1, pp. 55–60). NIH Public Access. <https://doi.org/10.1016/j.dnarep.2013.10.010>
- Abplanalp, J., Leutert, M., Frugier, E., Nowak, K., Feurer, R., Kato, J., Kistemaker, H. V. A., Filippov, D. V., Moss, J., Cafilisch, A., & Hottiger, M. O. (2017). Proteomic analyses identify ARH3 as a serine mono-ADP-ribosylhydrolase. *Nature Communications*, 8(1). <https://doi.org/10.1038/s41467-017-02253-1>
- Aguirre, N., Beal, M. F., Matson, W. R., & Bogdanov, M. B. (2005). Increased oxidative damage to DNA in an animal model of amyotrophic lateral sclerosis. *Free Radical Research*, 39(4), 383–388. <https://doi.org/10.1080/10715760400027979>
- Ali, A. A. E., Jukes, R. M., Pearl, L. H., & Oliver, A. W. (2009). Specific recognition of a multiply phosphorylated motif in the DNA repair scaffold XRCC1 by the FHA domain of human PNK. *Nucleic Acids Research*, 37(5), 1701–1712. <https://doi.org/10.1093/nar/gkn1086>
- Ali, R., Al-Kawaz, A., Toss, M. S., Green, A. R., Miligy, I. M., Mesquita, K. A., Seedhouse, C., Mirza, S., Band, V., Rakha, E. A., & Madhusudan, S. (2018). Targeting PARP1 in XRCC1-deficient sporadic invasive breast cancer or preinvasive ductal carcinoma in situ induces synthetic lethality and chemoprevention. *Cancer Research*, 78(24), 6818–6827. <https://doi.org/10.1158/0008-5472.CAN-18-0633>
- Álvarez-Quilón, A., Wojtaszek, J. L., Mathieu, M. C., Patel, T., Appel, C. D., Hustedt, N., Rossi, S. E., Wallace, B. D., Setiapura, D., Adam, S., Ohashi, Y., Melo, H., Cho, T., Gervais, C., Muñoz, I. M., Grazzini, E., Young, J. T. F., Rouse, J., Zinda, M., ... Durocher, D. (2020). Endogenous DNA 3' Blocks Are Vulnerabilities for BRCA1 and BRCA2 Deficiency and Are Reversed by the APE2 Nuclease. *Molecular Cell*, 78(6), 1152-1165.e8. <https://doi.org/10.1016/j.molcel.2020.05.021>
- Belanich, M., Randall, T., Pastor, M. A., Kibitel, J. T., Alas, L. G., Dolan, M. E., Schold, S. C., Gander, M., Lejeune, F. J., Li, B. F. L., White, A. B., Wasserman, P., Citron, M. L., & Yarosh, D. B. (1996). Intracellular localization and intercellular heterogeneity of the human DNA repair protein O6-methylguanine-DNA methyltransferase. *Cancer Chemotherapy and Pharmacology*,

- 37(6), 547–555. <https://doi.org/10.1007/s002800050427>
- Belousova, E. A., Ishchenko, A. A., & Lavrik, O. I. (2018). DNA is a New Target of Parp3. *Scientific Reports*, 8(1), 4176. <https://doi.org/10.1038/s41598-018-22673-3>
- Biernacka, A., Zhu, Y., Skrzypczak, M., Forey, R., Pardo, B., Grzelak, M., Nde, J., Mitra, A., Kudlicki, A., Crosetto, N., Pasero, P., Rowicka, M., & Ginalski, K. (2018). i-BLESS is an ultra-sensitive method for detection of DNA double-strand breaks. *Communications Biology*, 1(1). <https://doi.org/10.1038/s42003-018-0165-9>
- Bonfiglio, J. J., Fontana, P., Zhang, Q., Colby, T., Gibbs-Seymour, I., Atanassov, I., Bartlett, E., Zaja, R., Ahel, I., & Matic, I. (2017). Serine ADP-Ribosylation Depends on HPF1. *Molecular Cell*, 65(5), 932-940.e6. <https://doi.org/10.1016/j.molcel.2017.01.003>
- Breslin, C., Hornyak, P., Ridley, A., Rulten, S. L., Hanzlikova, H., Oliver, A. W., & Caldecott, K. W. (2015a). The XRCC1 phosphate-binding pocket binds poly (ADP-ribose) and is required for XRCC1 function. *Nucleic Acids Research*, 43(14), 6934–6944. <https://doi.org/10.1093/nar/gkv623>
- Breslin, C., Hornyak, P., Ridley, A., Rulten, S. L., Hanzlikova, H., Oliver, A. W., & Caldecott, K. W. (2015b). The XRCC1 phosphate-binding pocket binds poly (ADP-ribose) and is required for XRCC1 function. *Nucleic Acids Research*, 43(14), 6934–6944. <https://doi.org/10.1093/nar/gkv623>
- Breslin, C., Mani, R. S., Fanta, M., Hoch, N., Weinfeld, M., & Caldecott, K. W. (2017). The Rev1 interacting region (RIR) motif in the scaffold protein XRCC1 mediates a low-affinity interaction with polynucleotide kinase/phosphatase (PNKP) during DNA single-strand break repair. *Journal of Biological Chemistry*, 292(39), 16024–16031. <https://doi.org/10.1074/jbc.M117.806638>
- Broustas, C. G., & Lieberman, H. B. (2014). DNA Damage Response Genes and the Development of Cancer Metastasis. *Radiation Research*, 181(2), 111–130. <https://doi.org/10.1667/rr13515.1>
- Bryant, H. E., Schultz, N., Thomas, H. D., Parker, K. M., Flower, D., Lopez, E., Kyle, S., Meuth, M., Curtin, N. J., & Helleday, T. (2005). Specific killing of BRCA2-deficient tumours with inhibitors of poly(ADP-ribose) polymerase. *Nature*, 434(7035), 913–917. <https://doi.org/10.1038/nature03443>
- Caldecott, K. W. (2019). XRCC1 protein; Form and function. *DNA Repair*, 81. <https://doi.org/10.1016/j.dnarep.2019.102664>
- Caldecott, K. W., Tucker, J. D., Stanker, L. H., & Thompson, L. H. (1995a). Characterization of the XRCC1-DNA ligase complex in vitro and its absence from mutant hamster cells. In *Nucleic Acids Research* (Vol. 23, Issue 23). <https://academic.oup.com/nar/article->

abstract/23/23/4836/2400732

- Caldecott, K. W., Tucker, J. D., Stanker, L. H., & Thompson, L. H. (1995b). Characterization of the XRCC1-DNA ligase complex in vitro and its absence from mutant hamster cells. In *Nucleic Acids Research* (Vol. 23, Issue 23).
- Ciccia, A., & Elledge, S. J. (2010). The DNA Damage Response: Making It Safe to Play with Knives. In *Molecular Cell* (Vol. 40, Issue 2, pp. 179–204). NIH Public Access.  
<https://doi.org/10.1016/j.molcel.2010.09.019>
- Clements, P. M., Breslin, C., Deeks, E. D., Byrd, P. J., Ju, L., Bieganski, P., Brenner, C., Moreira, M. C., Taylor, A. M. R., & Caldecott, K. W. (2004). The ataxia-oculomotor apraxia 1 gene product has a role distinct from ATM and interacts with the DNA strand break repair proteins XRCC1 and XRCC4. *DNA Repair*, 3(11), 1493–1502.  
<https://doi.org/10.1016/j.dnarep.2004.06.017>
- Coppede, F., & Migliore, L. (2010). DNA Repair in Premature Aging Disorders and Neurodegeneration. *Current Aging Science*, 3(1), 3–19.  
<https://doi.org/10.2174/1874609811003010003>
- Crimella, C., Cantoni, O., Guidarelli, A., Vantaggiato, C., Martinuzzi, A., Fiorani, M., Azzolini, C., Orso, G., Bresolin, N., & Bassi, M. T. (2011). A novel nonsense mutation in the APTX gene associated with delayed DNA single-strand break removal fails to enhance sensitivity to different genotoxic agents. *Human Mutation*, 32(4). <https://doi.org/10.1002/humu.21464>
- Cristini, A., Ricci, G., Britton, S., Salimbeni, S., Huang, S. yin N., Marinello, J., Calsou, P., Pommier, Y., Favre, G., Capranico, G., Gromak, N., & Sordet, O. (2019). Dual Processing of R-Loops and Topoisomerase I Induces Transcription-Dependent DNA Double-Strand Breaks. *Cell Reports*, 28(12), 3167-3181.e6. <https://doi.org/10.1016/j.celrep.2019.08.041>
- Cuneo, M. J., & London, R. E. (2010). Oxidation state of the XRCC1 N-terminal domain regulates DNA polymerase  $\beta$  binding affinity. *Proceedings of the National Academy of Sciences of the United States of America*, 107(15), 6805–6810. <https://doi.org/10.1073/pnas.0914077107>
- Dedes, K. J., Wilkerson, P. M., Wetterskog, D., Weigelt, B., Ashworth, A., & Reis-Filho, J. S. (2011). Synthetic lethality of PARP inhibition in cancers lacking BRCA1 and BRCA2 mutations. In *Cell Cycle* (Vol. 10, Issue 8, pp. 1192–1199). Taylor and Francis Inc.  
<https://doi.org/10.4161/cc.10.8.15273>
- Della-Maria, J., Hegde, M. L., McNeill, D. R., Matsumoto, Y., Tsai, M. S., Ellenberger, T., Wilson, D. M., Mitra, S., & Tomkinson, A. E. (2012). The interaction between polynucleotide kinase phosphatase and the DNA repair protein XRCC1 is critical for repair of DNA alkylation damage

- and stable association at DNA damage sites. *Journal of Biological Chemistry*, 287(46), 39233–39244. <https://doi.org/10.1074/jbc.M112.369975>
- Desai, S. D., Li, T. K., Rodriguez-Bauman, A., Liu, L. F., & Rubin, E. H. (2001). Ubiquitin/26s proteasome-mediated degradation of topoisomerase I as a resistance mechanism to camptothecin in tumor cells. *Cancer Research*, 61(15), 5926–5932. <http://www.ncbi.nlm.nih.gov/pubmed/11479235>
- Dianova, I. I., Sleeth, K. M., Allinson, S. L., Parsons, J. L., Breslin, C., Caldecott, K. W., & Dianov, G. L. (2004). XRCC1-DNA polymerase  $\beta$  interaction is required for efficient base excision repair. *Nucleic Acids Research*, 32(8), 2550–2555. <https://doi.org/10.1093/nar/gkh567>
- El-Khamisy, S. F., Hartsuiker, E., & Caldecott, K. W. (2007). TDP1 facilitates repair of ionizing radiation-induced DNA single-strand breaks. *DNA Repair*, 6(10), 1485–1495. <https://doi.org/10.1016/j.dnarep.2007.04.015>
- El-Khamisy, S. F., Saifi, G. M., Weinfeld, M., Johansson, F., Helleday, T., Lupski, J. R., & Caldecott, K. W. (2005). Defective DNA single-strand break repair in spinocerebellar ataxia with axonal neuropathy-1. *Nature*, 434(7029), 108–113. <https://doi.org/10.1038/nature03314>
- Emerson, C. H., Lopez, C. R., Ribes-Zamora, A., Polleys, E. J., Williams, C. L., Yeo, L., Zaneveld, J. E., Chen, R., & Bertuch, A. A. (2018). Ku DNA end-binding activity promotes repair fidelity and influences end-processing during nonhomologous end-joining in *Saccharomyces cerevisiae*. *Genetics*, 209(1), 115–128. <https://doi.org/10.1534/genetics.117.300672>
- Fagerberg, L., Hallstrom, B. M., Oksvold, P., Kampf, C., Djureinovic, D., Odeberg, J., Habuka, M., Tahmasebpoor, S., Danielsson, A., Edlund, K., Asplund, A., Sjostedt, E., Lundberg, E., Szigartyo, C. A. K., Skogs, M., Ottosson Takanen, J., Berling, H., Tegel, H., Mulder, J., ... Uhlen, M. (2014). Analysis of the human tissue-specific expression by genome-wide integration of transcriptomics and antibody-based proteomics. *Molecular and Cellular Proteomics*, 13(2), 397–406. <https://doi.org/10.1074/mcp.M113.035600>
- Fan, J., Otterlei, M., Wong, H. K., Tomkinson, A. E., & Wilson, D. M. (2004). XRCC1 co-localizes and physically interacts with PCNA. *Nucleic Acids Research*, 32(7), 2193–2201. <https://doi.org/10.1093/nar/gkh556>
- Fang, Q., Andrews, J., Sharma, N., Wilk, A., Clark, J., Slyskova, J., Koczor, C. A., Lans, H., Prakash, A., & Sobol, R. W. (2019). Stability and sub-cellular localization of DNA polymerase  $\beta$  is regulated by interactions with NQO1 and XRCC1 in response to oxidative stress. *Nucleic Acids Research*, 47(12), 6269–6286. <https://doi.org/10.1093/nar/gkz293>
- Fortini, P., Pascucci, B., Parlanti, E., Sobol, R. W., Wilson, S. H., & Dogliotti, E. (1998). Different

- DNA polymerases are involved in the short- and long-patch base excision repair in mammalian cells. *Biochemistry*, 37(11), 3575–3580. <https://doi.org/10.1021/bi972999h>
- Grundy, G. J., Polo, L. M., Zeng, Z., Rulten, S. L., Hoch, N. C., Paomephan, P., Xu, Y., Sweet, S. M., Thorne, A. W., Oliver, A. W., Matthews, S. J., Pearl, L. H., & Caldecott, K. W. (2016). PARP3 is a sensor of nicked nucleosomes and monoribosylates histone H2B Glu2. *Nature Communications*, 7. <https://doi.org/10.1038/ncomms12404>
- Gryk, M. R., Marintchev, A., Maciejewski, M. W., Robertson, A., Wilson, S. H., & Mullen, G. P. (2002). Mapping of the interaction interface of DNA polymerase  $\beta$  with XRCC1. *Structure*, 10(12), 1709–1720. [https://doi.org/10.1016/S0969-2126\(02\)00908-5](https://doi.org/10.1016/S0969-2126(02)00908-5)
- Hanssen-Bauer, A., Solvang-Garten, K., Sundheim, O., Peña-Diaz, J., Andersen, S., Slupphaug, G., Krokan, H. E., Wilson, D. M., Akbari, M., & Otterlei, M. (2011). XRCC1 coordinates disparate responses and multiprotein repair complexes depending on the nature and context of the DNA damage. *Environmental and Molecular Mutagenesis*, 52(8), 623–635. <https://doi.org/10.1002/em.20663>
- Hanzlikova, H., Gittens, W., Krejcikova, K., Zeng, Z., & Caldecott, K. W. (2017). *Overlapping roles for PARP1 and PARP2 in the recruitment of endogenous XRCC1 and PNKP into oxidized chromatin*. *Nucleic Acids Research*. <https://doi.org/10.1093/nar/gkw1246>
- Hanzlikova, H., Kalasova, I., Demin, A. A., Pennicott, L. E., Cihlarova, Z., & Caldecott, K. W. (2018). The Importance of Poly(ADP-Ribose) Polymerase as a Sensor of Unligated Okazaki Fragments during DNA Replication. *Molecular Cell*, 71(2), 319. <https://doi.org/10.1016/J.MOLCEL.2018.06.004>
- Havali-Shahriari, Z., Weinfeld, M., & Glover, J. N. M. (2017). Characterization of DNA Substrate Binding to the Phosphatase Domain of the DNA Repair Enzyme Polynucleotide Kinase/Phosphatase. *Biochemistry*, 56(12), 1737–1745. <https://doi.org/10.1021/acs.biochem.6b01236>
- Hereditary Ataxia Overview - GeneReviews® - NCBI Bookshelf*. (n.d.). Retrieved August 4, 2020, from <https://www.ncbi.nlm.nih.gov/books/NBK1138/>
- Hirano, M., Yamamoto, A., Mori, T., Lan, L., Iwamoto, T. A., Aoki, M., Shimada, K., Furiya, Y., Kariya, S., Asai, H., Yasui, A., Nishiwaki, T., Imoto, K., Kobayashi, N., Kiriya, T., Nagata, T., Konishi, N., Itoyama, Y., & Ueno, S. (2007). DNA single-strand break repair is impaired in aprataxin-related ataxia. *Annals of Neurology*, 61(2), 162–174. <https://doi.org/10.1002/ana.21078>
- Hoch, N. C., Hanzlikova, H., Rulten, S. L., Tétreault, M., Komulainen, E., Ju, L., Hornyak, P., Zeng, Z., Gittens, W., Rey, S. A., Staras, K., Mancini, G. M. S., McKinnon, P. J., Wang, Z. Q., Wagner,

- J. D., Yoon, G., & Caldecott, K. W. (2017b). XRCC1 mutation is associated with PARP1 hyperactivation and cerebellar ataxia. *Nature*, *541*(7635), 87–91.  
<https://doi.org/10.1038/nature20790>
- Horton, J. K., Stefanick, D. F., Çağlayan, M., Zhao, M. L., Janoshazi, A. K., Prasad, R., Gassman, N. R., & Wilson, S. H. (2018). XRCC1 phosphorylation affects aprataxin recruitment and DNA deadenylation activity. *DNA Repair*, *64*, 26–33. <https://doi.org/10.1016/j.dnarep.2018.02.004>
- Iles, N., Rulten, S., El-Khamisy, S. F., & Caldecott, K. W. (2007). APLF (C2orf13) Is a Novel Human Protein Involved in the Cellular Response to Chromosomal DNA Strand Breaks. *Molecular and Cellular Biology*, *27*(10), 3793–3803. <https://doi.org/10.1128/mcb.02269-06>
- Iyama, T., & Wilson, D. M. (2013). DNA repair mechanisms in dividing and non-dividing cells. *DNA Repair*, *12*(8), 620–636. <https://doi.org/10.1016/j.dnarep.2013.04.015>
- Jeppesen, D. K., Bohr, V. A., & Stevnsner, T. (2011). DNA repair deficiency in neurodegeneration. In *Progress in Neurobiology* (Vol. 94, Issue 2, pp. 166–200). NIH Public Access.  
<https://doi.org/10.1016/j.pneurobio.2011.04.013>
- Kalасova, I., Hanzlikova, H., Gupta, N., Li, Y., Altmüller, J., Reynolds, J. J., Stewart, G. S., Wollnik, B., Yigit, G., & Caldecott, K. W. (2019). Novel PNKP mutations causing defective DNA strand break repair and PARP1 hyperactivity in MCSZ. *Neurology: Genetics*, *5*(2).  
<https://doi.org/10.1212/NXG.0000000000000320>
- Katyal, S., El-Khamisy, S. F., Russell, H. R., Li, Y., Ju, L., Caldecott, K. W., & McKinnon, P. J. (2007). TDP1 facilitates chromosomal single-strand break repair in neurons and is neuroprotective in vivo. *EMBO Journal*, *26*(22), 4720–4731.  
<https://doi.org/10.1038/sj.emboj.7601869>
- Kedar, P. S., Kim, S. J., Robertson, A., Hou, E., Prasad, R., Horton, J. K., & Wilson, S. H. (2002). Direct interaction between mammalian DNA polymerase  $\beta$  and proliferating cell nuclear antigen. *Journal of Biological Chemistry*, *277*(34), 31115–31123.  
<https://doi.org/10.1074/jbc.M201497200>
- Kim, N., Huang, S. Y. N., Williams, J. S., Li, Y. C., Clark, A. B., Cho, J. E., Kunkel, T. A., Pommier, Y., & Jinks-Robertson, S. (2011). Mutagenic processing of ribonucleotides in DNA by yeast topoisomerase I. *Science*, *332*(6037), 1561–1564. <https://doi.org/10.1126/science.1205016>
- King, B. S., Cooper, K. L., Liu, K. J., & Hudson, L. G. (2012). Poly(ADP-ribose) contributes to an association between Poly(ADP-ribose) polymerase-1 and xeroderma pigmentosum complementation group A in nucleotide excision repair. *Journal of Biological Chemistry*, *287*(47), 39824–39833. <https://doi.org/10.1074/jbc.M112.393504>



- Klungland, A., & Lindahl, T. (1997). Second pathway for completion of human DNA base excision-repair: Reconstitution with purified proteins and requirement for DNase IV (FEN1). *EMBO Journal*. <https://doi.org/10.1093/emboj/16.11.3341>
- Komulainen, E., Badman, J., Rey, S., Rulten, S., Ju, L., Fennell, K., Mckinnon, P. J., Staras, K., & Caldecott, K. W. (2020). *Aberrant PARP1 Activity Couples DNA Breaks to Deregulated Presynaptic Calcium Signalling and Lethal Seizures*. 1–14. <https://doi.org/https://doi.org/10.1101/431916>
- Kondo, N., Takahashi, A., Ono, K., & Ohnishi, T. (2010). DNA damage induced by alkylating agents and repair pathways. In *Journal of Nucleic Acids* (Vol. 2010). J Nucleic Acids. <https://doi.org/10.4061/2010/543531>
- Kordon, M., Zarębski, M., Solarczyk, K., Ma, H., Pederson, T., & Dobrucki, J. (2019). Direct, sensitive and specific detection of individual single- or double-strand DNA breaks by fluorescence microscopy. *BioRxiv*, 772269. <https://doi.org/10.1101/772269>
- Lan, L., Nakajima, S., Oohata, Y., Takao, M., Okano, S., Masutani, M., Wilson, S. H., & Yasui, A. (2004). In situ analysis of repair processes for oxidative DNA damage in mammalian cells. *Proceedings of the National Academy of Sciences of the United States of America*, 101(38), 13738–13743. <https://doi.org/10.1073/pnas.0406048101>
- Langelier, M. F., Zandarashvili, L., Aguiar, P. M., Black, B. E., & Pascal, J. M. (2018). NAD<sup>+</sup> analog reveals PARP-1 substrate-blocking mechanism and allosteric communication from catalytic center to DNA-binding domains. *Nature Communications*, 9(1). <https://doi.org/10.1038/s41467-018-03234-8>
- Leal, A., Bogantes-Ledezma, S., Ekici, A. B., Uebe, S., Thiel, C. T., Sticht, H., Berghoff, M., Berghoff, C., Morera, B., Meisterernst, M., & Reis, A. (2018). The polynucleotide kinase 3'-phosphatase gene (PNKP) is involved in Charcot-Marie-Tooth disease (CMT2B2) previously related to MED25. *Neurogenetics*, 19(4), 215–225. <https://doi.org/10.1007/s10048-018-0555-7>
- Lee, Y., Katyal, S., Li, Y., El-Khamisy, S. F., Russell, H. R., Caldecott, K. W., & McKinnon, P. J. (2009). The genesis of cerebellar interneurons and the prevention of neural DNA damage require XRCC1. *Nature Neuroscience*, 12(8), 973–980. <https://doi.org/10.1038/nn.2375>
- Levin, D. S., McKenna, A. E., Motycka, T. A., Matsumoto, Y., & Tomkinson, A. E. (2000). Interaction between PCNA and DNA ligase I is critical for joining of Okazaki fragments and long-patch base-excision repair. *Current Biology*, 10(15), 919–922. [https://doi.org/10.1016/S0960-9822\(00\)00619-9](https://doi.org/10.1016/S0960-9822(00)00619-9)
- Lévy, N., Martz, A., Bresson, A., Spenlehauer, C., de Murcia, G., & Ménissier-de Murcia, J. (2006).

- XRCC1 is phosphorylated by DNA-dependent protein kinase in response to DNA damage. *Nucleic Acids Research*, 34(1), 32–41. <https://doi.org/10.1093/nar/gkj409>
- Li, G. M. (2008). Mechanisms and functions of DNA mismatch repair. In *Cell Research* (Vol. 18, Issue 1, pp. 85–98). Cell Res. <https://doi.org/10.1038/cr.2007.115>
- Li, M., Lu, L. Y., Yang, C. Y., Wang, S., & Yu, X. (2013). The FHA and BRCT domains recognize ADP-ribosylation during DNA damage response. *Genes and Development*, 27(16), 1752–1768. <https://doi.org/10.1101/gad.226357.113>
- Lieber, M. R. (2010). The Mechanism of Double-Strand DNA Break Repair by the Nonhomologous DNA End-Joining Pathway. *Annual Review of Biochemistry*, 79(1), 181–211. <https://doi.org/10.1146/annurev.biochem.052308.093131>
- Ljungquist, S., Kenne, K., Olsson, L., & Sandström, M. (1994a). Altered DNA ligase III activity in the CHO EM9 mutant. *Mutation Research-DNA Repair*, 314(2), 177–186. [https://doi.org/10.1016/0921-8777\(94\)90081-7](https://doi.org/10.1016/0921-8777(94)90081-7)
- Ljungquist, S., Kenne, K., Olsson, L., & Sandström, M. (1994b). Altered DNA ligase III activity in the CHO EM9 mutant. *Mutation Research-DNA Repair*, 314(2), 177–186. [https://doi.org/10.1016/0921-8777\(94\)90081-7](https://doi.org/10.1016/0921-8777(94)90081-7)
- Lodato, M. A., Rodin, R. E., Bohrson, C. L., Coulter, M. E., Barton, A. R., Kwon, M., Sherman, M. A., Vitzthum, C. M., Luquette, L. J., Yandava, C. N., Yang, P., Chittenden, T. W., Hatem, N. E., Ryu, S. C., Woodworth, M. B., Park, P. J., & Walsh, C. A. (2018). Aging and neurodegeneration are associated with increased mutations in single human neurons. *Science*, 359(6375), 555–559. <https://doi.org/10.1126/science.aao4426>
- Loizou, J. I., El-Khamisy, S. F., Zlatanou, A., Moore, D. J., Chan, D. W., Qin, J., Sarno, S., Meggio, F., Pinna, L. A., & Caldecott, K. W. (2004). The protein kinase CK2 facilitates repair of chromosomal DNA single-strand breaks. *Cell*, 117(1), 17–28. [https://doi.org/10.1016/S0092-8674\(04\)00206-5](https://doi.org/10.1016/S0092-8674(04)00206-5)
- Luczak, M. W., & Zhitkovich, A. (2018). Monoubiquitinated  $\gamma$ -H2AX: Abundant product and specific biomarker for non-apoptotic DNA double-strand breaks. *Toxicology and Applied Pharmacology*, 355, 238–246. <https://doi.org/10.1016/j.taap.2018.07.007>
- Lyras, L., Cairns, N. J., Jenner, A., Jenner, P., & Halliwell, B. (1997). An assessment of oxidative damage to proteins, lipids, and DNA in brain from patients with Alzheimer's disease. *Journal of Neurochemistry*, 68(5), 2061–2069. <https://doi.org/10.1046/j.1471-4159.1997.68052061.x>
- Mani, R. S., Karimi-Busheri, F., Fanta, M., Caldecott, K. W., Cass, C. E., & Weinfeld, M. (2004). Biophysical characterization of human XRCC1 and its binding to damaged and undamaged DNA.

- Biochemistry*, 43(51), 16505–16514. <https://doi.org/10.1021/bi048615m>
- Marintchev, A., Gryk, M. R., & Mullen, G. P. (2003). Site-directed mutagenesis analysis of the structural interaction of the single-strand-break repair protein, X-ray cross-complementing group 1, with DNA polymerase  $\beta$ . In *Nucleic Acids Research* (Vol. 31, Issue 2, pp. 580–588). <https://doi.org/10.1093/nar/gkg159>
- Matsumoto, Y., Kim, K., & Bogenhagen, D. F. (1994). Proliferating cell nuclear antigen-dependent abasic site repair in *Xenopus laevis* oocytes: an alternative pathway of base excision DNA repair. *Molecular and Cellular Biology*, 14(9), 6187–6197. <https://doi.org/10.1128/mcb.14.9.6187>
- Moreira, M. C., Barbot, C., Tachi, N., Kozuka, N., Uchida, E., Gibson, T., Mendonça, P., Costa, M., Barros, J., Yanagisawa, T., Watanabe, M., Ikeda, Y., Aoki, M., Nagata, T., Coutinho, P., Sequeiros, J., & Koenig, M. (2001). The gene mutated in ataxia-ocular apraxia 1 encodes the new HIT/Zn-finger protein aprataxin. *Nature Genetics*, 29(2), 189–193. <https://doi.org/10.1038/ng1001-189>
- Mortusewicz, O., Rothbauer, U., Cardoso, M. C., & Leonhardt, H. (2006a). Differential recruitment of DNA ligase I and III to DNA repair sites. *Nucleic Acids Research*, 34(12), 3523–3532. <https://doi.org/10.1093/nar/gkl492>
- Mortusewicz, O., Rothbauer, U., Cardoso, M. C., & Leonhardt, H. (2006b). Differential recruitment of DNA ligase I and III to DNA repair sites. *Nucleic Acids Research*, 34(12), 3523–3532. <https://doi.org/10.1093/nar/gkl492>
- Nanetti, L., Cavalieri, S., Pensato, V., Erbetta, A., Pareyson, D., Panzeri, M., Zorzi, G., Antozzi, C., Moroni, I., Gellera, C., Brusco, A., & Mariotti, C. (2013). SETX mutations are a frequent genetic cause of juvenile and adult onset cerebellar ataxia with neuropathy and elevated serum alpha-fetoprotein. *Orphanet Journal of Rare Diseases*, 8(1). <https://doi.org/10.1186/1750-1172-8-123>
- O'Connor, E., Vandrovcova, J., Bugiardini, E., Chelban, V., Manole, A., Davagnanam, I., Wiethoff, S., Pittman, A., Lynch, D. S., Efthymiou, S., Marino, S., Manzur, A. Y., Roberts, M., Hanna, M. G., Houlden, H., Matthews, E., & Wood, N. W. (2018). Mutations in XRCC1 cause cerebellar ataxia and peripheral neuropathy. *Journal of Neurology, Neurosurgery and Psychiatry*, 89(11), 1230–1232. <https://doi.org/10.1136/jnnp-2017-317581>
- Pion, E., Ullmann, G. M., Amé, J. C., Gérard, D., De Murcia, G., & Bombarda, E. (2005). DNA-induced dimerization of poly(ADP-ribose) polymerase-1 triggers its activation. *Biochemistry*, 44(44), 14670–14681. <https://doi.org/10.1021/bi050755o>
- Plo, I., Liao, Z. Y., Barceló, J. M., Kohlhagen, G., Caldecott, K. W., Weinfeld, M., & Pommier, Y. (2003). Association of XRCC1 and tyrosyl DNA phosphodiesterase (Tdp1) for the repair of

- topoisomerase I-mediated DNA lesions. *DNA Repair*, 2(10), 1087–1100.  
[https://doi.org/10.1016/S1568-7864\(03\)00116-2](https://doi.org/10.1016/S1568-7864(03)00116-2)
- Polo, L. M., Xu, Y., Hornyak, P., Garces, F., Zeng, Z., Hailstone, R., Matthews, S. J., Caldecott, K. W., Oliver, A. W., & Pearl, L. H. (2019). Efficient Single-Strand Break Repair Requires Binding to Both Poly(ADP-Ribose) and DNA by the Central BRCT Domain of XRCC1. *Cell Reports*.  
<https://doi.org/10.1016/j.celrep.2018.12.082>
- Pommier, Y., Barcelo, J. M., Rao, V. A., Sordet, O., Jobson, A. G., Thibaut, L., Miao, Z. H., Seiler, J. A., Zhang, H., Marchand, C., Agama, K., Nitiss, J. L., & Redon, C. (2006). Repair of Topoisomerase I-Mediated DNA Damage. In *Progress in Nucleic Acid Research and Molecular Biology* (Vol. 81, pp. 179–229). Prog Nucleic Acid Res Mol Biol. [https://doi.org/10.1016/S0079-6603\(06\)81005-6](https://doi.org/10.1016/S0079-6603(06)81005-6)
- Prasad, R., Beard, W. A., Strauss, P. R., & Wilson, S. H. (1998). Human DNA polymerase  $\beta$  deoxyribose phosphate lyase: Substrate specificity and catalytic mechanism. *Journal of Biological Chemistry*, 273(24), 15263–15270. <https://doi.org/10.1074/jbc.273.24.15263>
- Prasad, R., Dianov, G. L., Bohr, V. A., & Wilson, S. H. (2000). FEN1 stimulation of DNA polymerase  $\beta$  mediates an excision step in mammalian long patch base excision repair. *Journal of Biological Chemistry*, 275(6), 4460–4466. <https://doi.org/10.1074/jbc.275.6.4460>
- Richard, P., Feng, S., Tsai, Y. L., Li, W., Rinchetti, P., Muhith, U., Irizarry-Cole, J., Stolz, K., Sanz, L. A., Hartono, S., Hoque, M., Tadesse, S., Seitz, H., Lotti, F., Hirano, M., Chédin, F., Tian, B., & Manley, J. L. (2020). SETX (senataxin), the helicase mutated in AOA2 and ALS4, functions in autophagy regulation. *Autophagy*. <https://doi.org/10.1080/15548627.2020.1796292>
- Rouleau, M., Aubin, R. A., & Poirier, G. G. (2004). Pol (ADP-ribosyl)ated chromatin domains: Access granted. In *Journal of Cell Science* (Vol. 117, Issue 6, pp. 815–825).  
<https://doi.org/10.1242/jcs.01080>
- Rulten, S. L., Cortes-Ledesma, F., Guo, L., Iles, N. J., & Caldecott, K. W. (2008). APLF (C2orf13) Is a Novel Component of Poly(ADP-Ribose) Signaling in Mammalian Cells. *Molecular and Cellular Biology*, 28(14), 4620–4628. <https://doi.org/10.1128/mcb.02243-07>
- Santos-Pereira, J. M., & Aguilera, A. (2015). R loops: New modulators of genome dynamics and function. In *Nature Reviews Genetics* (Vol. 16, Issue 10, pp. 583–597). Nature Publishing Group.  
<https://doi.org/10.1038/nrg3961>
- Scholz, C., Golas, M. M., Weber, R. G., Hartmann, C., Lehmann, U., Sahn, F., Schmidt, G., Auber, B., Sturm, M., Schlegelberger, B., Illig, T., Steinemann, D., & Hofmann, W. (2018). Rare compound heterozygous variants in PNKP identified by whole exome sequencing in a German

- patient with ataxia-oculomotor apraxia 4 and pilocytic astrocytoma. In *Clinical Genetics* (Vol. 94, Issue 1, pp. 185–186). Blackwell Publishing Ltd. <https://doi.org/10.1111/cge.13216>
- Sharifi, R., Morra, R., Denise Appel, C., Tallis, M., Chioza, B., Jankevicius, G., Simpson, M. A., Matic, I., Ozkan, E., Golia, B., Schellenberg, M. J., Weston, R., Williams, J. G., Rossi, M. N., Galehdari, H., Krahn, J., Wan, A., Trembath, R. C., Crosby, A. H., ... Ahel, I. (2013). Deficiency of terminal ADP-ribose protein glycohydrolase TARG1/C6orf130 in neurodegenerative disease. *EMBO Journal*, *32*(9), 1225–1237. <https://doi.org/10.1038/emboj.2013.51>
- Sharma, R., Kumar, D., Jha, N. K., Jha, S. K., Ambasta, R. K., & Kumar, P. (2017). Re-expression of cell cycle markers in aged neurons and muscles: Whether cells should divide or die? In *Biochimica et Biophysica Acta - Molecular Basis of Disease* (Vol. 1863, Issue 1, pp. 324–336). Elsevier B.V. <https://doi.org/10.1016/j.bbadis.2016.09.010>
- Slade, D., Dunstan, M. S., Barkauskaite, E., Weston, R., Lafite, P., Dixon, N., Ahel, M., Leys, D., & Ahel, I. (2011). The structure and catalytic mechanism of a poly(ADP-ribose) glycohydrolase. *Nature*, *477*(7366), 616–622. <https://doi.org/10.1038/nature10404>
- Sparks, J. L., Chon, H., Cerritelli, S. M., Kunkel, T. A., Johansson, E., Crouch, R. J., & Burgers, P. M. (2012). RNase H2-Initiated Ribonucleotide Excision Repair. *Molecular Cell*, *47*(6), 980–986. <https://doi.org/10.1016/j.molcel.2012.06.035>
- Sugasawa, K. (2010). Regulation of damage recognition in mammalian global genomic nucleotide excision repair. In *Mutation Research - Fundamental and Molecular Mechanisms of Mutagenesis* (Vol. 685, Issues 1–2, pp. 29–37). Elsevier. <https://doi.org/10.1016/j.mrfmmm.2009.08.004>
- Szabó, A., Papp, A., & Nagymajtényi, L. (n.d.). EFFECTS OF 3-NITROPROPIONIC ACID IN RATS: GENERAL TOXICITY AND FUNCTIONAL NEUROTOXICITY \*. In *hrcak.srce.hr*. Retrieved August 4, 2020, from [https://hrcak.srce.hr/index.php?show=clanak\\_download&id\\_clanak\\_jezik=143](https://hrcak.srce.hr/index.php?show=clanak_download&id_clanak_jezik=143)
- Takashima, H., Boerkoel, C. F., John, J., Saifi, G. M., Salih, M. A. M., Armstrong, D., Mao, Y., Quioco, F. A., Roa, B. B., Nakagawa, M., Stockton, D. W., & Lupski, J. R. (2002). Mutation of TDP1, encoding a topoisomerase I-dependent DNA damage repair enzyme, in spinocerebellar ataxia with axonal neuropathy. *Nature Genetics*, *32*(2), 267–272. <https://doi.org/10.1038/ng987>
- Taylor, R. M., Wickstead, B., Cronin, S., & Caldecott, K. W. (1998). Role of a BRCT domain in the interaction of DNA ligase III- $\alpha$  with the DNA repair protein XRCC1. *Current Biology*, *8*(15), 877–880. [https://doi.org/10.1016/s0960-9822\(07\)00350-8](https://doi.org/10.1016/s0960-9822(07)00350-8)
- Tebbs, R. S., Flannery, M. L., Meneses, J. J., Hartmann, A., Tucker, J. D., Thompson, L. H., Cleaver, J. E., & Pedersen, R. A. (1999). Requirement for the *Xrcc1* DNA Base Excision Repair Gene

- during *Early Mouse Development*. <http://www.idealibrary.com>
- Tebbs, R. S., Thompson, L. H., & Cleaver, J. E. (2003). Rescue of Xrcc1 knockout mouse embryo lethality by transgene- complementation. *DNA Repair*, 2(12), 1405–1417. <https://doi.org/10.1016/j.dnarep.2003.08.007>
- Verheijen, B. M., Vermulst, M., & van Leeuwen, F. W. (2018). Somatic mutations in neurons during aging and neurodegeneration. In *Acta Neuropathologica* (Vol. 135, Issue 6, pp. 811–826). Springer Verlag. <https://doi.org/10.1007/s00401-018-1850-y>
- Vidal, A. E., Boiteux, S., Hickson, I. D., & Radicella, J. P. (2001a). XRCC1 coordinates the initial and late stages of DNA abasic site repair through protein-protein interactions. *EMBO Journal*, 20(22), 6530–6539. <https://doi.org/10.1093/emboj/20.22.6530>
- Vidal, A. E., Boiteux, S., Hickson, I. D., & Radicella, J. P. (2001b). XRCC1 coordinates the initial and late stages of DNA abasic site repair through protein-protein interactions. *EMBO Journal*, 20(22), 6530–6539. <https://doi.org/10.1093/emboj/20.22.6530>
- Vyas, S., Matic, I., Uchima, L., Rood, J., Zaja, R., Hay, R. T., Ahel, I., & Chang, P. (2014). Family-wide analysis of poly(ADP-ribose) polymerase activity. *Nature Communications*, 5, 4426. <https://doi.org/10.1038/ncomms5426>
- Wang, H., Guo, W., Mitra, J., Hegde, P. M., Vandoorne, T., Eckelmann, B. J., Mitra, S., Tomkinson, A. E., Van Den Bosch, L., & Hegde, M. L. (2018). Mutant FUS causes DNA ligation defects to inhibit oxidative damage repair in Amyotrophic Lateral Sclerosis. *Nature Communications*, 9(1), 3683. <https://doi.org/10.1038/s41467-018-06111-6>
- Wiest, N. E., & Tomkinson, A. E. (2019). SUMO ning the base excision repair machinery for differentiation . *The EMBO Journal*, 38(1). <https://doi.org/10.15252/embj.2018101147>
- Wilson, D. M., & McNeill, D. R. (2007). Base excision repair and the central nervous system. In *Neuroscience* (Vol. 145, Issue 4, pp. 1187–1200). Pergamon. <https://doi.org/10.1016/j.neuroscience.2006.07.011>
- Wong, H. K., Kim, D., Hogue, B. A., McNeill, D. R., & Wilson, D. M. (2005). DNA damage levels and biochemical repair capacities associated with XRCC1 deficiency. *Biochemistry*, 44(43), 14335–14343. <https://doi.org/10.1021/bi051161o>
- Wong, H. K., & Wilson, D. M. (2005). XRCC1 and DNA polymerase  $\beta$  interaction contributes to cellular alkylating-agent resistance and single-strand break repair. *Journal of Cellular Biochemistry*, 95(4), 794–804. <https://doi.org/10.1002/jcb.20448>
- Yang, N., Galick, H., & Wallace, S. S. (2004). Attempted base excision repair of ionizing radiation damage in human lymphoblastoid cells produces lethal and mutagenic double strand breaks. *DNA*

- Repair*, 3(10), 1323–1334. <https://doi.org/10.1016/j.dnarep.2004.04.014>
- Yao, B., & Jin, P. (2014). Cytosine modifications in neurodevelopment and diseases. In *Cellular and Molecular Life Sciences* (Vol. 71, Issue 3, pp. 405–418). NIH Public Access. <https://doi.org/10.1007/s00018-013-1433-y>
- Yao, N. Y., Schroeder, J. W., Yurieva, O., Simmons, L. A., & O'Donnell, M. E. (2013). Cost of rNTP/dNTP pool imbalance at the replication fork. *Proceedings of the National Academy of Sciences of the United States of America*, 110(32), 12942–12947. <https://doi.org/10.1073/pnas.1309506110>
- Yasuhara, T., Hara, K., Sethi, K. D., Morgan, J. C., & Borlongan, C. V. (2007). Increased 8-OHdG levels in the urine, serum, and substantia nigra of hemiparkinsonian rats. *Brain Research*, 1133(1), 49–52. <https://doi.org/10.1016/j.brainres.2006.11.072>
- Yoon, G., & Caldecott, K. W. (2018). Nonsyndromic cerebellar ataxias associated with disorders of DNA single-strand break repair. In *Handbook of Clinical Neurology* (Vol. 155, pp. 105–115). Elsevier B.V. <https://doi.org/10.1016/B978-0-444-64189-2.00007-X>
- Zecca, L., Youdim, M. B. H., Riederer, P., Connor, J. R., & Crichton, R. R. (2004). Iron, brain ageing and neurodegenerative disorders. In *Nature Reviews Neuroscience* (Vol. 5, Issue 11, pp. 863–873). Nat Rev Neurosci. <https://doi.org/10.1038/nrn1537>
- Zheng, J., Winderickx, J., Franssens, V., & Liu, B. (2018). A Mitochondria-Associated Oxidative Stress Perspective on Huntington's Disease. In *Frontiers in Molecular Neuroscience* (Vol. 11). Frontiers Media S.A. <https://doi.org/10.3389/fnmol.2018.00329>

**Online sources:**

URL1: <https://www.genetex.com/Article/Support/Index/poster-library>

URL2: <https://www.genecards.org/cgi-bin/carddisp.pl?gene=PARP1#expression>

URL3: <https://www.genecards.org/cgi-bin/carddisp.pl?gene=PARP2#expression>

URL4: <https://www.genecards.org/cgi-bin/carddisp.pl?gene=PARP3#expression>

URL5: <https://www.ncbi.nlm.nih.gov/gene/7515#gene-expression>

URL6: <https://www.ncbi.nlm.nih.gov/books/NBK1138/>